A STUDY OF MOISTURE INDUCED MATERIAL LOSS OF HOT MIX ASPHALT (HMA)

by

Uma Maheswar Arepalli

A Dissertation

Submitted to the Faculty

of the

WORCESTER POLYTECHNIC INSTITUTE

in partial fulfillment of the requirements for the

Degree of Doctor of Philosophy

in

Civil Engineering

February 2018

APPROVED:

_____	_____
Dr. Rajib. B. Mallick, Major Advisor, CEE	Dr. Mingjiang Tao, CEE
_____	_____
Dr. Nima Rahbar, CEE	Dr. Michael Radzicki, SD

Abstract

Susceptibility of Hot Mix Asphalt (HMA) mixes to moisture induced damage is one of the main reasons for premature failures of asphalt pavements. Hence, the evaluation of mixes for the moisture susceptibility is an essential part of the mix design. The existing methods are found to be in-sufficient to characterize mixes in terms of their moisture damage potential, and many studies have been conducted to establish an improved methodology that can better address the issue. Most of these methods involve the determination of changes in mix properties due to moisture conditioning in the laboratory or to verify the mix performance in the field or the laboratory. In the field moisture susceptible mixes are also found to lose material to extents that are dependent upon the properties of the mix and materials. So far, there has been no comprehensive study to investigate the loss of materials due to moisture induced damage. The objective of this study was to identify and evaluate a conditioning and a test method that can be used on a regular basis to detect moisture susceptible mixes and to understand the combined problem of moisture induced material loss and change in strength/stiffness of the mix. The Moisture Induced Stress Tester (MIST), Ultrasonic Pulse Velocity (UPV), Dynamic Modulus in Indirect tensile mode, and Indirect Tensile Strength (ITS) tests were utilized in the study. The effluent from the MIST was checked for the gradation of dislodged aggregates and the Dissolved Organic Carbon (DOC) content. A system dynamics (SD) approach was also adopted to investigate the problem and establish a model to reproduce field observations. The results showed that the use of MIST in combination with UPV or ITS is able to identify moisture susceptible mixes, in particular for mixes with the potential of aggregate breakdown. The mixes with a higher loss of asphalt binder during conditioning exhibit higher tensile strengths, and those with a loss of finer materials, which is indicative of aggregate breakdown, show a lower tensile strength. For the mixes used in this study, the rate of change in indirect tensile strength during moisture conditioning was found to be strongly correlated to the pre-conditioning modulus of the mix. A step-by-step framework to characterize the moisture susceptible mixes was presented.

Keywords: HMA, asphalt, seismic modulus, indirect tensile strength, system dynamics, dissolved organic carbon, fineness modulus, Moisture Induced Stress Tester, dynamic modulus, moisture damage.

Dedication

I dedicate this dissertation to my father Simhadri Arepalli, without whose support and encouragement this would not have possible. It is also dedicated to my village Lankalakoderu, West Godavari, AP, India, the place where I born and brought up!

Acknowledgement

First and foremost, I would like to express sincerest thanks to my advisor Prof. Rajib. B. Mallick, for giving me the opportunity to pursue a doctoral degree from the United States. My Ph.D. would not have possible without his kind support and guidance, not only academically but also personally. I am greatly thankful to him for arranging various funding opportunities through research assistantship, professional development and grants to attend conferences.

I would like to thank my dissertation committee members – Prof. Mingjiang Tao, Prof. Nima Rahbar and Prof. Michael Radzicki for all their support from the beginning with their valuable suggestions at the appropriate time, and to monitor the research to meet the standards of the Ph.D. dissertation. A special thanks go to Prof. Paul Mathisen for all his generous help with one of the parts of the research. I would also like to thank various researchers – Prof. Soheil Nazarian, Texas-El Paso; Ilker Boz, Penn State University; Dr. Lily Poulikakos and Dr. Michele Griffa, Empa, Switzerland; Mr. Andrew Butler, LSBC, WPI, for their opinions and contributions at different stages of this research. A big thanks go to Maine Department of Transportation for funding the project and providing the material especially the valuable field samples for the research. My sincere thanks go to our lab managers – Mr. Don Pellegrino and Mr. Russ Lang, who were very resourceful in the laboratory. I thank our department head Prof. Tahar El-korchi for all his efficient coordination to run the department smoothly, and for his support in getting my teaching assistantship (TA). I would also thank all of my TA course professors – Prof. Salazar, Prof. Lepage, Prof. Mathisen, Prof. Pitreforte and Prof. Mallick, for their kind support, due to which I could able spend good amount of time towards my research. I would also thank our department office staff - Marylou and Cindy for their great help with all the works related to office.

I would like to thank my fellow students and friends – Ram Kumar Veeraragavan, Wenwen Yao, Ryan Worsman, Nivedya MK, Mohammed Salhi, Baillie McNally and Sravan Katepalli for their help and support at different stages of this long journey.

I would like to thank my wife Vineela for all her love and company during the entire course of the study. I thank God for his wonderful gift through our new-born Praneesha, during my final stages of Ph.D. Last but not the least, I would like to thank my parents, siblings, in-laws, friends and relatives for all their encouragement and support throughout my Ph.D.

Table of Contents

List of Figures

List of Tables

Chapter 1

Introduction

1.1 Overview

A significant amount of research has been conducted in the last few decades on the evaluation of moisture damage of Hot Mix Asphalt (HMA). Various modes of failures have been identified, and methods of testing have been developed (Kakar et al. 2015; Kiggundu and Roberts 1988). Typically, for routine testing, HMA mixes are conditioned to simulate the action of moisture and then tested, and the test results are compared to those from pre-conditioned mixes to determine the potential of moisture damage (Solaimanian et al. 2003). However, not much work is available for the identification of moisture susceptible mixes where the material loss in the wheel-path is due to the breakdown of the material under the combined action of traffic and moisture. This moisture induced material loss could be a loss of coated/uncoated aggregates or loss of binder compounds due to the presence of moisture and traffic.

1.2 Problem statement

The partial or complete loss of material within 2-3 years of construction in the traffic wheel path in the presence of moisture was noticed by a state Department of Transportation in few of their mixes. Regularly used moisture susceptibility tests are unable to detect the problem during mix design. The obvious reason is that the currently available tests are not appropriate – or more precisely, either the conditioning or the test or both are not appropriate. Hence, a research study was initiated to understand and characterize the mixes that are susceptible to moisture induced material loss.

1.3 Research Objectives

The objectives of the research were as follows:

- To simulate moisture induced loss of materials in mixes in the laboratory
- To identify and evaluate a test method that can be used on a regular basis to detect moisture susceptible mixes

1.4 Dissertation Outline

The dissertation is organized in 7 chapters as described below.

Chapter 1 presents an introduction that includes an overview, problem statement and research objectives, and the dissertation outline.

Chapter 2 presents a summary of general literature related to the field of research with an objective to identify suitable methods for the current study. The outcomes of the literature study were summarized at the end of the chapter. The literature study includes moisture damage mechanisms, moisture damage studies along with studies that studied moisture induced material loss.

Chapter 3 presents the major methods that were considered in the study and the corresponding literature reviews.

Chapter 4 presents the preliminary study, in four parts, that was conducted to identify a methodology to characterize the moisture susceptible mixes and also to identify and evaluate the loss of material.

Chapter 5 presents the main study that was conducted to characterize the moisture susceptible mixes with the proposed methodology based on the preliminary study.

Chapter 6 presents a study to understand moisture induced material loss of Hot Mix Asphalt with the use of system dynamics modeling.

Chapter 7 presents a framework to evaluate moisture susceptibility of Hot Mix Asphalt.

References

Kakar, M. R., Hamzah, M. O., and Valentin, J. (2015). "A review on moisture damages of hot and warm mix asphalt and related investigations." *Journal of Cleaner Production*, 99, 39-58.

Kiggundu, B. M., and Roberts, F. L. (1988). "Stripping in HMA mixtures: State-of-the-art and critical review of test methods." National Center for Asphalt Technology.

Solaimanian, M., Harvey, J., Tahmoressi, M., and Tandon, V. (2003). "Test methods to predict moisture sensitivity of hot-mix asphalt pavements." *Transportation Research Board National Seminar. San Diego, California*, 77-110.

Chapter 2

Literature Review - General

2.1 Moisture damage phenomena

The primary cause of moisture induced damage in Hot Mix Asphalt (HMA) is the cohesive failure of asphalt mixture and/or adhesive failure of aggregates and asphalt binder interface (Airey and Choi 2002). These failures can occur in different forms depending on the factors involved. Table 2.1 lists various micro and macro mechanisms that could be responsible for moisture damage, and also possible responses of the system. Kringos and Scarpas (2005) studied the gradual development of damage in open graded asphalt mixes due to water infiltration and identified desorption, diffusion and dispersion as fundamental processes that are involved in the moisture damage phenomena. In stationary condition, water diffuses into mastic and causes mastic-aggregate interface failure. Over time, the diffusion causes cohesive mastic failure. On the other hand, the water flow itself can cause advective transport of mastic, irrespective of diffusion, depending upon the velocity of water flow. The extents of these processes depend upon the porosity, velocity of water flow, and the mechanical and chemical characteristics of HMA components. Copeland et al. (2007) described the water damage in asphalt mixes as the cohesive failure in the mastic, adhesive failure at the asphalt-aggregate interface, and breakdown of aggregates.

Table 2.1. Moisture Damage theories and mechanisms (Mehrara and Khodaii 2013)

Mechanisms		**Response of the system**
Micro	**Macro**	
Adhesion theories: Mechanical, Chemical reaction, Molecular orientation, Surface energy, Weak boundary	Formation of excess pore pressure, Hydraulic scouring and Physical erosion of asphalt	Detachment, Displacement, Dispersion of the mastic, film rupture and micro-crack, Desorption, Spontaneous emulsification

The characteristics of asphalt mixture and its components affect the moisture susceptibility of the mixes. A complete list of determining characteristics and their favorable properties that are related to moisture susceptibility were presented in Mehrara and Khodaii 2013.

2.2 Moisture damage studies

The percentage of asphalt coating retention on aggregate surfaces under different testing conditions has been utilized as a qualitative measure to evaluate the stripping potential of loose mixtures (Kiggundu and Roberts 1988; Tunnicliff and Root 1982). Net absorption, chemical and surface reaction methods were utilized to evaluate moisture damage of loose mixtures quantitatively (Curtis et al. 1993; Kiggundu and Roberts 1988; Solaimanian et al. 2003). Various energy based methods and advanced techniques have been introduced and utilized as measures of cohesion or adhesion. Adhesive energy concepts, and a pull off test method (Pull-off Strength of Coatings using Portable Adhesion Tester, Pneumatic Adhesion Tensile Testing Instrument, PATTI) and its variations (Bitumen Bond Strength (BBS) have been utilized to evaluate the effect of water on both adhesive and cohesive bond strengths (Bahia et al. 2007; Canestrari et al. 2010; Chaturabong and Bahia 2016; Cho and Kim 2010; Copeland et al. 2007; Moraes et al. 2011; Youtcheff and Aurilio 1997). Adhesion bond has been evaluated with wetting of moisture on substrate tests (Wasiuddin et al. 2011), contact angle, mechanical interlocking, and physicochemical adhesion due to surface free energy and bonding due to interfacial chemical reaction (Bhasin 2006; Bhasin et al. 2007; Johnson and Freeman 2002; Petrie 2006; Terrel and Shute 1989). Asphalt properties that can affect the bond strength have been identified as polarity and constitution, viscosity, film thickness and surface energy (Bahia et al. 2007; Xiao et al. 2007). Aggregates selectively absorb some components of asphalt, especially sulfoxides and carboxylic acids, and less of aromatic compounds, and their types and quantities affect the bond strength (Petersen et al. 1982; Plancher et al. 1977; Robertson 2000). While rough surface with greater area is favorable for the adhesive bond, the presence of porosity with trapped air, moisture and dust reduce the bond strength (Castan and Cartellas 1968; Yoon and Tarrer 1988).

The dynamic shear rheometer (DSR) has been used to determine the effect of moisture on the properties of different types of fillers in asphalt mix mastic (Kvasnak and Williams 2007; Moraes et al. 2011) and a continuum damage mechanics model to explain adhesive and cohesive damage has been presented (Shakiba et al. 2013). Recent developments include a tensile test

method for measuring adhesion strength between binders and aggregates (Merusi et al. 2013), the sequentially coupled model with cohesive zone fracture concept (Caro et al. 2010) and an integration of this concept with pull off testing experiments (Ban et al. 2011). Bhasin and Little (2007) determined the bond strength between aggregate and asphalt binder from surface energies measured by using universal sorption device. Pan et al. (2008) utilized Fourier Transform Infrared (FTIR) spectroscopy technique to evaluate the emulsification of asphalt binder in the presence of most common deicer - sodium acetate. The authors also suggested other analytical methods such as the Mass Spectroscopy (MS) and Nuclear Magnetic Resonance (NMR) spectroscopy to detect the new materials possibly generated in the emulsification process. Bhasin and Little (2009) utilized microcalorimeter, which can measure surface energy, to characterize adhesion between asphalt binders and aggregates.

For regular mix design testing of HMA, the moisture damage potential is predicted by using the AASHTO T283 method (AASHTO 2001; Lottman 1977; Lottman 1978). Kringos et al. (2009) have presented the many reasons for variability in the results from this test: the wide variability in pore spaces and resulting moisture concentrations, weakening in indirect tensile strength samples, and variability in stresses in samples of different sizes. They emphasized the need for the consideration of the moisture ingress time. The effect of pavement saturation on the moisture damage has also been demonstrated (Choubane et al. 2000). The Hamburg Wheel Tracking (HWT) test has been utilized extensively by many researchers (Aschenbrener 1995; Aschenbrener and Currier 1993) for comparison of the performance of mixes. Yin et al. (2014) have developed new HWT test parameters to evaluate mixture resistance to rutting and stripping separately by avoiding post-compaction duration assumptions and also possible bias introduced from fitting creep and stripping phase lines in the conventional method. Copeland et al. (2007) have compared the results of pull off test with those from DSR and Hamburg wheel tracking tests, and Cross et al. (2000) had used the Asphalt Pavement Analyzer (APA) to test the moisture susceptibility of HMA. A test method for quantitative evaluation of stripping using ultrasonic energy in HMA has been presented (McCann and Sebaaly 2001), and the Model Mobile Load Tester (MMLS) has been used to evaluate mixes under combined wet-high temperature-trafficked systems (Mallick et al. 2005). In the environmental conditioning system (ECS) (Al-Swailmi et al. 1992) a membrane-encapsulated specimen is subjected to cycles of temperature, loading, and

moisture conditioning. Solaimanian et al. (2006) have recommended the dynamic modulus testing of ECS-conditioned HMA as a potentially good method for identifying moisture susceptible mixes. Lu and Harvey (2006) examined the potential of flexural beam fatigue test to evaluate the moisture sensitivity of HMA and developed a test protocol. Airey et al. (2005) developed a test method "Saturation Ageing Tensile Stiffness (SATS)" using Nottingham Asphalt Tester (NAT) to assess combined aging/moisture sensitivity of high modulus base asphalt mixtures. Birgisson et al. (2003) utilized ultrasonic pulse velocity test for monitoring changes in HMA integrity from exposure to moisture. The effect of pore water pressure and saturation on de-bonding of mixes, the effect of permeability and vehicle speed on pore water pressure in pavements, and the use of the Moisture Induced Stress Tester (MIST) have been investigated by a number of researchers (Birgisson et al. 2007; Buchanan et al. 2004; Cross et al. 2000; Jimenez 1974; Kiggundu and Roberts 1988; Mallick et al. 2003; Novak et al. 2002; Pinkham et al. 2013). In general, they have recommended an equipment for generating cyclic pore pressure as a tool for the evaluation of mixes within a reasonable amount of time. Finally, the need for the consideration of moisture damage in Mechanistic-Empirical (ME) design of pavements has been emphasized (Apeagyei 2016; Vargas-Nordcbeck 2016).

2.3 Identification of loss of material

In a moisture damage study that was conducted by Varveri et al. (2016) upon porous asphalt mixes using the MIST, erosion of fine material was reported with the increase of cycles at and above 8,000. Zofka et al. (2014) analyzed the post MIST water samples using Fourier transform (FT-IR) and identified traces of leached asphalt in the water samples. Song et al. (2011) determined the chemical composition of water soluble asphalt compounds using Gas chromatography-mass spectrometry (GC/MS). Many asphalt leaching studies reported the leaching of Poly Aromatic Hydrocarbons (PAH) from asphalt pavements (Brantley and Townsend 1999; Kriech et al. 2002). Though these amounts were below detection limits of the Environmental Protection Agency (EPA), the studies confirm the leaching of asphalt compounds.

The outcomes of the literature study can be summarized as follows.

- Current AASHTO T 283 method is not efficient and cyclic pore pressure generation equipment such as MIST has shown good potential to simulate moisture induced damage in the laboratory

- There is a potential for non-destructive ultrasonic pulse velocity test to characterize moisture susceptible mixes
- No comprehensive study have been conducted to evaluate the loss of material, in terms of coated and uncoated aggregates and binder compounds, which could contribute to the moisture induced damage and deterioration of mixes in the field.

References

AASHTO (2001). "Resistance of compacted bituminous mixture to moisture induced damage,T283–89." *Part II: Tests*, Standard Specifications for Transportation Materials and Methods and Sampling and Testing, Washington D.C.

Airey, G. D., and Choi, Y.-K. (2002). "State of the Art Report on Moisture Sensitivity Test Methods for Bituminous Pavement Materials." *Road Materials and Pavement Design*, 3(4), 355-372.

Airey, G. D., Choi, Y. K., Collop, A. C., Moore, A. J., and Elliott, R. C. (2005). "Combined laboratory ageing/moisture sensitivity assessment of high modulus base asphalt mixtures (with discussion)." *Journal of the Association of Asphalt Paving Technologists*, 74.

Al-Swailmi, S., Scholz, V., and Terrel, L. (1992). "Development and evaluation of test system to induce and monitor moisture damage to asphalt concrete mixtures." *Transportation Research Record: Journal of the Transportation Research Board*, 1353, 39.

Apeagyei, A., J. Grenfell and G. Airey (2016). "Incorporating Moisture Effects into Mechanistic-Empirical Design of Asphalt Pavements." *Presented at the 95th Annual Meeting of the Transportation Research Board*Washington D.C.

Aschenbrener, T. (1995). "Evaluation of Hamburg wheel-tracking device to predict moisture damage in hot-mix asphalt." *Transportation Research Record: Journal of the Transportation Research Board*, 1492, 193.

Aschenbrener, T., and Currier, G. (1993). "Influence of testing variables on the results from the Hamburg Wheel-Tracking Device." *Final Report*, Colorado Department of Transportation, p 116.

Bahia, H., Hanz, A., Kanitpong, K., and Wen, H. (2007). "Testing methods to determine aggregate/asphalt adhesion properties and potential moisture damage." *WHRP 07-02, Wisconsin Highway Research Program*, Madison, Wisconsin, p 107.

Ban, H., Kim, Y.-R., and Pinto, I. (2011). "Integrated experimental-numerical approach for estimating material-specific moisture damage characteristics of binder-aggregate interface." *Transportation Research Record: Journal of the Transportation Research Board*(2209), 9-17.

Bhasin, A. (2006). "Development of methods to quantify bitumen-aggregate adhesion and loss of adhesion due to water." Ph.D. dissertation, Texas A&M University, College Station, Tex.

Bhasin, A., Little, D., Vasconcelos, K., and Masad, E. (2007). "Surface free energy to identify moisture sensitivity of materials for asphalt mixes." *Transportation Research Record: Journal of the Transportation Research Board*(2001), 37-45.

Bhasin, A., and Little, D. N. (2007). "Characterization of aggregate surface energy using the universal sorption device." *Journal of Materials in Civil Engineering*, 19(8), 634-641.

Bhasin, A., and Little, D. N. (2009). "Application of microcalorimeter to characterize adhesion between asphalt binders and aggregates." *Journal of Materials in Civil Engineering*, 21(6), 235-243.

Birgisson, B., Roque, R., and Page, G. (2003). "Ultrasonic pulse wave velocity test as a tool for monitoring changes in HMA mixture integrity due to exposure to moisture." *Proc., Annual Transportation Research Board Meeting*.

Birgisson, B., Roque, R., Page, G., and Wang, J. (2007). "Development of new moisture-conditioning procedure for hot-mix asphalt." *Transportation Research Record: Journal of the Transportation Research Board*(2001), 46-55.

Brantley, A. S., and Townsend, T. G. (1999). "Leaching of pollutants from reclaimed asphalt pavement." *Environmental Engineering Science*, 16(2), 105-116.

Buchanan, M. S., Moore, V., Mallick, R., O'Brien, S., and Regimand, A. (2004). "Accelerated moisture susceptibility testing of hot mix asphalt (HMA) mixes." *83rd annual meeting of the Transportation research board, Washington, D.C.* .

Canestrari, F., Cardone, F., Graziani, A., Santagata, F. A., and Bahia, H. U. (2010). "Adhesive and cohesive properties of asphalt-aggregate systems subjected to moisture damage." *Road Materials and Pavement Design*, 11(sup1), 11-32.

Caro, S., Masad, E., Bhasin, A., and Little, D. (2010). "Coupled micromechanical model of moisture-induced damage in asphalt mixtures." *Journal of Materials in Civil Engineering*, 22(4), 380-388.

Castan, M., and Cartellas, E. (1968). "Rising of binder to the surface of an open-graded bituminous mix." *No. 33*, Bullentinde Liaison des Laboratories Routiers, 77-84.

Chaturabong, P., and Bahia, H. U. (2016). "Effect of Moisture on Cohesion of Asphalt Mastics and Bonding with Surface of Aggregates." *Proc., Transportation Research Board 95th Annual Meeting*.

Cho, D.-W., and Kim, K. (2010). "The mechanisms of moisture damage in asphalt pavement by applying chemistry aspects." *KSCE Journal of Civil Engineering*, 14(3), 333-341.

Choubane, B., Page, G., and Musselman, J. (2000). "Effects of water saturation level on resistance of compacted hot-mix asphalt samples to moisture-induced damage." *Transportation Research Record: Journal of the Transportation Research Board*(1723), 97-106.

Copeland, A. R., Kringos, N., Youtcheff Jr, J. S., and Scarpas, T. (2007). "Measurement of Aggregate–Mastic Bond Strength in Presence of Moisture: Combined Experimental-Computational Study." *Proc., Transportation Research Board 86th Annual Meeting*.

Copeland, A. R., Kringos, N., Youtcheff Jr, J. S., and Scarpas, T. (2007). "Measurement of Aggregate–Mastic Bond Strength in Presence of Moisture: Combined Experimental-Computational Study." *86th Annual Meeting of the Transportation Research Board, Washington, D.C.* .

Cross, S. A., Voth, M. D., and Fager, G. A. (2000). "Effects of sample preconditioning on asphalt pavement analyzer wet rut depths." *Proceedings of Mid-Continent Transportation Symposium*, 20-23.

Curtis, C. W., Ensley, K., and Epps, J. (1993). "Fundamental properties of asphalt-aggregate interactions including adhesion and absorption." *SHRP-A-341. Strategic Highway Research Program*, National Research Council, Washington, D.C., p 603.

Jimenez, R. (1974). "Testing for debonding of asphalt from aggregates." *Transportation Research Record: Journal of the Transportation Research Board*(515), 1-17.

Johnson, D. R., and Freeman, R. B. (2002). "Rehabilitation techniques for stripped asphalt pavements." *Report No. FHWA/MT-002-003/8123*, Western Transportation Institute, Bozeman, Montana, p 164.

Kiggundu, B. M., and Roberts, F. L. (1988). "Stripping in HMA mixtures: State-of-the-art and critical review of test methods." *NCAT Report No. 88-2*, National Center for Asphalt Technology, Auburn University, Auburn, AL, p 44.

Kriech, A., Kurek, J., Osborn, L., Wissel, H., and Sweeney, B. (2002). "Determination of polycyclic aromatic compounds in asphalt and in corresponding leachate water." *Polycyclic Aromatic Compounds*, 22(3-4), 517-535.

Kringos, N., Azari, H., and Scarpas, A. (2009). "Identification of parameters related to moisture conditioning that cause variability in modified Lottman test." *Transportation Research Record: Journal of the Transportation Research Board*(2127), 1-11.

Kringos, N., and Scarpas, A. (2005). "Raveling of asphaltic mixes due to water damage: computational identification of controlling parameters." *Transportation research record: journal of the transportation research board*(1929), 79-87.

Kvasnak, A., and Williams, R. C. (2007). "Evaluation of the Interaction Effects between Asphalt Binders and Fillers Using a Moisture Susceptibility Test (With Discussion)." *Journal of the association of asphalt paving technologists*, 76.

Lottman, R. (1977). "Predicting Moisture Induced Damage to Asphaltic Concrete - Field Evaluation." *NCHRP Report. 246*, Transportation Research Board, National Highway Research Council, Washington, D.C., p 20.

Lottman, R. (1978). "Predicting moisture-induced damage to asphaltic concrete." *NCHRP Report 192*, Transportation Research Board, National Research Council, Washington, D.C., p 46.

Lu, Q., and Harvey, J. T. (2006). "Evaluation of moisture sensitivity of hot mix asphalt by flexural beam fatigue test." *Asphalt Concrete: Simulation, Modeling, and Experimental Characterization*, 124-133.

Mallick, R. B., Gould, J. S., Bhattacharjee, S., Regimand, A., James, L. H., and Brown, E. R. (2003). "Development of a rational procedure for evaluation of moisture susceptibility of asphalt paving mixes." *82nd Annual meeting of the TRB Meeting. Washington, D.C.*

Mallick, R. B., Pelland, R., and Hugo, F. (2005). "Use of accelerated loading equipment for determination of long term moisture susceptibility of hot mix asphalt." *International Journal of Pavement Engineering*, 6(2), 125-136.

McCann, M., and Sebaaly, P. (2001). "Quantitative evaluation of stripping potential in hot-mix asphalt, using ultrasonic energy for moisture-accelerated conditioning." *Transportation research record: journal of the transportation research board*(1767), 48-49.

Mehrara, A., and Khodaii, A. (2013). "A review of state of the art on stripping phenomenon in asphalt concrete." *Construction and Building Materials*, 38, 423-442.

Merusi, F., Caruso, A., Chiapponi, L., and Giuliani, F. (2013). "Mechanical Analysis of Failure Processes at Bitumen/Aggregate Interface." *92nd Annual Meeting of the Transportation Research Board, Washington, D.C.* .

Moraes, R., Velasquez, R., and Bahia, H. (2011). "Measuring the effect of moisture on asphalt-aggregate bond with the bitumen bond strength test." *Transportation Research Record: Journal of the Transportation Research Board*(2209), 70-81.

Novak, M., Birgisson, B., and McVay, M. (2002). "Effects of permeability and vehicle speed on pore pressure in hot mix asphalt pavements." *Proc., Transportation Research Board Meeting, Washington, DC*.

Pan, T., He, X., and Shi, X. (2008). "Laboratory investigation of acetate-based deicing/anti-icing agents deteriorating airfield asphalt concrete." *Asphalt Paving Technology-Proceedings*, 77, 773.

Petersen, J., Plancher, H., Ensley, E., Venable, R., and Miyake, G. (1982). "Chemistry of asphalt-aggregate interaction: relationship with pavement moisture-damage prediction test." *Transportation Research Record: Journal of the Transportation Research Board*(843), 95-104.

Petrie, E. M. (2006). "Handbook of adhesives and sealants." McGraw-Hill, New York, p 267.

Pinkham, R., Cote, S. A., Mallick, R. B., Tao, M., Bradbury, R. L., and Regimand, A. (2013). "Use of Moisture Induced Stress Testing to Evaluate Stripping Potential of Hot Mix Asphalt (HMA)." *92nd Annual Meeting of the Transportation Research Board, Washington, D.C.*

Plancher, H., Dorrence, S., and Petersen, J. (1977). "Identification of chemical types in asphalts strongly adsorbed at the asphalt-aggregate interface and their relative displacement by water." *Journal of the Association of Asphalt Paving Technologists*, 46, 151-175.

Robertson, R. E. (2000). "Chemical properties of asphalts and their effects on pavement performance." *Transportation Research Circular 499, TRB*, National Research Council, Washington, D.C., p 46.

Shakiba, M., Al-Rub, R., Darabi, M., You, T., Masad, E., and Little, D. (2013). "Continuum coupled moisture-mechanical damage model for asphalt concrete." *Transportation Research Record: Journal of the Transportation Research Board*(2372), 72-82.

Solaimanian, M., Fedor, D., Bonaquist, R., Soltani, A., and Tandon, V. (2006). "Simple performance test for moisture damage prediction in asphalt concrete (with discussion)." *Journal of the Association of Asphalt Paving Technologists*, 75, 345-380.

Solaimanian, M., Harvey, J., Tahmoressi, M., and Tandon, V. (2003). "Test methods to predict moisture sensitivity of hot-mix asphalt pavements." *Proc., Moisture Sensitivity of Asphalt Pavements-A National Seminar*.

Song, Y., Wang, C., and Zhang, Y. (2011). "Determination of the Chemical Composition in Asphalt Aqueous Solutions by SPE and GC/MS." *Petroleum Science and Technology*, 29(15), 1590-1595.

Terrel, R. L., and Shute, J. W. (1989). "Summary report on water sensitivity." *SHRP-A/IR-89-003, Strategic Highway Program*, National Research Council, Washington, D.C.

Tunnicliff, D. G., and Root, R. E. "ANTISTRIPPING ADDITIVES IN ASPHALT CONCRETE--STATE-OF-THE-ART 1981." *Proc., Association of Asphalt Paving Technologists Proceedings*.

Vargas-Nordcbeck, A., F. Leiva-Villacorta , J. Aguiar-Moya , L Loria-Salazar (2016). "Evaluating Moisture Susceptibility of AC Mixtures through Simple Performance Tests." *Presented at the 95th Annual Meeting of the Transportation Research Board, Washington, D.C.*

Varveri, A., Avgerinopoulos, S., and Scarpas, A. (2016). "Experimental evaluation of long-and short-term moisture damage characteristics of asphalt mixtures." *Road Materials and Pavement Design*, 17(1), 168-186.

Wasiuddin, N., Saltibus, N., and Mohammad, L. (2011). "Novel moisture-conditioning method for adhesive failure of hot-and warm-mix asphalt binders." *Transportation Research Record: Journal of the Transportation Research Board*(2208), 108-117.

Xiao, F., Amirkhanian, S., and Juang, C. H. (2007). "Rutting resistance of rubberized asphalt concrete pavements containing reclaimed asphalt pavement mixtures." *Journal of Materials in Civil Engineering*, 19(6), 475-483.

Yin, F., Arambula, E., Lytton, R., Martin, A., and Cucalon, L. (2014). "Novel method for moisture susceptibility and rutting evaluation using hamburg wheel tracking test." *Transportation Research Record: Journal of the Transportation Research Board*(2446), 1-7.

Yoon, H. H., and Tarrer, A. R. (1988). "Effect of aggregate properties on stripping." *Transportation Research Record: Journal of the Transportation Research Board*(1171), 37-43.

Youtcheff, J., and Aurilio, V. (1997). "Moisture sensitivity of asphalt binders: evaluation and modeling of the pneumatic adhesion test results." *Proc., Proceedings of the annual conference-Canadian technical asphalt association*, POLYSCIENCE PUBLICATIONS INC., 180-200.

Zofka, A., Maliszewski, M., and Bernier, A. (2014). "Alternative moisture sensitivity test." *Proc., Environmental Engineering. Proceedings of the International Conference on Environmental Engineering. ICEE*, Vilnius Gediminas Technical University, Department of Construction Economics & Property, 1.

Chapter 3

Experimental Methods

The following experimental methods were utilized in the research.

3.1 Moisture conditioning

The Moisture Induced Stress Tester (MIST), a relatively new device (Buchanan et al. 2004) (ASTM D7870-13) was selected as the conditioning method for the following reasons:

1. The pressurized cycles of MIST can represent the action of traffic under moist conditions, which was suspected to be the reason for the loss of material in the wheel paths.
2. It is able to characterize moisture susceptible mixes in a better way than the AASHTO T 283 method (Chen and Huang 2008; Mallick et al. 2005).
3. The MIST is:
    i. Easy to operate, simple in process and less time consuming.
    ii. Able to accomodate any standard size of HMA sample.

The working principle of MIST is to apply pressurized cycles by means of a bladder which inflates and deflates, upon a HMA sample which is submerged in water inside a chamber. The number of cycles, temperature of the water and pressure and can be controlled. ASTM D7870 recommends the use of 3500 Cycles at 60^0C and 276 kPa for moisture conditioning of asphalt mixes. Table 3.1 gives the details of study parameters and inferences that have been obtained by researchers who have worked with the MIST, and Table 3.2 shows the various MIST protocols that have been used in the earlier studies.

T**able 3.1. Summary of studies conducted with the MIST**

Study Parameters	Moisture Susceptibility tests	Inferences
Poor performing aggregate mix that was not identified by regular moisture susceptibility test – AASHTO T 283; Effect of Lime (Mallick et al. 2005)	MMLS3, MIST and AASHTO T283 with multiple F/T cycles *Mechanical Tests:* Indirect Tensile Strength (ITS)	1. MIST and MMLS3 were able to identify the poor performing aggregate mix whereas regular AASHTO T 283 test was not able to differentiate. 2. Adding lime increased the retained tensile strength of poor performing aggregate mix by 5% under MIST conditioning.
Effect of Coarse aggregate angularity, Amine based anti-strip additives, and effectiveness of performance tests-Superpave SPT and IDT (Chen and Huang 2008)	F-T, MIST *Mechanical Tests:* Simple Performance Test (SPT)-Dynamic Modulus and Creep, Superpave Indirect Tensile Test (IDT)-Resilient Modulus and strength	(i) MIST or F-T conditioning showed almost similar results. (ii) An increase in in MIST or F-T conditioning cycles increases the moisture damage in HMA mixtures. (iii) Use of amine-based antistrip additives showed better resistance whereas increase in CAA levels did not show significant effect, against moisture damage. (iv) SPT and the Superpave IDT tests combined with MIST or F-T were effective in characterizing lab-measured moisture susceptible HMA mixtures.

Table 3.1. Summary of studies conducted with the MIST (Contd..)

Study Parameters	Moisture Susceptibility tests	Inferences
Plant produced foamed WMA with high percentages of RAP, HMA; effectiveness of performance tests- Superpave SPT and IDT (Shu et al. 2012)	AASHTO T283, MIST, Asphalt Pavement Analyzer (APA) Hamburg wheel tracking test, *Mechanical Tests:* ITS , Superpave SPT and IDT	1. MIST and AASHTO T283 F–T conditioning showed different effects on the properties of the HMA mixtures due to the difference in moisture induced mechanisms. Higher damage to IDT strength was noticed with F-T whereas MIST causes more damage to resilient modulus and dissipated creep strain energy limit (DCSEf). 2. HMA and WMA mixes showed an equivalent moisture damage resistance while incorporation of RAP increased the resistance to moisture damage in both mixes. 3. Superpave SPT and IDT tests were found effective in characterizing moisture susceptible asphalt mixtures and also the results of the three performance tests were consistent to characterize HMA and WMA mixtures against moisture damage.
Alternate moisture conditioning method- MIST (Bernier 2012)	MIST, AASHTO T 283; *Mechanical Tests:* ITS	-The tensile strength results were found similar for HMA mixes with MIST and AASHTO T 283 whereas they are different for WMA mixes.
Use of MIST to evaluate stripping potential of HMA (Pinkham et al. 2012)	MIST; *Mechanical Tests:* ITS, MR	-The net changes in the values of M_R and ITS before and after MIST confirms the changes due to stripping or moisture damage that was simulated by MIST conditioning.

Table 3.1. Summary of studies conducted with the MIST (Contd..)

Study Parameters	Moisture Susceptibility tests	Inferences
Ranking HMA moisture sensitivity tests (Schram and Williams 2012)	MIST, HWTD, AASHTO T 283, DM, FN	-The overall test rankings found better for MIST test parameters – Swell and TSR than AASHTO T 283. -Also, the authors suggested considering MIST and Hamburg for further evaluation on the basis of testing time and simplicity.
To simulate observed field moisture damage in the laboratory (Pinkham et al. 2013)	MIST; Resilient Modulus, ITS	-MIST conditioning simulated the moisture damage which was evident from significant change in resilient modulus, BSG, and also through visual investigation
New moisture susceptibility evaluation method (Azari and Mohseni 2013)	MIST, Vacuum Saturation; Incremental Repeated Load Permanent Deformation Test (iRLPD)	-MIST conditioning caused significant damage, though, including vacuum saturation before MIST, still severe the damage to the specimens.

Table 3.1. Summary of studies conducted with the MIST (Contd..)

Study Parameters	Moisture Susceptibility tests	Inferences
Moisture susceptibility of cement emulsified asphalt mortar (CEAM) with different asphalt contents (Rutherford et al. 2014)	MIST; ITS	-MIST Conditioning reduced the strength of CEAM up to 20% -Increase of asphalt content decreased the tensile strength ratio making CEAM more susceptible to moisture induced damage
Sensitivity of MIST to moisture induced damage, effectiveness of Dynamic Modulus (DM) with MIST (Tarefder et al. 2014)	MIST, AASHTO T 283; DM, ITS	-A decrease in DM was observed due to MIST conditioning indicating the sensitivity of MIST to moisture induced damage -The results of dynamic modulus ratio (DMR) are close to tensile strength ratio (TSR) obtained from AASHTO T283 indicating the effectiveness of DM with MIST in characterizing moisture susceptible asphalt mixes - Increase in moisture damage was found with increase in number of cycles
MIST parameters and moisture damage, Models to predict loss in E* from moisture susceptibility test to use with ME design (Weldegiorgis and Tarefder 2014)	MIST, AASHTO T 283; DM, ITS	-Moisture damage caused by MIST is a function of its parameters – number of cycles, temperature and pressure -Rupture of binder film due to pore pressure cycles and subsequent adhesion failure between aggregate and binder film was identified as one of the mechanisms of MIST conditioning. It was recognized from the visual inspection of conditioned samples. -Two models (MIST-cycles & MIST-pressure) were developed to predict loss in E* due to moisture conditioning which could be helpful in ME pavement design

Table 3.1. Summary of studies conducted with the MIST (Contd..)

Study Parameters	Moisture Susceptibility tests	Inferences
To evaluate MIST as a means of accelerated moisture susceptibility test (Zofka et al. 2014)	MIST, AASHTO T 283; ITS	-MIST and AASHTO T 283 showed similar results for HMA and WMA foamed mixes.
Effect of pore pressure cycles on HMA using MIST and DM (Tarefder et al. 2014)	MIST, AASHTO T283;ITS, DM	- The MIST conditioning along with dynamic modulus test was sensitive to characterize moisture susceptible mixes. The MIST results at 3500 cycles were close to the AASHTO T283 test results.
Evaluate laboratory test methods suitable for identifying PFC mixture susceptible to raveling and loss of drainability (Edith et al. 2015)	MIST, Hamburg; Cantabro LA abrasion, ITS	-Results of ITS and Cantabro LA abrasion confirms the damage created by MIST

Table 3.1. Summary of studies conducted with the MIST (Contd..)

Study Parameters	Moisture Susceptibility tests	Inferences
Moisture conditioning effects on chemical and mechanical properties of HMA (Ahmad et al. 2016)	MIST, AASHTO T283;ITS, Beam Fatigue test	-The changes in the chemical properties of the binder were observed with both MIST and AASHTO T 283 conditioning and the changes are different for various cycles of conditioning
Investigation of good and poor mixes, in terms of moisture susceptibility, using MIST (Mallick et al. 2016)	MIST; ITS, Es	-The change in seismic modulus due to MIST was significant for poor mixes whereas it is insignificant for bad mixes
MIST Conditioning protocol research – Bath and Cyclic conditioning phase, and respective durations (Varveri et al. 2016)	MIST, ITS	-For the similar MIST conditioning (Short term) cycles, the increase in bath conditioning (Long term) time increased the moisture damage and vice versa - The effect of long term bath conditioning such as diffusion etc. was significant for the mixtures containing softer binder than a harder binder whereas it is converse for short term conditioning.

Table 3.1. Summary of studies conducted with the MIST (Contd..)

Study Parameters	Moisture Susceptibility tests	Inferences
WMA Moisture Susceptibility, Alternative Moisture conditioning protocol other than modified lottman protocol, Specimen drying methods (Yin et al. 2016)	MIST, Modified Lottman, Hot Water Bath Mechanical/Performance tests: IDT, M_R, APA	-A moisture damage equivalent to modified lottman protocol was found with 1000 cycles MIST at 40psi pressure and 60^0C temperature and 3-day hot water bath at 60^0C - A higher M_R and IDT values were found with specimen drying methods of SSD and Core dry than air dry and oven dry methods. So, it was recommended to use CoreDry, 48 hour air dry at 60^0C, or the 24-hr over dry at 60^0C as specimen drying methods after moisture conditioning and before testing for mechanical properties.

Table 3.2. Various MIST Protocols used in the Literature

Adhesion Phase		Cycle Phase			Dwell Phase		Reference
Temp. (^{0}C)	**Period (hr)**	**Cycles (No.)**	**Temp. (^{0}C)**	**Pressure (psi)**	**Temp. (^{0}C)**	**Period (hr)**	
-	-	5000	60	30	-	-	Mallick et al. (2005)
-	-	500, 1000	40	40	-	-	Chen and Huang (2008)
-	-	1000	40	40	-	-	Shu et al. (2012)
-	-	3500	60	40	-	-	Bernier (2012)
-	-	2000	60	30			Pinkham et al. (2012)
-	-	3000	60	40			Schram and Williams (2012)
W and W/O Vacuum@25mm for 30 min.		N/A	40	40,60	-	-	Azari and Mohseni (2013)
-	-	5000	60	40	-	-	Pinkham et al. (2013)
-	-	500	60	40	-	-	Rutherford et al. (2014)
-	-	3500, 7000	60	40	-	-	Tarefder et al. (2014)
-	-	3500, 7000, 10500	40,50, 60	40,55, 70	-	-	Weldegiorgis and Tarefder (2014)
-	-	3500	60	40	-	-	Zofka et al. (2014)
-	-	1000	60	40	-	-	Edith et al. (2015)
-	-	3500	60	70	-	-	Nicholls et al. (2015)
-	-	3500	60	40	25	2	Tarefder and Ahmad (2015)
-	-	3500	60	40	25	2	Ahmad et al. (2016)
-	-	15000	25	20			Mallick et al. (2016)
-	-	4000	60	70	20	2	Varveri et al. (2016)
-	-	1000,2000	60	40	-	-	Yin et al. (2016)

The intensity of moisture induced damage in the MIST has been reported to be a function of the number of cycles and the duration of pre MIST soaking of sample in water or dwell. Tarefder et al. (2014) found significant damage when doubling the cycles from 3,500 to 7,000. Varveri et al. (2016) reported a greater reduction of strength of the mix with longer pre MIST dwell period.

In this study, the various MIST conditioning process involved the use of 15,000 cycles at 138 kPa and 25^0C, 10,000 and 5,000 cycles at 207 kPa and 60^0C with a pre MIST dwell of 20 hours at 60^0C (for different phases), on specimens with 7±1% air voids. The dwell period was used to allow the water to diffuse into the asphalt-aggregate interface and the cycles of pulses were added to allow the development of the potential of the advective transfer of mastic under pressure.

3.2 Pre and post-conditioning tests: Dynamic Modulus in Indirect Tensile (IT) mode

The dynamic modulus (|E*|) test in the indirect tensile mode (Kim et al. 2004) was selected. This method was selected over the conventional compressive mode because of its relevancy for fatigue cracking models that utilize tensile strain, and the ability to use thin samples, which allows conditioning of three samples in the MIST simultaneously. The dynamic modulus is estimated using the following equation:

$$|E^*(\omega)| = -\frac{2|P^*|}{\pi a d}\frac{\beta_1\gamma_2 - \beta_2\gamma_1}{\gamma_2|V^*| - \beta_2|U^*|} \quad (3.1)$$

Where,

$|P^*|$ = applied load amplitude (N);

a = loading strip width (m);

d = thickness of specimen (m);

$|V^*|$ = average vertical displacement magnitude (m);

$|U^*|$ = average horizontal displacement magnitude (m); and

β_1, β_2, γ_1, γ_2 = geometric coefficients for different gauge lengths

3.3 Pre and post conditioning tests: Seismic Modulus (E_s) with the Ultrasonic Pulse Velocity (UPV) Test

The seismic modulus (E_s) test was selected because of the following reasons: 1. It is a fast and nondestructive test; 2. It has been extensively evaluated, found to be sensitive to key properties and moisture susceptibility of HMA (Nazarian et al. 2002; Birgisson et al. 2003; Maser and

Mallick 2006); 3. Guidelines are available for this test for quality control of HMA (Ultrasonic Pulse Velocity Device: User's manual, 2006). A commercially available Ultrasonic Pulse Velocity equipment (V-Meter, ASTM C 597-09) was utilized. The method works on the basic principle that the velocity of a pulse of a compressional wave through a medium depends on the elastic properties and density of the medium. The P waves (longitudinal compression) transmitted through the thickness of the sample are detected by sensors, and the time for travel (t_v) is displayed, which is used with the bulk density of the sample (ρ) to calculate the bulk constrained modulus and then the seismic modulus (E_s), which can be converted to design modulus (E_d) (Equation 3.2 to 3.5).

$$V_p = \frac{H}{t_v} \text{ ---------- (3.2)}$$

$$M_V = \rho \times {V_p}^2 \text{ ---------- (3.3)}$$

$$E_s = M_V \times \frac{(1+\mu)\times(1-2\mu)}{1-\mu} \text{ ---------- (3.4)}$$

$$E_d = \frac{E_s}{3.2} \times Temperature\ Correction\ Factor \text{ -- (3.5)}$$

Temperature correction factor = 0.95 (for a test temperature of 21^0C (70^0F))

Where,

V_p = velocity of wave; t_v = time of travel; ρ = density; μ = Poisson's ratio

A number of studies have been conducted with the use of nondestructive tests (NDT) on HMA. Stephenson (1968) used compression wave velocity technique to study the transitional temperatures where the dynamic properties of HMA undergo a significant change. Celaya and Nazarian (2008) and Rojas et al. (1999) have developed quality control guidelines for the construction of HMA layers with the use of NDT. Rojas et al. (1999) evaluated HMA mixes in the laboratory using ultrasonic pulse velocity (UPV) test and concluded that the seismic modulus increases with a decrease in the voids in the total mix (VTM) and decreases with a decrease in the binder viscosity; however, the impact of the viscosity was found to become less pronounced as the VTM increased. Norambuena-Contreras et al. (2010) have examined two types of mixes - dense and porous using ultrasonic direct test to determine dynamic modulus. The authors identified the difference in transmission time between two types of mixes due to the difference in porosity, which resulted in longer propagation times for the porous mix. Birgisson et al. (2003) evaluated the ultrasonic pulse wave velocity test for monitoring moisture damage effects in asphalt mixtures and studied the effects of saturation levels, aggregate structure and aggregate type on mixture

conditioning. The results demonstrated the sensitivity of seismic modulus to effects of moisture damage and a decrease in low-strain modulus with an increase in level of saturation. A visual investigation of failed specimens indicated cohesive and adhesive failures, and breakage of aggregate failures for conditioned dense graded, granite and unconditioned limestone aggregate mixes respectively. Arabani et al. (2009) evaluated the effect of various HMA mix parameters with the UPV, which was found to be sensitive to changes in the asphalt content, filler content, percent of fractured particles, gradation type and compaction method of the HMA. For a specific gradation, increasing the filler content was found to result in an increase in the low-strain modulus values.

A lowering of E_s, due to moisture effect, can happen in two ways – 1. Due to the effect of pore pressure because of presence of water in the pores, and 2. Due to the loss of integrity of the mix, as a result of loss in cohesion or adhesion or breakdown of material. E_s has been found to be sensitive to moisture effects (Birgisson et al. 2003; Nazarian et al. 2006). Note that the pore water effect will be more significant and long lasting where a relatively greater amount of water is absorbed by aggregates, and/or where the pore sizes are small and facilitate capillary action, which helps in retaining water (fine graded mix). In mixes with higher voids or low absorption aggregates, the effect of pore water pressure may get reduced quickly after the moisture conditioning process (Birgisson et al. 2003) and hence a relatively quick test is more appropriate for the detection of pore water effects in such a case. The estimated E_s values can be transformed to design modulus (E_d) to estimate the loss in structural capacity or life as a result of moisture damage, with the help of available data/relationships (Aouad et al. 1993; Nazarian et al. 2006) or with newly developed data. Good agreements between moduli measured by seismic methods and laboratory and field methods have been reported (Saeed and Hall 2002).

3.4 Pre and post-conditioning tests: Indirect Tensile Strength (ITS) test

The Indirect Tensile Strength (ITS) test was selected as it has been widely used by the pavement community as a test to evaluate loss of cohesion and adhesion in HMA mixes, specifically with respect to moisture damage. However, note that while the ITS is traditionally utilized in conjunction with a typical moisture conditioning process, such as freeze-thaw and/or conditioning in water at an elevated temperature, in this study samples were tested dry, and after the MIST conditioning process.

References

Ahmad, M., Mannan, U. A., Islam, M. R., and Tarefder, R. A. (2016). "Effects of Moisture Conditioning on Chemical and Mechanical Properties of Asphalt Concrete." *Transportation Research Board 95th Annual Meeting*.

Aouad, M. F., Stokoe, I., Kenneth, H., and Briggs, R. C. (1993). "Stiffness of asphalt concrete surface layer from stress wave measurements." *Transportation Research Record*(1384).

Arabani, M., Kheiry, P. T., and Ferdosi, B. (2009). "Laboratory Evaluation of the Effect of HMA Mixt Parameters on Ultrasonic Pulse Wave Velocities." *Road Materials and Pavement Design*, 10(1), 223-232.

Azari, H., and Mohseni, A. (2013). "Improvement of the Test Method for Determining Moisture Damage Resistance." *Multi-Scale Modeling and Characterization of Infrastructure Materials*, Springer, 109-125.

Bernier, A. K. (2012). "Laboratory and Field Evaluation of Two Warm-Mix Additives in Connecticut and Validation of an Alternative Moisture Susceptibility Test."

Birgisson, B., Roque, R., and Page, G. (2003). "Ultrasonic pulse wave velocity test for monitoring changes in hot-mix asphalt mixture integrity from exposure to moisture." *Transportation Research Record: Journal of the Transportation Research Board*(1832), 173-181.

Buchanan, M. S., Moore, V., Mallick, R., O'Brien, S., and Regimand, A. (2004). "Accelerated moisture susceptibility testing of hot mix asphalt (HMA) mixes." *83rd Transportation research board annual meeting*.

Celaya, M., and Nazarian, S. (2008). "Implementation of quality management of hot-mix asphalt with seismic methods." *Transportation Research Record: Journal of the Transportation Research Board*(2057), 99-106.

Chen, X., and Huang, B. (2008). "Evaluation of moisture damage in hot mix asphalt using simple performance and superpave indirect tensile tests." *Construction and Building Materials*, 22(9), 1950-1962.

Edith, A., Estakhri, C. K., and Scullion, T. (2015). "Evaluation of Laboratory Test Methods to Address Performance Issues of Porous Friction Courses." *Transportation Research Board 94th Annual Meeting*Washington D.C.

Kim, Y., Seo, Y., King, M., and Momen, M. (2004). "Dynamic modulus testing of asphalt concrete in indirect tension mode." *Transportation Research Record: Journal of the Transportation Research Board*(1891), 163-173.

Mallick, R. B., Pelland, R., and Hugo, F. (2005). "Use of accelerated loading equipment for determination of long term moisture susceptibility of hot mix asphalt." *International Journal of Pavement Engineering*, 6(2), 125-136.

Mallick, R. B., Tao, M., Worsman, R., Daniel, J. S., and McCarthy, L. M. (2016). "Risk-Based Quantification of Loss of Pavement Life of Hot-Mix Asphalt Pavements due to Use of Moisture-Susceptible Mixes." *Transportation Research Board 95th Annual Meeting*.

Maser, K., and Mallick, R. B. (2006). "Use of Nondestructive Testing for Detection of Damaged Subsurface Layers in Asphalt Pavements." *NDE Conference on Civil Engineering, St. Louis MO.* , 87-97.

Nazarian, S., Yuan, D., Tandon, V., and Arellano, M. (2002). "Quality management of flexible pavement layers with seismic methods." The Center for Transportation Infrastructure Systems, The University of Texas at El Paso., p 34.

Nicholls, C., Wayman, M., Mollenhauer, K., McNally, C., Tabakovic, A., Varveri, A., Cassidy, S., Shahmohammadi, R., and Taylor, R. (2015). "Effect of using of reclaimed asphalt and/or lower temperature asphalt on the availability of the road network." *6th International Conference Bituminous Mixtures and Pavements*Thessaloniki, Greece.

Norambuena-Contreras, J., Castro-Fresno, D., Vega-Zamanillo, A., Celaya, M., and Lombillo-Vozmediano, I. (2010). "Dynamic modulus of asphalt mixture by ultrasonic direct test." *Ndt & E International*, 43(7), 629-634.

Pinkham, R., Cote, S. A., Mallick, R. B., and Tao, M. (2012). "Use of MIST to evaluate stripping potential of HMA - Maine DOT."

Pinkham, R., Cote, S. A., Mallick, R. B., Tao, M., Bradbury, R. L., and Regimand, A. (2013). "Use of Moisture Induced Stress Testing to Evaluate Stripping Potential of Hot Mix Asphalt (HMA)." *Transportation Research Board 92nd Annual Meeting*.

Rojas, J., Nazarian, S., Tandon, V., and Yuan, D. (1999). *Quality management of asphalt-concrete layers using wave propagation techniques*, University of Texas at El Paso.

Rutherford, T., Wang, Z., Shu, X., Huang, B., and Clarke, D. (2014). "Laboratory investigation into mechanical properties of cement emulsified asphalt mortar." *Construction and Building Materials*, 65, 76-83.

Saeed, A., and Hall, J. W. (2002). "Comparison of non-destructive testing devices to determine in situ properties of asphalt concrete pavement layers." *Pavement Evaluation Conference, Roanoke, Virginia, USA*.

Schram, S., and Williams, R. C. (2012). "Ranking of HMA Moisture Sensitivity Tests in Iowa." *Transportation Research Board, National Research Council, Washington, DC*.

Shu, X., Huang, B., Shrum, E. D., and Jia, X. (2012). "Laboratory evaluation of moisture susceptibility of foamed warm mix asphalt containing high percentages of RAP." *Construction and Building Materials*, 35, 125-130.

Stephenson, R. W. (1968). "Temperature effects of the compressional wave velocities of asphalt-aggregate mixtures." Doctoral, Oklahoma State University.

Tarefder, R., and Ahmad, M. (2015). "Pore Structure Evaluation of Asphalt Concrete and Its Influence on Permeability and Moisture Damage." *Transportation Research Board 94th Annual Meeting*.

Tarefder, R. A., Weldegiorgis, M. T., and Ahmad, M. (2014). "Assessment of the Effect of Pore Pressure Cycles on Moisture Sensitivity of Hot Mix Asphalt Using MIST Conditioning and Dynamic Modulus." *Journal of Testing and Evaluation*, 42(6), 1-11.

Varveri, A., Avgerinopoulos, S., and Scarpas, A. (2016). "Experimental evaluation of long-and short-term moisture damage characteristics of asphalt mixtures." *Road Materials and Pavement Design*, 17(1), 168-186.

Weldegiorgis, M. T., and Tarefder, R. A. (2014). "Towards a mechanistic understanding of moisture damage in asphalt concrete." *Journal of Materials in Civil Engineering*, 27(3), 04014128.

Yin, F., Martin, A. E., and Arámbula-Mercado, E. (2016). "Warm-Mix Asphalt Moisture Susceptibility Evaluation for Mix Design and Quality Assurance." *Transportation Research Record: Journal of the Transportation Research Board*, 2575, 39-47.

Zofka, A., Maliszewski, M., and Bernier, A. (2014). "Alternative moisture sensitivity test." *Environmental Engineering. Proceedings of the International Conference on*

Environmental Engineering. ICEE, Vilnius Gediminas Technical University, Department of Construction Economics & Property, 1.

Chapter 4. Preliminary Study

The preliminary study is presented in four different parts as follows:

Part 1 includes the study that was conducted to identify the moisture susceptible mixes among the most commonly used Maine DOT mixes using MIST conditioning.

Part 2 includes the study that was conducted to finalize the nondestructive mechanical test that can be combined with MIST conditioning to determine the moisture induced damage.

Part 3 includes the study that was conducted on an identified moisture susceptible mix with an accelerated loading equipment – Model Mobile Load Simulator (MMLS3).

Part 4 includes the study that was conducted to finalize a methodology to identify and analyze the loss of material.

4.1 Part 1: Study of Twenty Six HMA mixes from MDOT

4.1.1 Objectives

The objective of this phase of the study was to investigate the potential of MIST conditioning method in identifying the two known poor performing mixes, in terms of moisture susceptibility, that was not recognized by regular test methods.

4.1.2 Materials

Twenty six loose plant-produced Maine DOT mixes, with two known poor performers (PI & HOU mixes) based on field performance, were considered for the study. Table 4.1.1 and 4.1.2 shows the gradation and mix design information of the selected mixes.

Table 4.1.1. Stockpile Gradation (Percentage passing sieve sizes) – Loose Plant mixes

S. No.	Mix ID	Sieve Size, mm									
		25	**12.5**	**9.5**	**4.75**	**2.36**	**1.18**	**0.6**	**0.3**	**0.15**	**0.075**
1	AUG	100	100	95-100	64-78	47-55	33-41	21-27	11-15	5-9	2.5-6.5
2	DUR	100	100	95-100	60-73	46-54	36-44	23-29	11-15	5-9	2.6-6.6
3	PARK	100	90-100	80-90	61-75	53-58	41-49	24-30	11-15	6-10	4.0-6.0
4	L-S	100	95-100	63-77	44-52	29-37	19-25	19-25	10-14	5-9	2.0-6.0
5	AUB	100	100	95-100	62-76	46-54	35-43	23-29	12-16	5-9	2.0-6.0
6	RUM	100	100	95-100	62-76	45-53	32-40	21-27	12-16	6-10	2.8-6.8
7	PI	100	100	95-100	65-79	43-51	24-32	15-21	10-14	6-10	3.9-7.0
8	HOU	100	100	95-100	63-77	45-53	30-38	17-23	9-13	5-9	4.0-7.0
9	P30	100	100	95-100	60-73	46-54	36-44	23-29	11-15	5-9	2.6-6.6
10	P47	100	100	95-100	60-73	46-54	36-44	23-29	11-15	5-9	2.6-6.6
11	D49	100	100	95-100	60-73	46-54	36-44	23-29	11-15	5-9	2.6-6.6
12	P48	100	93-100	79-90	50-64	40-48	32-40	20-26	10-14	5-9	2.5-6.0
13	P49	100	93-100	79-90	50-64	40-48	32-40	20-26	10-14	5-9	2.5-6.0
14	CP	100	100	95-100	64-78	47-55	33-41	21-27	11-15	5-9	2.5-6.5
15	LS68	100	100	95-100	63-77	44-52	29-37	19-25	10-14	5-9	2.0-6.0
16	GT30	100	100	95-100	62-76	46-54	35-43	23-29	12-16	5-9	2.0-6.0
17	LS66	100	100	95-100	63-77	44-52	29-37	19-25	10-14	5-9	2.0-6.0
18	M	100	100	95-100	61-75	46-54	31-39	18-24	11-15	6-10	3.8-7.0
19	NC74	100	92-100	77-90	48-62	35-43	22-30	13-19	8-12	5-9	3.0-6.0
20	SN61	100	91-100	78-90	53-67	40-48	28-36	18-24	9-13	5-9	2.5-6.0
21	FW34	100	100	95-100	65-79	45-53	29-37	18-24	11-15	6-10	3.0-7.0
22	SH	100	100	95-100	65-79	43-51	24-32	15-21	10-14	6-10	3.9-7.0
23	NCP55	100	92-100	79-90	46-60	35-43	25-33	16-22	10-14	5-9	2.0-6.0
24	NC30	--Not Available--									
25	NCP16	--Not Available--									
26	NCP93	--Not Available--									

Table 4.1.2. Mix Design Information – Loose Plant Mixes

S. No.	Mix ID	ESAL'S	Ndesign	NMAS	Optimum AC, %	Binder Grade	Material and respective Proportions
1	AUG	3<10	50	9.5mm (FG)	6.4	PG 64-28	9.5mm (25%), WSS (22%), Washed Manufactured Sand (11%), Wahsed Sand (22%), RAP (20%)
2	DUR	3<10	50	9.5mm (FG)	6.3	PG 64-28	9.5mm (33%), DSS (14%), Sand (33%), Fine RAP (8%), 3/8 RAP (12%)
3	PARK	0.3<3	75	12.5mm (FG)	5.7	PG 58-28	12.5mm (12%), 9.5mm (10%), Sand (49%), Blend Sand (14%), RAP (15%)
4	L-S	0.3<3	75	9.5mm (FG)	6.2	PG 64-28	9.5mm (30%), Sand (25%), Washed Stone Dust (25%), RAP (20%)
5	AUB	3<10	50	9.5mm (FG)	6.6	PG 64-28	9.5mm (40%), Dust (16%), Sand (44%)
6	RUM	3<10	75	9.5mm (FG)	6.1	PG 64-28	9.5mm (33%), Sand (16%), WSS (17%), DSS (14%), RAP (20%)
7	PI	3<10	50	9.5mm (FG)	6.6	PG 58-28	Washed Ledge Sand (29%), 12.5mm (13%), Crusher Sand (38%), Sand (10%), RAP (10%)
8	HOU	0.3<3	50	9.5mm (FG)	6.5	PG 58-28	12.5mm (35%), Ledge Sand (35%), Washed Sand (30%)
9	P30	3<10	50	9.5mm (FG)	6.3	PG 64-28	9.5mm (33%), DSD (14%), Sand (33%), Fine RAP (8%), 3/8 RAP (12%)
10	P47	3<10	50	12.5mm (FG)	5.3	PG 64-28	9.5mm (33%), DSD (14%), Sand (33%), Fine RAP (8%), 3/8 RAP (12%)
11	D49	3<10	50	9.5mm (FG)	6.3	PG 64-28	9.5mm (33%), DSD (14%), Sand (33%), Fine RAP (8%), 3/8 RAP (12%)
12	P48	3<10	75	12.5mm (FG)	5.3	PG 64-28	12.5mm (21%), 9.5mm (22%), DSD (11%), Sand (26%), Fine RAP (15%), 1/2RAP (5%)
13	P49	3<10	75	12.5mm (FG)	5.3	PG 64-28	12.5mm (21%), 9.5mm (22%), DSD (11%), Sand (26%), Fine RAP(15%), 1/2RAP(5%)

Table 4.1.2. Mix Design Information – Loose Plant Mixes (Contd….)

S. No.	Mix ID	ESAL'S	Ndesign	NMAS	Optimum AC, %	Binder Grade	Material and respective Proportions
14	CP	3<10	75	9.5mm (FG)	6.2	PG64E-28(70)	9.5mm (25%), WSS (22%), Washed Manufactured Sand (11%), Wahsed Sand (22%), RAP (20%)
15	LS68	0.3<3	75	9.5mm (FG)	6.2	PG 64-28	9.5mm (30%), Sand (25%), WSD (25%), RAP (20%)
16	GT30	3<10	50	9.5mm (FG)	6.6	PG 64-28	9.5mm (40%), Dust (16%), Sand (44%)
17	LS66	0.3<3	75	9.5mm (FG)	6.2	PG 64-28	9.5mm (30%), Sand (25%), WSD (25%), RAP (20%)
18	M	3<10	50	9.5mm (FG)	6.0	PG 64-28	9.5mm (23%), Sand (32%), Crushed Sand (15%), Washed Ledge Sand (10%), RAP (20%)
19	NC74	3<10	75	12.5mm (FG)	5.5	PG64E-28(70)	12.5mm (17%), 9.5 MINUS (15%), 9.5mm (15%), Sand (20%), Washed Ledge Sand (13%), RAP (20%)
20	SN61	3<10	50	12.5mm (FG)	5.8	PG 64-28	12.5mm (25%), 9.5mm (10%), WSS (18%), Washed Manufactured Sand (9%), Washed Sand (18%), RAP (20%)
21	FW34	0.3<3	50	9.5mm (FG)	6.5	PG 64-28	9.5mm (24%), WSS (39%), Sand (17%), RAP (20%)
22	SH	3<10	50	9.5mm (FG)	6.6	PG 64-28	Washed Ledge Sand (29%), 12.5mm (13%), Crusher Sand (38%), Sand (10%), RAP (10%)
23	NCP55	3<10	75	12.5mm (FG)	5.2	PG 64-28	12.5mm (22%), 9.5mm (25%), Crushed Sand(12%), Sand(21%), RAP(20%)
24	NC30	--Not Available--					
25	NCP16	--Not Available--					
26	NCP93	--Not Available--					

4.1.3 Methods

4.1.3.1 Moisture Conditioning

A MIST conditioning protocol of 10,000 Cycles at 25^0C temperature and 207 kPa (30psi) pressure was used for this study.

4.1.3.2 Modulus

Dynamic modulus in IT mode and Seismic modulus were determined using the methods as described in Chapters 3.2 and 3.3, respectively.

4.1.3.3 Strength

Indirect tensile strength was determined using the method described in Chapter 3.4.

4.1.4 Test Plan

Figure 4.1.1 shows the test plan for this part of the study.

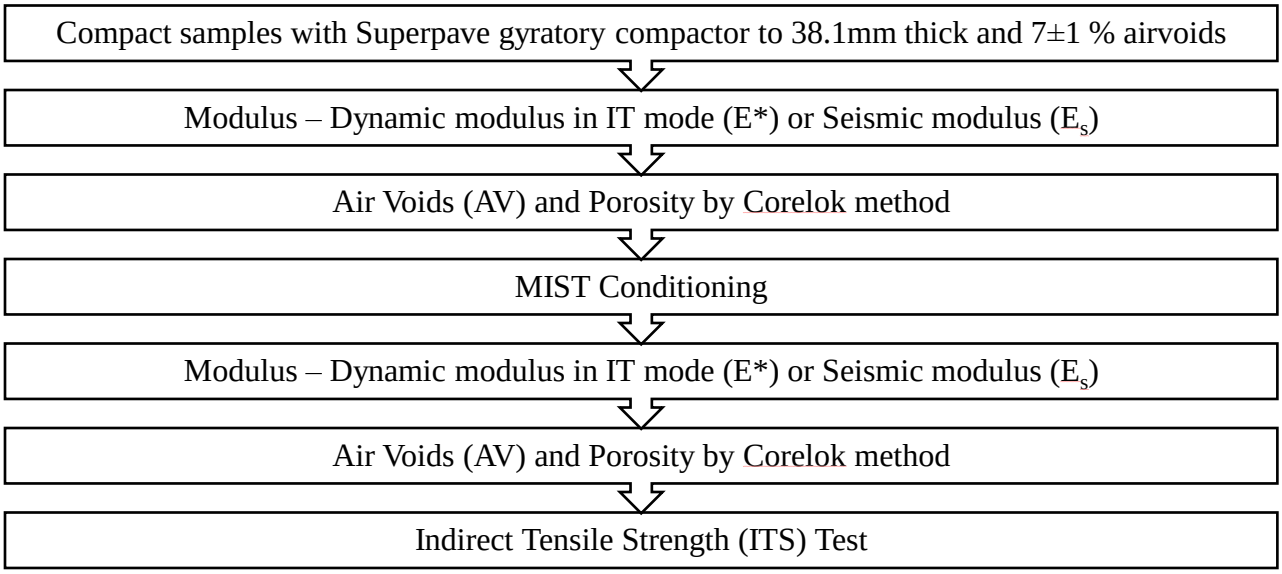

Figure 4.1.1 Test Plan – Preliminary study: Part 1

Note: Porosity was determined using GravitySuite™ software which uses the following equation: $\% \text{ Porosity} = \left(\frac{\rho_2 - \rho_1}{\rho_2}\right) \times 100$

Where, ρ_2 = the CoreLok vacuum sealed density of compacted sample

ρ_2 = Density of the vacuum sealed sample after opening under water

4.1.5 Results and Discussion

Table 4.1.3 and 4.1.4 show the results of volumetric and mechanical tests.

Table 4.1.3. Test results – Loose plant mixes - Dynamic modulus in IT mode (E*)

S. No.	Mix ID	Before MIST Conditioning				After MIST Conditioning				
		Air Voids (%)	Porosity (%)	E*@ 10Hz (Mpa)	E*@ 1Hz (Mpa)	Air Voids (%)	Porosity (%)	E*@ 10Hz (Mpa)	E*@ 1Hz (Mpa)	ITS (kPa)
1	AUG	7.1	5.8	2731	964	6.5	6.0	2736	921	562
2	DUR	5.5	4.1	3552	1444	4.9	3.6	4270	1543	665
3	PARK	7.0	5.3	4340	1653	6.5	5.1	3640	1400	609
4	L-S	6.6	5.7	3197	1378	6.2	5.9	3001	1258	678
5	AUB	7.4	4.4	3016	1164	6.8	3.7	3395	1023	619
6	RUM	7.0	5.4	3508	1509	6.2	4.9	3236	1332	624
7	PI	6.2	4.6	3150	979	5.8	5.3	3308	1203	458
8	HOU	6.5	5.1	3964	1640	6.1	5.6	3404	1294	501

Table 4.1.4. Test results – Loose plant mixes - Seismic Modulus (Es)

S. No.	Mix ID	Before MIST Conditioning				After MIST Conditioning				
		Air Voids (%)	Porosity (%)	Es (Mpa)	Ed (Mpa)	Air Voids (%)	Porosity (%)	Es (Mpa)	Ed (Mpa)	ITS (kPa)
9	P30	7.3	5.3	11204	3501	5.8	3.1	11271	3522	676
10	P47	7.2	6.3	13669	4271	6.2	3.8	13881	4338	758
11	D49	7.2	6.7	11463	3582	6.0	3.9	11083	3464	806
12	P48	6.7	5.6	13560	4238	5.7	3.3	13270	4147	824
13	P49	6.8	5.4	13758	4299	5.8	3.2	13669	4272	1034
14	CP	6.4	5.3	12244	3826	5.0	3.6	12602	3938	925
15	LS68	7.3	6.2	11182	3494	5.8	3.3	11486	3590	582
16	GT30	8.3	7.5	9985	3120	7.4	4.5	10130	3165	646
17	LS66	6.5	5.7	12249	3828	5.2	3.2	12374	3867	859
18	M	7.2	6.5	11514	3598	6.3	3.9	11496	3592	625
19	NC74	6.7	5.7	13780	4306	5.6	4.9	14291	4466	754
20	SN61	6.8	6.0	13486	4214	5.7	3.2	13410	4191	881
21	FW34	7.0	5.8	12417	3880	5.8	4.0	12289	3840	674
22	NCP55	6.5	5.4	13816	4317	5.4	3.4	13543	4232	707
23	SH	6.6	5.7	14091	4404	5.4	3.1	14139	4418	627
24	NC30	7.0	6.4	12754	3986	5.9	3.4	12600	3937	654
25	NCP16	6.7	5.7	12221	3819	5.2	3.3	12305	3845	716
26	NCP93	6.7	5.6	12248	3827	5.4	3.4	12615	3942	717

E* - Dynamic Modulus in IT mode; Es – Seismic Modulus; Ed – Design Modulus

4.1.5.1 Volumetric Properties

Air Voids (AV)

All of the mixes showed a decrease in air voids due to moisture conditioning (Figure 4.1.2). This indicates compaction during the pressurized cycles of water in the MIST chamber.

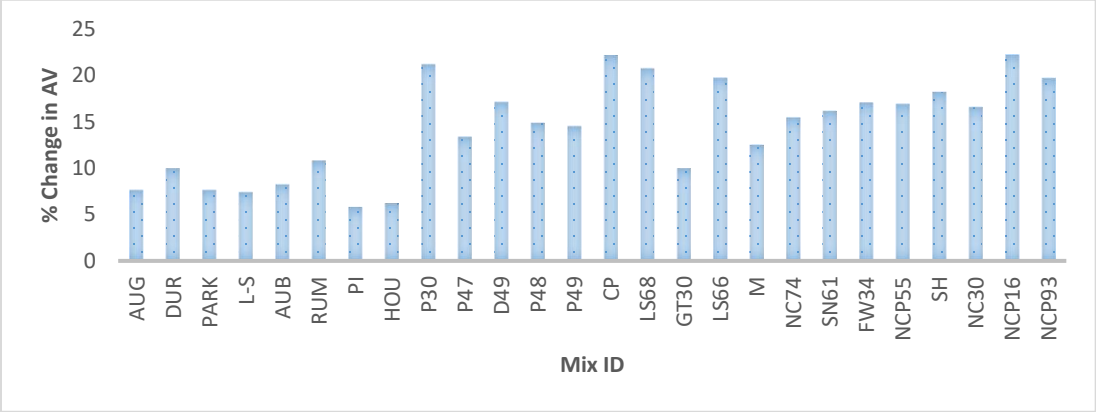

Figure 4.1.2. % change in Air Voids (AV) due to MIST conditioning for various mixes

Note: % Change refers to ((Pre-Post)/Pre)*100

Porosity

A decrease in porosity of mixes due to MIST conditioning was found in most cases except for a few mixes that includes the two poor performers – PI and HOU (Figure 4.1.3). The increase in porosity in poor performers may be due to the breakage of aggregates during moisture conditioning.

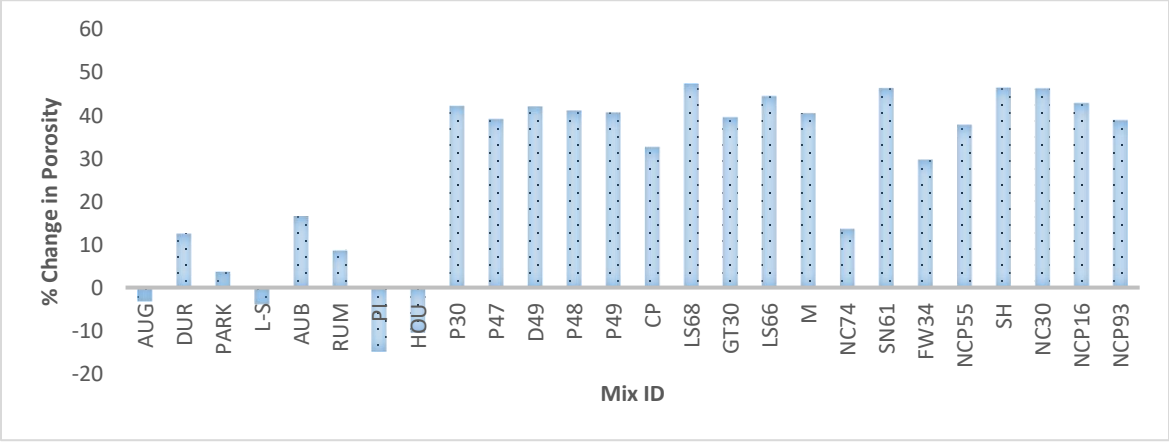

Figure 4.1.3. % change in Porosity due to MIST conditioning for various mixes

4.1.5.2 Modulus

An increase or decrease in modulus was found for the various mixes due to moisture conditioning (Figure 4.4). The two known poor performers showed highest percentage change in modulus at 1Hz frequency (Figure 4.4(b)). A statistical analysis conducted upon the mix modulus (E* and Es) values before and after MIST conditioning showed significant difference in E* for PI mix (at 1Hz) and HOU mix (at 10Hz) (Table 4.1.5).

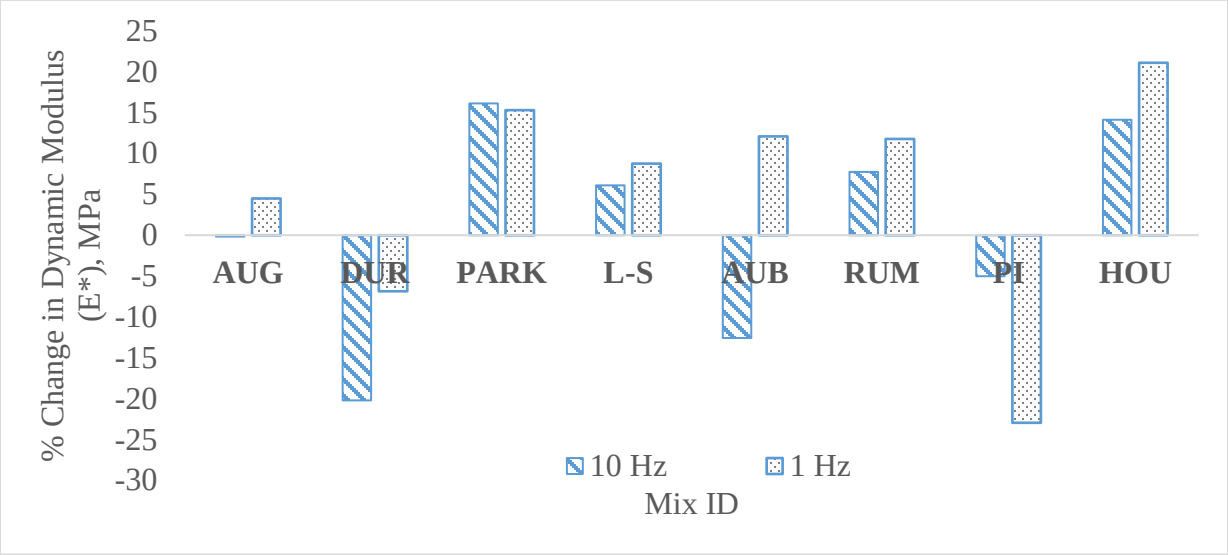

(a) Percentage change in Dynamic Modulus (E*) at 10Hz and 1Hz

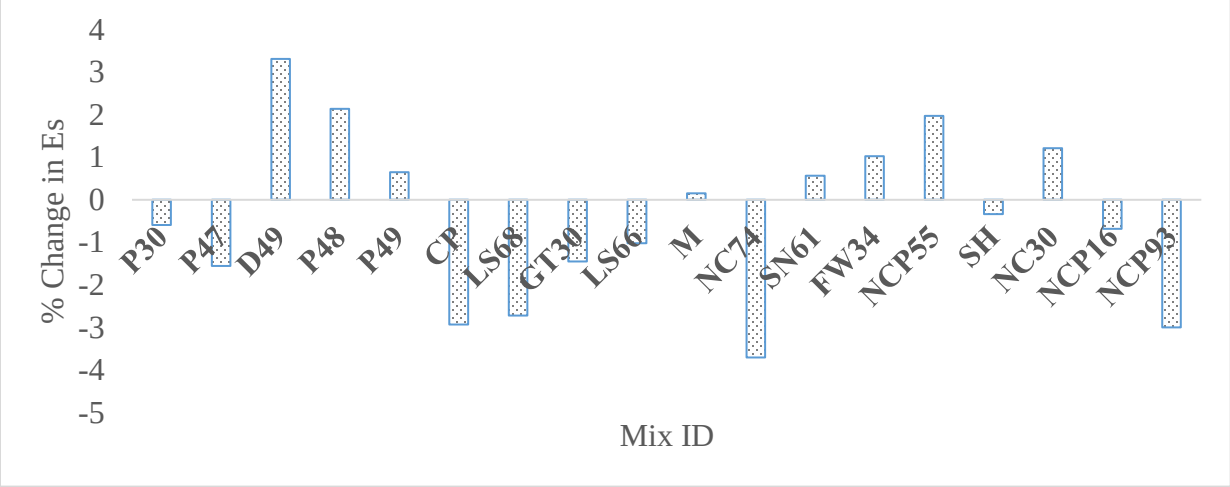

(b) Percentage change in Es

Figure 4.1.4. Percentage change in Modulus due to MIST conditioning for various mixes

Table 4.1.5. Results of Paired t test @ 95% Confidence Level – Change in Modulus (E* and Es) before and after the MIST conditioning

	Mix	Mean	Std. Deviation	Std. Error Mean	t	df	Sig. (2-tailed)
Dynamic Modulus (E*) @ 10Hz	AUG	-5.0	525.8	303.6	-0.016	2	0.988
	DUR	-504.8	445.9	222.9	-2.264	3	0.109
	PARK	700.0	346.6	200.1	3.498	2	0.073
	L-S	195.7	221.0	127.6	1.534	2	0.265
	AUB	-379.3	501.1	289.3	-1.311	2	0.320
	RUM	272.0	538.5	310.9	0.875	2	0.474
	PI	-158.3	380.8	219.9	-0.720	2	0.546
	HOU	559.7	218.3	126.0	4.441	2	**0.047**
Dynamic Modulus (E*) @ 1Hz	AUG	43.3	131.2	75.7	0.572	2	0.625
	DUR	-99.7	18.8	10.9	-9.171	2	**0.012**
	PARK	196.7	135.3	67.7	2.907	3	0.0621
	L-S	141.0	73.7	42.6	3.311	2	0.08
	AUB	-379.3	501.1	289.3	-1.311	2	0.32
	RUM	177.7	276.3	159.5	1.114	2	0.381
	PI	-225.0	87.5	50.5	-4.455	2	**0.047**
	HOU	346.0	174.5	100.7	3.434	2	0.075
Seismic Modulus (Es)	P30	-66.3	116.5	67.2	-0.986	2	0.428
	P47	-212.7	305.0	176.1	-1.208	2	0.351
	D49	379.7	860.8	497.0	0.764	2	0.525
	P48	289.7	228.5	132.0	2.195	2	0.159
	P49	89.0	227.9	131.6	0.676	2	0.569
	CP	-358.7	302.3	174.5	-2.055	2	0.176
	LS68	-304.7	268.4	155.0	-1.966	2	0.188
	GT30	-145.0	94.6	54.6	-2.655	2	0.117
	LS66	-125.7	57.1	33.0	-3.814	2	0.062
	M	18.0	108.3	62.5	0.288	2	0.8
	NC74	-510.3	209.9	121.2	-4.21	2	0.052
	SN61	76.3	191.5	110.6	0.69	2	0.561
	FW34	127.3	88.5	51.1	2.491	2	0.13
	NCP55	273.0	189.4	109.3	2.497	2	0.13
	SH	-47.0	224.7	129.7	-0.362	2	0.752
	NC30	154.0	175.6	101.4	1.519	2	0.268
	NCP16	-83.3	39.8	23.0	-3.624	2	0.068
	NCP93	-366.7	203.4	117.4	-3.122	2	0.089

4.1.5.3 Strength

Although no significant correlation was found between the regularly obtained test data and performance, it was noted that only the poor performing mixes showed post-MIST ITS of ≤500 kPa, contained coarse aggregates with high Micro-Deval values and fine aggregates with high absorption, lower PG (PG 58 instead of PG 64) asphalt binder (appropriate PG for the project), and no or relatively low RAP percentage (Table 4.1.6 & Figure 4.1.5).

Table 4.1.6. Aggregate properties and Post MIST tensile strength

S. No.	Mix ID	Coarse Micro Deval, %	Fine Aggregate Absorption, %	PG Grade	RAP content,%
1	AUG	12	1.3	PG 64-28	20
2	DUR	27	0.4	PG 64-28	20
3	PARK	11	1	PG 58-28	15
4	L-S	13	0.7	PG 64-28	20
5	AUB	14	0.7	PG 64-28	0
6	RUM	10	0.2	PG 64-28	20
7	**PI-E**	**15**	**1.8**	**PG 58-28**	**10**
8	**HOU**	**16**	**1.3**	**PG 58-28**	**0**
9	P30	27	0.4	PG 64-28	20
10	P47	20	0.4	PG 64-28	20
11	D49	27	0.4	PG 64-28	20
12	P48	20	0.4	PG 64-28	20
13	P49	20	0.4	PG 64-28	20
14	CP	13	0.6	PG64E-28(70)	20
15	LS68	13	0.7	PG 64-28	20
16	GT30	14	0.7	PG 64-28	0
17	LS66	13	0.7	PG 64-28	20
18	M	11	0.9	PG 64-28	20
19	NC74	17	0.9	PG64E-28(70)	20
20	SN61	13	1.2	PG 64-28	20
21	FW34	13	1.9	PG 64-28	20
22	NCP55	18	0.5	PG 64-28	20
23	SH	15	1.8	PG 64-28	10
24	NC30	Mix Information Not Available			
25	NCP16	Mix Information Not Available			
26	NCP93	Mix Information Not Available			

The mixes (**in bold**) were identified as poor performers in terms of moisture damage in the filed

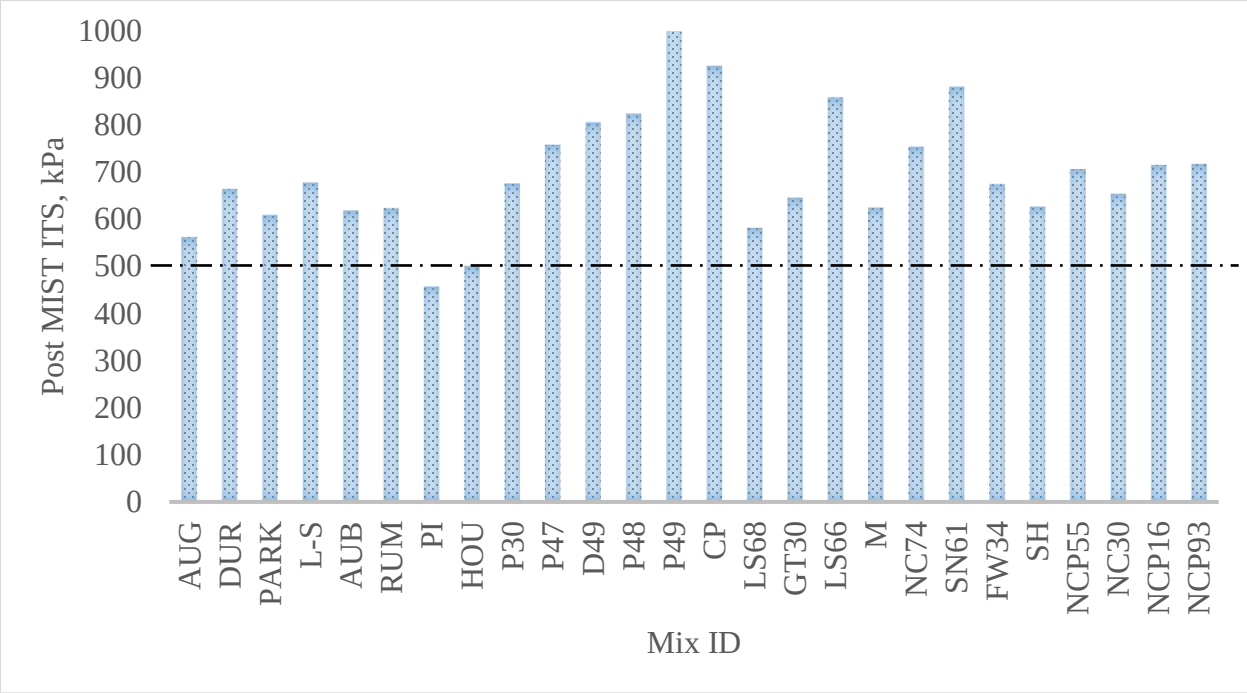

Figure 4.1.5. Post-MIST ITS values for the various mixes

4.1.6 Conclusions

- The post MIST Indirect Tensile Strength (ITS) values were able to identify the two poor performing mixes
- The dynamic modulus in indirect tension (IT) mode at any single protocol (10Hz frequency/1Hz frequency) was unable to identify the two poor performing mixes.
- Keeping in view of the effect of compaction from moisture conditioning, the MIST protocol could be revised.

Part 2: Study of laboratory compacted mixes – Moisture Susceptible versus Non-Moisture Susceptible

4.2.1 Objectives

The objective of this phase of the study was to finalize a nondestructive mechanical test based on its sensitivity to capture changes in mix properties due to moisture induced damage.

4.2.2 Materials

A PG 64-28 grade asphalt binder and two aggregates, PI (moisture susceptible) and SM (non-moisture susceptible), passing MDOT specifications (Maine DOT 2014), were selected. The mix design specifications are shown in Table 4.2.1.

Table 4.2.1. **Mix design information for PI and SM mixes**

PI mix

NMAS: 12.5 mm (Fine-Graded); N_{design}: 50 gyrations; Asphalt Binder: PG 64-28

Material	Proportions (%)	Sieve Size (mm)	Percent Passing
19 mm	12	19	100
12.5 mm	17	12.5	90-100
9.5 mm	19	9.5	78-90
Classifier Sand	22	4.75	64-78
Sand	10	2.36	38-46
RAP	20	1.18	23-31
Asphalt Content	5.9	0.60	14-20
		0.30	8-12
		0.15	5-9
		0.075	3.9-6.0

SM mix

NMAS: 12.5 mm (Coarse-Graded); N_{design}: 75 gyrations; Asphalt Binder: PG 64-28

Material		Sieve Size (mm)	Percent Passing
19 mm	16	19	100
12.5 mm	18	12.5	90-100
9.5 mm	25	9.5	74-88
Sand	21	4.75	43-57
RAP	20	2.36	31-39
Asphalt Content	5.4	1.18	20-28
		0.60	13-19
		0.30	8-12
		0.15	5-9
		0.075	3.5-7.0

4.2.3 Methods

4.2.3.1 Moisture Conditioning

A MIST conditioning protocol of 15,000 Cycles at 25^{o}C temperature and 138 kPa pressure was used for this study.

4.2.3.2 Modulus

Dynamic modulus in IT mode (E*) and seismic modulus (Es) were determined using the methods described in chapter 3.2 and 3.3, respectively.

4.2.3.3 Strength

Indirect tensile strength was determined using the method described in Chapter 3.4.

4.2.4 Test Plan

Figure 4.2.1 shows the test plan for this part of the study.

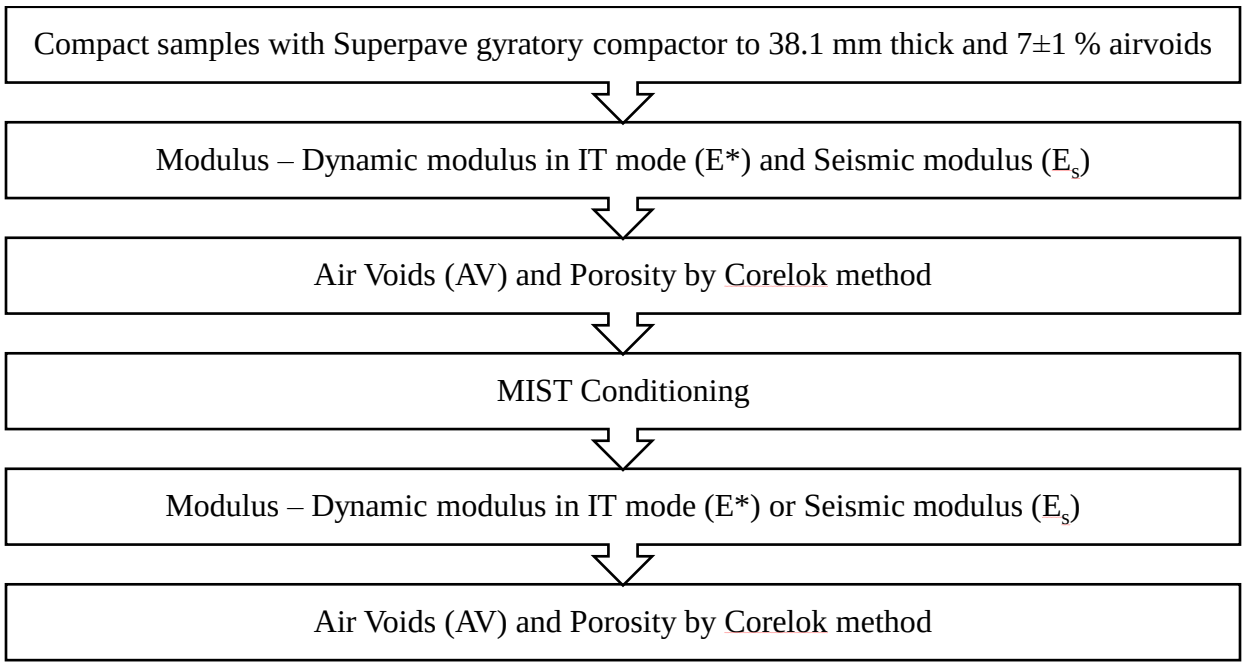

Figure 4.2.1 Test Plan – Preliminary study: Part 2

4.2.5 Results and Discussion

4.2.5.1 Review of Maine DOT data

Petrographic examination indicated the source of PI (hardness, 4.5 Mohs) and SM (hardness, 6.5 Mohs) as soft limestone and Andesite (igneous rock), respectively. The retained tensile strength (AASHTO T283) for the PI mix was found to be 92%. The results of Hamburg test (45^{o}C) on plant produced mixes (Figure 4.2.2) show that the PI mix fails to meet the <12.5 mm rut depth criterion at 13,000 passes, and has a very low stripping inflection point of 5,000. The SM mix has an average rut depth of 3.9 mm, whereas the PI mix has a rut depth of 6.4 mm at 10,000 passes, and a significantly higher pass versus rut depth slope, indicating a major contribution of stripping towards rutting (Aschenbrener 1995). The approved aggregate test data and Figure 4.2.2 point out the challenge – even though it can be confirmed by conducting a *destructive* test, how does one

detect moisture susceptibility during regular mix design and consider the risk of using it in structural design?

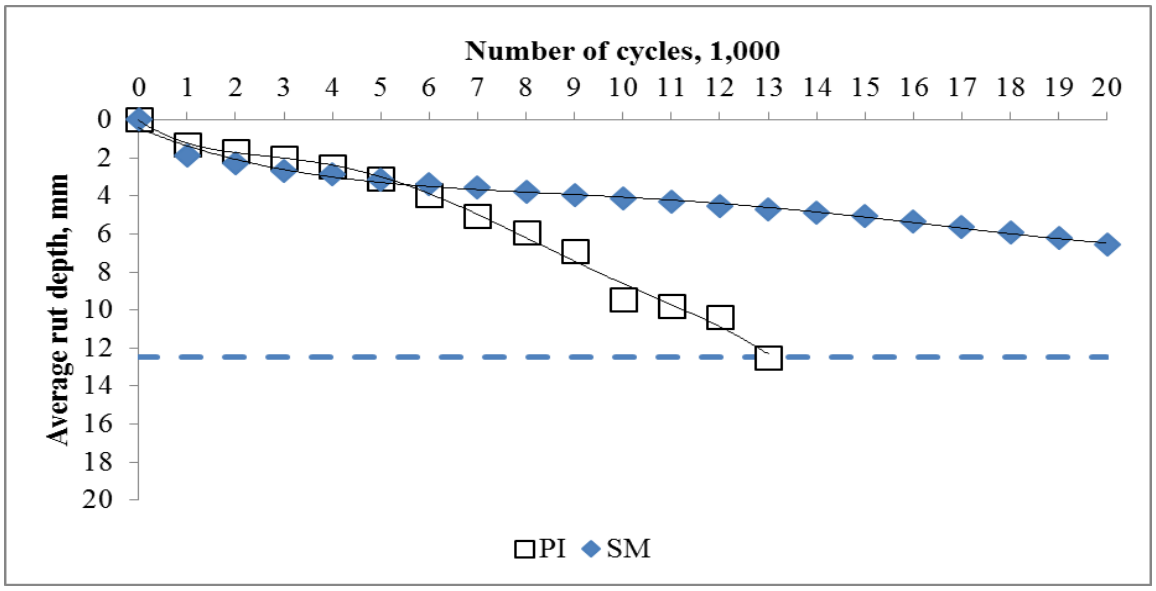

Figure 4.2.2 Hamburg Wheel tracking test results – PI and SM mixes

4.2.5.2 Modulus

Table 4.2.2 shows the results of dynamic modulus in IT mode (E*) and seismic modulus (Es) tests on PI and SM mixes. Statistical analyses of the Es values (Table 4.2.3) showed a significant difference between the post and pre-MIST moduli of the PI mix samples (Paired sample t-test at 1% significance level; the post-MIST values are lower) and no difference in the case of the SM mix. The results provide evidence that seismic testing is sensitive to the effects of moisture damage. The results also show the inability of the E* to differentiate the two mixes.

Table 4.2.2 Results of E* and E_s Tests

Results of Dynamic Modulus tests				
Mix	E* **at 10 Hz before MIST, MPa**	E* **at 10 Hz after MIST, MPa**	E* **at 1 Hz before MIST, MPa**	E* **at 1 Hz after MIST, MPa**
PI	1,463	1,515	2,57	2,76
	1,881	2,691	4,52	4,81
	4,253	4,752	7,50	7,86
	2,980	2,765	5,70	5,43
	2,969	2,165	4,64	5,01
	2,659	2,605	6,20	4,86
SM	3,321	3,334	6,55	7,26
	3,207	2,886	6,94	7,42
	2,971	2,922	4,64	5,43
	2,767	4,200	4,69	6,26
	3,542	3,947	6,48	7,00
	4,126	5,136	1,091	1,535

Results of Seismic Tests		
Mix	**E_s before MIST conditioning, MPa**	**E_s after MIST conditioning MPa**
PI	13,772	12,518
	14,947	13,695
	17,361	15,799
	15,810	15,072
	14,937	13,956
	16,236	14,798
SM	17,088	16,888
	16,264	16,388
	14,887	14,567
	15,951	15,712
	16,869	16,239
	16,799	16,996

Table 4.2.3 Results of Paired t test @ 95% Confidence Level – Change in Modulus (E* and Es) before and after the MIST conditioning

Mix	Mean	Std. Deviation	Std. Error Mean	t	df	Sig. (2-tailed)
E* at 10Hz						
PI	-48	563.83	230.18	-0.2085	5	0.843
SM	-415.17	679.56	277.43	-1.4965	5	0.195
E* at 1Hz						
PI	-93.53	116.77	47.67	-1.9619	5	0.107
SM	-216.55	208.45	85.1	-2.5447	5	0.052
Seismic Modulus (Es)						
PI	1203.86	301.82	123.217	9.7702	5	**0.000**
SM	178.056	303.649	123.96	1.4364	5	0.210

Effect of Moisture on Seismic Modulus

The method of drying of specimens prior to MIST conditioning and the mode of seismic testing were identified as topics that needed further research. This is because of three reasons:

1. The presence of water inside samples affects the travel time of the ultrasonic pulse;
2. The amount of water inside samples is dependent on the gradation, absorption and porosity of the mix/sample;
3. The mode of seismic test (compression/shear wave) needs to be appropriate to minimize the effects of residual moisture from MIST conditioning upon the travel time measurements. In general, shear waves do not travel through liquid media due to the nature of their propagation whereas compression waves do travel and get affected from the type of media. So it would of interest to study further the impacts of these wave transducers to accurately capture the changes in mix properties from moisture damage.

The presence of water inside a post-MIST sample, after 72-hours of laboratory countertop fan-drying at 25^{o}C was confirmed through X-ray micro-tomography of a PI mix sample (Figure 4.2.3).

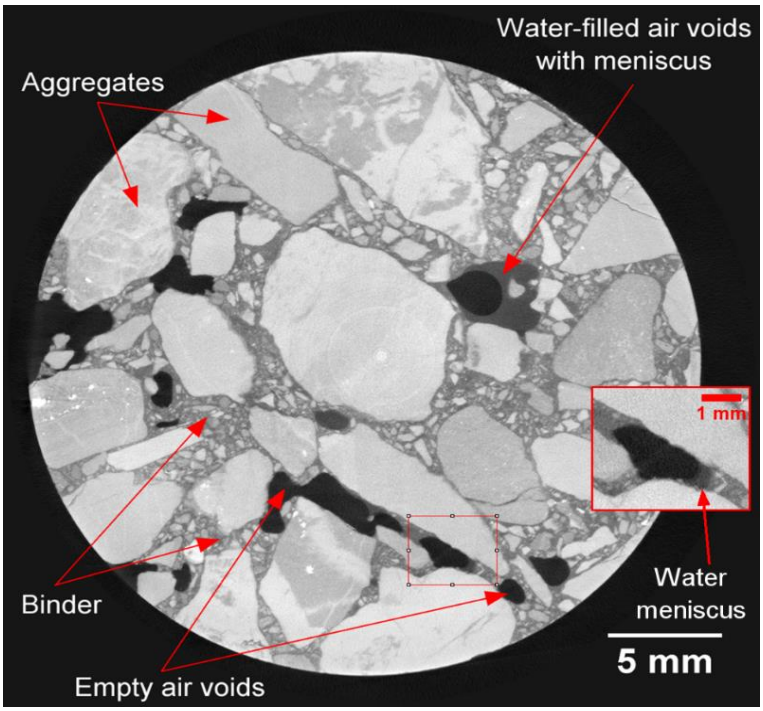

Figure 4.2.3 2D cross-section from the 3D image (tomogram) of part of the M-P-2 sample (a 30 mm diameter core from the original full sample). The 3D image was obtained by X-ray micro-tomography. The voxel value is proportional to density and the 4th power of the elemental atomic number. The rectangle indicates a region of interest magnified and included as an inset in the bottom right part of the figure, zooming onto air voids which clearly show a water meniscus. Other, larger air voids show even larger water menisci, being more saturated with remaining water; Air void and the porosity of this sample changed from 5.9 to 5.2%, and from 6.4 to 4.1, respectively, after MIST conditioning.

Moisture Induced Stress Test (MIST) conditioning parameters

The average change in air voids after MIST conditioning was observed to be 0.6 and 0.5% (absolute value, POST-Pre MIST), whereas the change in porosity was found to be 2.0 and 2.9% (absolute value, POST-Pre MIST) for the SM and PI mixes, respectively. The decrease in both air voids and porosity indicate that the impact of MIST conditioning was more of a compacting nature rather than a "stripping" nature; and even if the PI samples showed a loss of modulus after MIST conditioning, part of that loss might have been masked by the increase in modulus due to a decrease in air voids. Therefore, to maximize its potential, the MIST conditioning process needs to be made severe enough to simulate the loss of material that is commonly observed in moisture damaged pavements. Also, the use of a sufficient dwell period, which can simulate the soaking period of water immediately after rain before significant traffic use, is needed. Two MIST conditioning

protocols were used to determine the effect on modulus; a conditioning process of 20 hour dwell at 60ºC, followed by 3,500 cycles at 276 kPa and 60ºC showed an average loss in modulus that is four times that of a conditioning process of no dwell, 15,000 cycles at 25ºC and 138 kPa (Table 4.2.2 & 4.2.4).

Table 4.2.4 Results of E_s at MIST conditioning of 20 hour dwell at 60ºC, followed by 3,500 cycles at 276 kPa and 60ºC - PI mix

Sample No.	E_s before MIST conditioning, MPa	E_s after MIST conditioning, MPa	% Reduction
1	13653	8712	36.2
2	12479	9798	21.5
3	13553	6812	49.7
Average			35.8

4.2.6 Conclusions

- Dynamic modulus test in indirect tension mode was unable to distinguish the moisture susceptible PI mix from the non-moisture susceptible SM mix;
- Seismic modulus obtained from the Ultrasonic Pulse Velocity (UPV) test was effective in distinguishing between moisture susceptible and non-moisture susceptible mixes;
- Moisture can linger in the internal pore spaces of moisture conditioned samples for a considerable amount of time;
- Further research is warranted in three areas:
    - Impact of specimen drying times on the amount of residual moisture;
    - Appropriate mode of seismic testing.

References

Aschenbrener, T. (1995). "Evaluation of Hamburg wheel-tracking device to predict moisture damage in hot-mix asphalt." *Transportation Research Record: Journal of the Transportation Research Board*, 1492, 193.

Maine DOT (2014). "Standard Specifications." Maine Department of Transportation, Maine.

Part 3: Study of a Moisture Susceptible Hot Mix Asphalt with Model Mobile Load Simulator (MMLS3)

4.3.1 Objective

The objective of the study was to investigate the performance of the moisture susceptible mix with and without the presence of water using an accelerated loading equipment – Model Mobile Load Simulator (MMLS3).

4.3.2 Model Mobile Load Simulator (MMLS3)

The Model Mobile Load Simulator (MMLS3) is a one third scaled accelerated loading equipment that has been used successfully to evaluate rutting performance and moisture damage of pavements in the field and the laboratory (De Vos et al. 2007; Huang et al. 2017; Walubita 2000). The MMLS3 is run using an appropriate number of load repititions (based on traffic level), speed, tire pressure, and axle load. The rut depth profile is measured at the end of the test. Also, it has the potential to maintain desired environmental conditions such as high temperature and moisture. The mechanical properties of the loaded mix can be obtained from mechanical tests that could be calculated on cores taken from trafficked slabs or samples.

Walubita et al. (2002) studied the performance of in-service asphalt pavements under various environmental conditions using the MMLS3 combined with laboratory fatigue tests. Decrease in fatigue life under wet trafficking due to water damage and an increase in fatigue life under dry and hot conditions due to material densification were reported from the study. Smit et al. (2003) validated the performance of MMLS3 by comparing the results from full-scale trafficking in combination with laboratory mechanical and performance tests. Hugo et al. (2004) developed interim guidelines for limits based on stiffness, strength and fatigue measurements that are combined with MMLS3, to evaluate the moisture susceptibility of tested pavements. The research also pointed out the need for shift functions to measure the accurate surface rutting under wet wandering conditions due to the unexpected surface deformation when compared to dry wandering studies. Mallick et al. (2005) evaluated and validated the performance of MMLS3 to characterize moisture susceptibility of mixes and the effect of lime on reducing moisture susceptibilty. De Vos et al. (2007) utilized MMLS3 and MMLS 10 (full-scale) in combination with Portable Seismic Pavement Analyzer (PSPA) to develop mechanistic-empirical design method for cement stabilized

sand bases. The study reported that the observed distress mechanisms and surface deformations under MMLS were similar to those found in pavement structures in the region. Huang et al. (2017) investigated the performance of various accelerated pavement testing (APT) equipment and concluded that the MMLS3 is an effective, economic and reliable trafficking tool to characterize the rutting and fatigue potential of pavement materials.

4.3.3 Materials

Laboratory compacted PI mix samples and field cores from the PI mix layer, and field cores from a non-moisture susceptible mix (WL) were used for the study. Table 4.3.1 shows the mix design information of the laboratory compacted samples and field cores.

Table 4.3.1. Mix design information of laboratory compacted samples and field cores

---

PI mix

ESAL'S: 3 to <10; NMAS: 12.5 mm (Fine-Graded); N_{design}: 50 gyrations; Asphalt Binder: PG 64-28; Optimum Asphalt Content: 5.9%

Material	Proportions (%)		Sieve Size (mm)	Percent Passing
	Lab Compacted[a]	Field Cores		
19 mm	86.25% (Quarry)	12	19	100
12.5 mm		17	12.5	90-100
9.5 mm		19	9.5	78-90
Classifier Sand		22	4.75	64-78
Sand	13.75%	10	2.36	38-46
RAP	--	20	1.18	23-31
			0.60	14-20
			0.30	8-12
			0.15	5-9
			0.075	3.9-6.0

WL Mix – Field Cores

ESAL'S: 3 to <10; NMAS: 12.5 mm (Fine-Graded); N_{design}: 75 gyrations; Asphalt Binder: PG 64-28; Optimum Asphalt Content: 5.3%

Material	Proportions	Sieve Size (mm)	Percent Passing
12.5 mm	22	19	100
9.5 mm	18	12.5	90-100
Washed Stone Screenings	16	9.5	80-90
Dry Stone Screenings	6	4.75	53-67
Sand	18	2.36	28-58
RAP	--	1.18	29-37
		0.60	20-26
		0.30	11-15
		0.15	6-10
		0.075	2-6

---

[a]Batches made by stockpile sizes after washing, drying and separating into different sizes based on the source (Quarry/ Natural Sand). Also, the RAP was replaced with virgin aggregates, proportionately, to have a control mix to compare with other laboratory test results.

4.3.4. Methods

4.3.3.1 Model Mobile Load Simulator (MMLS3)

A 1/3rd scaled model mobile load simulator (MMLS3) was utilized for the study. The various parameters considered for the test are shown in Table 4.3.2.

Table 4.3.2. MMLS3 testing conditions

Condition/Parameter	Value
Tire Pressure	690 kPa
Load	2.7 kN
Number of loads	12,000
Speed	12.6 Hz (1/4th Max. Speed)
Water Temperature (Wet run)	48±3 ^{0}C
Dry run temperature	25±3 ^{0}C
Ambient Temperature	25±3^{0}C

A total number of thirty, 50.8 mm high (150 mm diameter) compacted samples at three different air voids and asphalt contents (Table 4.3.3), in sets of three, in dry and wet heated conditioned were tested.

Table 4.3.3. Matrix of PI Lab compacted samples

Asphalt Content	Air Voids					
	5±1%		7±1% (Opt)		10±1%	
	Dry	Wet	Dry	Wet	Dry	Wet
Optimum – 1			XXX	XXX		
Optimum	XXX	XXX	XXX	XXX	XXX	XXX
Optimum + 1			XXX	XXX		

The field cores of PI and WL mixes, in sets of three, were tested in dry and wet heated conditions. Table 4.3.4 shows the matrix of PI and WL field cores.

Table 4.3.4. Matrix of PI and WL field cores

	Dry	Wet
PI Cores	XXX	XXX
Wells Cores	XXX	XXX

Three samples of similar conditions were tested each time. The volumetric parameters such as air voids, density, porosity and surface profiles of the samples were measured before and after the test.

4.3.5. Results and Discussion

4.3.5.1 Laboratory compacted samples of PI mix

Table 4.3.5 shows the volumetric properties before and after the MMLS loading and the rut depths.

Table 4.3.5. MMLS - Results of PI mix lab compacted Samples

Asphalt Content, %	Before MMLS			After MMLS			Max. Rut Depth, mm
	AV, %	Density, g/cc	Porosity, %	AV, %	Density, g/cc	Porosity, %	
	Dry Run						
5.9	5.5	2.360	3.594	3.7	2.370	4.244	0.43
5.9	6.4	2.336	4.099	4.5	2.350	4.533	0.48
5.9	9.7	2.256	3.957	7.4	2.278	4.346	1.00
4.9	8.0	2.332	4.582	7.0	2.358	4.693	0.45
6.9	7.3	2.281	5.692	6.1	2.310	5.615	0.62
	Wet-heated Run						
5.9	5.0	2.373	3.153	3.6	2.372	3.766	2.51
5.9	6.9	2.325	5.109	5.2	2.332	5.175	2.72
5.9	9.9	2.249	8.285	7.9	2.266	7.257	5.93
4.9	7.4	2.349	5.303	4.2	2.358	5.239	1.84
6.9	7.1	2.285	5.772	6.6	2.297	5.573	4.89

Figure 4.3.1 shows pictures of samples before and after MMLS dry and wet heated runs.

(i) Before Dry Run

(a) Before Wet Run

(ii) After Dry Run, 7±1% AV

(b) After Wet Run, 7±1% AV

(iii) After Dry run, 10±1% AV

(c) After Wet run, 10±1% AV

Figure 4.3.1. Laboratory compacted specimens of PI mix before and after MMLS runs

Effect of Air Voids

Figure 4.3.2 shows the results of rut depths for samples with different air voids – design (5±1%), construction (7±1%) and high (10±1%) under dry and wet-heated condition. Though there is a slight difference in rut depths at design and construction air voids, a higher difference was found (with high air voids) between the dry and wet-heated conditions. The rutting potential of the mixes was found to be higher under wet-heated conditions compared to dry conditions.This confirmed the significant combined impact of heat and moisture on the properties of HMA.

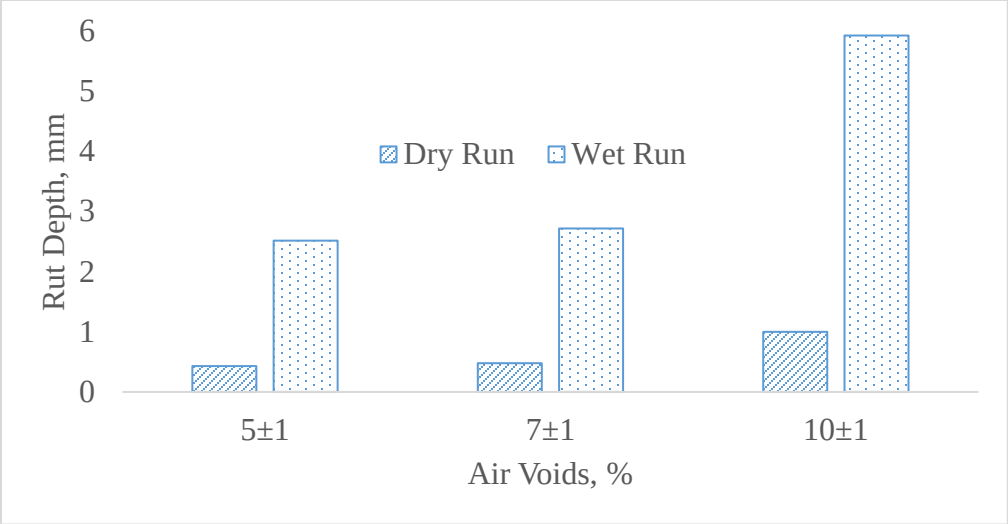

Figure 4.3.2 Average rut depth for different air voids under dry and wet-heated condition

Effect of Asphalt Content

Figure 4.3.3 shows the results of rut depths with different asphalt contents - around Optimum (4.9, 5.9 and 6.9) under dry and wet-heated condition. Higher rut depths were observed with increase in asphalt content under both dry and wet-heated conditions. The rut depth was significantly higher under wet-heated conditions, at higher asphalt content. This is due to the higher sensitivity of higher amounts of asphalt content to heat and moisture, which leads to failure in the mixes.

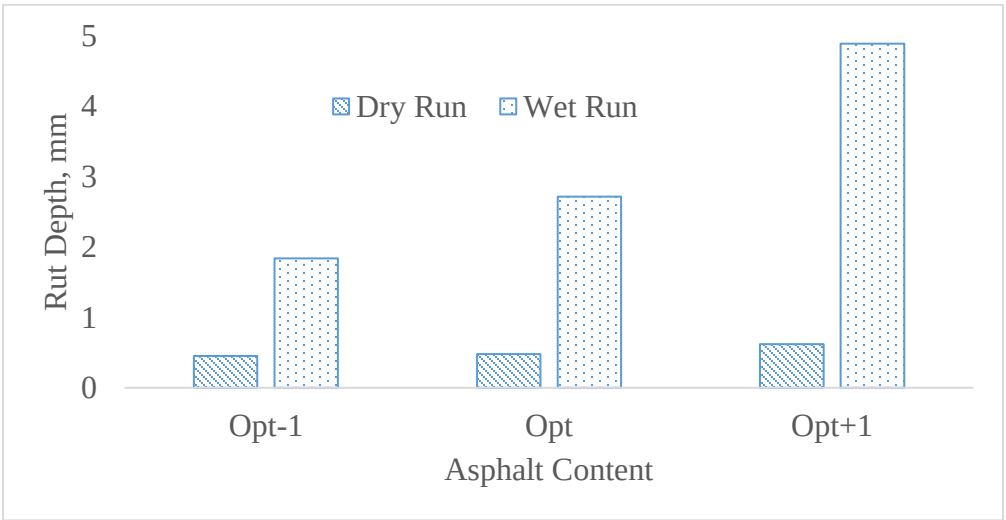

Figure 4.3.3 Average rut depth for different asphalt contents under dry and wet-heated condition

4.3.5.2 Field Cores of PI and WL mix

Table 6 & Figure 4.3.5 show the summary of average rut depths and a picture of samples after the wet-heated run for PI and WL mix cores. A higher amount of rut depth was observed for the PI mix compared to the WL mix.

Table 4.3.6. Results of PI and Wells Cores

Mix Type	Air Voids, %	Binder Content,%	Avg. Rut Depth, mm	
			Dry	Wet
PI Cores	5.5	5.9	1.11	6.60
WL Cores	5.5	5.3	0.39	5.89

(a) PI field core sample (b) WL field core sample

Figure 4.3.5. PI and WL mix core samples after Wet heated MMLS runs

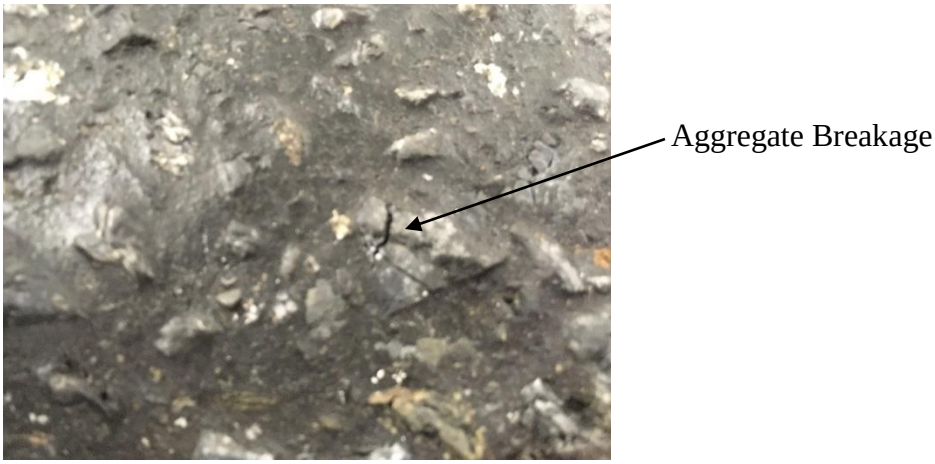

Figure 4.3.6. Picture showing broken PI mix aggregate after MMLS3 wet-heated run

Observations after MMLS wet-heated runs showed loss of material in the test bed and also evidence of aggregate breakage on the samples (Figure 4.3.6).

4.3.5.3 Discussion

Overall, the rut depths of laboratory compacted samples of the PI mix were in the range of 1.84 to 2.72 mm (excluding the samples with higher % air voids) under wet conditions which are comparable with the critical values of 1.8 to 3 mm depending on the traffic conditions (Mallick et al. 2005). Moisture damage was found to be severe for the laboratory samples with higher percentage of air voids and for field cores with rut depth values ranging from 5.89 – 6.60 mm.

4.3.6 Conclusions

The major conclusion from this phase of the study was that the rutting potential of mixes is increased significantly in the presence of heat and moisture.

References

De Vos, E., Hugo, F., Strauss, P., Prozzi, J., Fults, K., and Tayob, H. (2007). "Comparitive Scaled MMLS3 Tests vs. Full-Scale MLS10 Tests in Mozambique." *CD ROM Proceedings of the 86th Annual Meeting of the Transportation Research Board, Washington, DC*.

Huang, Y., Wang, L., and Xiong, H. (2017). "Evaluation of pavement response and performance under different scales of APT facilities." *Road Materials and Pavement Design*, 1-11.

Hugo, F., Smit, A. d. F., Pieter, P., Powell, B., and Bacchi, C. (2004). "Distress of hot mix asphalt on the NCAT test track due to accelerated wet trafficking with the MMLS3." *CD-ROM Proceedings Second International APT Conference*.

Mallick, R. B., Pelland, R., and Hugo, F. (2005). "Use of accelerated loading equipment for determination of long term moisture susceptibility of hot mix asphalt." *International Journal of Pavement Engineering*, 6(2), 125-136.

Smit, A., de Hugo, F., Rand, D., and Powell, B. (2003). "MMLS3 testing at the NCAT test track." *CD-ROM of TRB 82nd Annual Meeting, TRB, National Research Council*Washington DC.

Walubita, L. F. (2000). "Accelerated testing of an asphalt pavement with the third-scale model mobile load simulator (MMLS3)." Stellenbosch: Stellenbosch University.

Walubita, L. F., Hugo, F., and Martin, A. L. E. (2002). "Indirect tensile fatigue performance of asphalt after MMLS3 trafficking under different environmental conditions." *Journal of the South African Institution of Civil Engineering*, 44(3), 2-11.

Part 4: Study of Material Loss of HMA due to Moisture Damage

Field studies have frequently reported signs of materials loss (white streaks of aggregates and black patches of asphalt) associated with moisture damage in HMA pavements. Furthermore, MDOT has also reported loss of materials (the underlying HMA layer could be seen) for the PI mix, in the wheel path of the pavements. Hence, an effort was made to evaluate the type and the amount of both aggregate and asphalt binder, if any, that was lost from the mix during the moisture conditioning. The effluent from the MIST was collected for different samples. This effluent was found to consist of water, aggregates (broken, coated and uncoated) and was suspected to contain dissolved components from the asphalt binder. The effluent water was collected immediately and stored for further analysis to detect traces of asphalt binder in the effluent and determine the content. The aggregates were recovered from the effluent and subjected to sieve analysis for gradation.

4.4.1 Materials

Laboratory samples of PI and SM mixes were prepared to a target air void of 7± 1%. The mix design details are same as given in the Part 2 of the preliminary study.

4.4.2 Methods

4.4.2.1 Loss of Material – Aggregates

The recovered aggregates were weighed and the weight was reported as loss of material (LOM) in gm. Then fineness modulus was determined, after which a microscopic analysis was conducted. Also, a particle size counter was used to count the fine particles that were smaller than 75µ.

Fineness Modulus

The recovered aggregates were passed through a set of fine sieves ranging in opening sizes of 4.75 to 0.075 mm. The fineness modulus was then calculated as follows.

FM = (Σ Cumulative percent retained from 4.75 to 0.15 mm sieves)/100

Microscopic Analysis

Microscopic Analysis of aggregates were carried out using a stereoscope (regular light microscope). The pictures of different size of aggregates were taken at different magnifications from 1X to 4X.

Particle size counter

A Particle size counter (PC 2400PS, Chemtrac systems Inc.,) was used for the particle size analysis. The effluent sample was passed through the particle size counter and a preset program with different size ranges was used to count the number of particle.

4.4.2.2 Loss of Asphalt compounds

Flourometer

The 10-AU field fluorometer was used for the analysis. The fluorometer measures the parameters of fluorescence- its intensity and wavelength distribution of emission spectrum after excitation by a certain spectrum of light. These parameters are used to identify the presence and the amount of specific molecules in a medium.

Dissolved Organic Carbon (DOC)

The DOC analysis was conducted with a Shimadzu TOC-5000A analyzer, which uses combustion of carbon to CO_2 and analysis with a non-dispersive infrared (NDIR) gas detector to quantify total carbon. The DOC samples were prepared by filtering effluent water samples through GF/C glass fiber filter and preserved with 100µL of 6N HCl per 100ml of sample. The working standards of 8, 5, 2, and 0 ppm were used in the analysis. A 2ppm standard was kept along with DOC samples for analysis as a quality control measure. The type of analysis chosen was non-purgeable organic carbon (NPOC) with three injections for repetitive measurements of each standard or sample and a maximum of 5 with an allowable standard deviation of 200 and Co-variance of 2%.

Nuclear Magnetic Resonance (NMR)

Nuclear Magnetic Resonance (NMR) spectroscopy analysis was conducted with a Bruker Avance AVIII NMR Spectrometer. The samples for the analysis were prepared by filtering effluent water

through 0.45µm glass filters (Whatman, GF/C) and dissolving in deuterium oxide (D2O) and then transferring to NMR tubes for the spectroscopy analysis.

Gas Chromatography–Mass Spectrometry (GC-MS)

Agient 6890N-5973N GS/MSD gas chromatography with EI ionization mode and 70eV electronic energy was used to analyze the compounds. The ion source and interface temperatures were at 230^0C and 280^0C respectively. A HP-5MS (30 m 0.25 mm) chromatographic column was used at a flow volume of 1.0 mL/min. The column temperature was kept from 50 to 300^0C with a heating rate 10^0C/min and it was kept for 20 min at 300^0C. The carrier gas was helium injected in nonsplit way and the injection volume was 1.0 mL. The mass scan range was from 9 amu to 500 amu.

Solid Phase Extraction (SPE)

The SPE cartridge Superclean^{TM} ENVI-18 SPE tube (SUPELCO) with bed weight 500mg and volume 3ml, and the solvent methylene chloride were used for solid phase extraction. The extraction was carried in three stages. First, the cartridge was conditioned by pulling 3ml of methylene chloride completely, twice, using vacuum pump. A 3ml (approx.) of purified water was then pulled through the cartridge for equilibrium, which was also repeated in between washes and at the end to avoid drying of cartridge. Second, the sample was passed through the cartridge at a flow rate of 10ml/min approximately. After passing the entire sample of 500ml, the air was drawn through the cartridge for 10 min at full vacuum. Next, the elution was carried out, immediately, by soaking sorbent using low vacuum, and then drawing 3ml of methylene chloride through the cartridge into collection tubes, without vacuum. The extracted elute was then transferred to 1.5 ml glass vials for further analysis.

4.4.3 Results and Discussion

Table 4.4.1 shows the moisture induced material loss along with changes in mechanical properties due to MIST conditioning.

Table 4.4.1 Moisture induced loss of material

Mix	Air Voids (%)	Before MIST	After MIST		LOM (gm)	FM	Fluorescence	DOC (ppm)
		Seismic Modulus (Mpa)	Seismic Modulus (Mpa)	ITS (kPa)				
PI	6.2	14290	14466	447	1.62	1.29	6.34	1.934
PI	8.0	13286	12888	434				
PI	7.2	13152	13086	439				
SM	8.9	13412	13482	572	0.91	1.11	3.15	1.78
SM	7.5	13421	13397	507				
SM	7.6	13271	13422	564				

The results of effluent analysis showed differences in loss of material and leaching of asphalt compounds between the two mixes – PI and SM (Figure 4.4.1). The PI mix shows higher loss of material and fineness modulus than SM mix. The higher fineness modulus of PI mix indicates the coarseness of aggregate material that are lost due to MIST conditioning. The microscopic analysis conducted upon lost aggregate particles showed coated, uncoated and broken aggregates (Figure 4.4.2). Figure 4.4.3 shows the particle size distribution using particle size counter. The PI mix showed a finer gradation when compared to the SM mix. The values of fluorescence and DOC were found to be higher for the PI mix compared to those from the SM mix which indicates a higher loss of asphalt binder compounds from the PI mix (Figure 4.4.1).

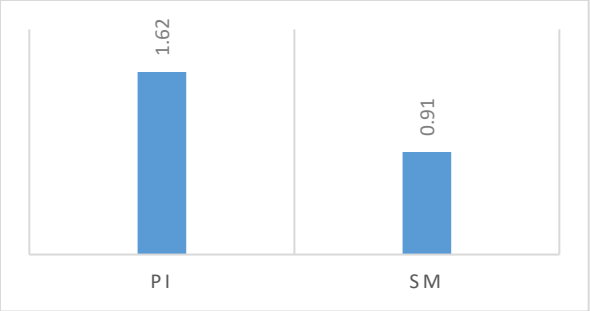

(a) Loss of material, gm

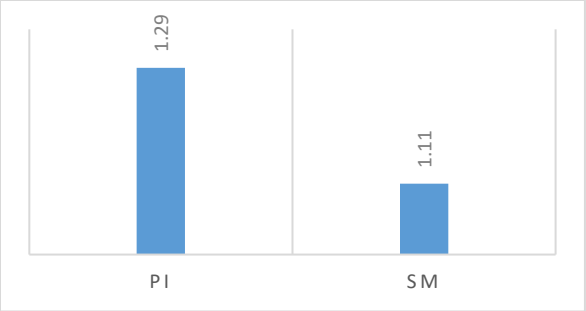

(b) Fineness Modulus

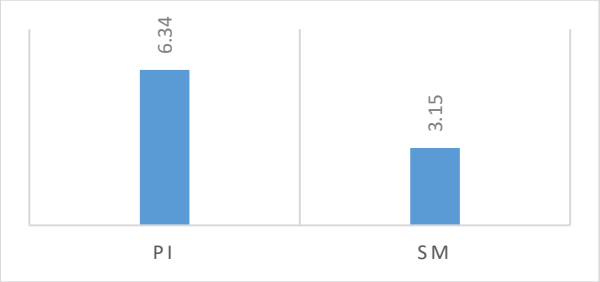

(c) Fluorescence

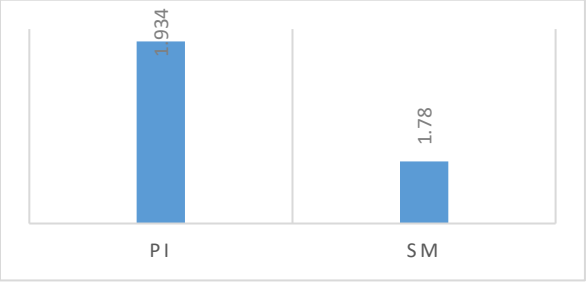

(d) DOC, ppm

Figure 4.4.1 Effluent Analysis – Results

1.18 mm 0.6 mm 0.3 mm 0.15 mm 0.075 mm

(a) PI mix

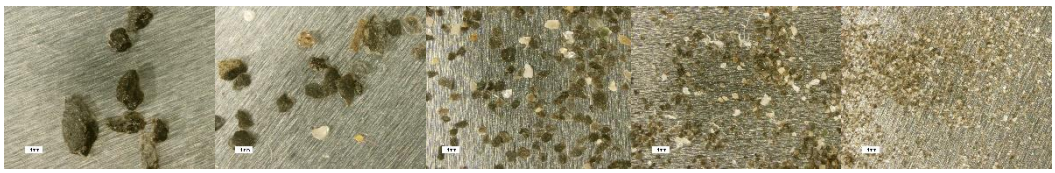

1.18 mm 0.6 mm 0.3 mm 0.15 mm 0.075 mm

(b) SM mix

Figure 4.4.2 Photos of typical materials collected from the effluent of MIST conditioning of samples with PI and SM mixes retained on different sieve sizes –1X Magnification

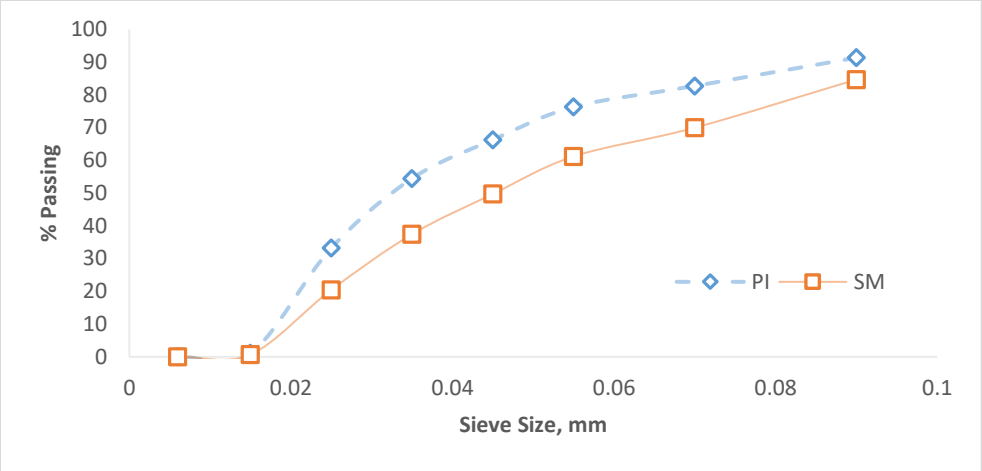

Figure 4.4.3 Particle size distribution using particle size counter; shows finer gradation for the PI mix

Nuclear magnetic resonance (NMR) spectroscopy

Figure 4.4.4 shows the results of NMR spectroscopy upon the three effluent water samples (E1 to E3) and tap water. The NMR did not show any peaks that confirm the presence of traces of asphalt binder. The sample E2 was repeated to achieve high S/N at 6X to check for any signals of aromatic compounds; however no peak was observed (Figure 4.4.5). Hence, NMR was not able to detect the low intensities of traces of asphalt compounds in effluent water that was obtained from MIST conditioning.

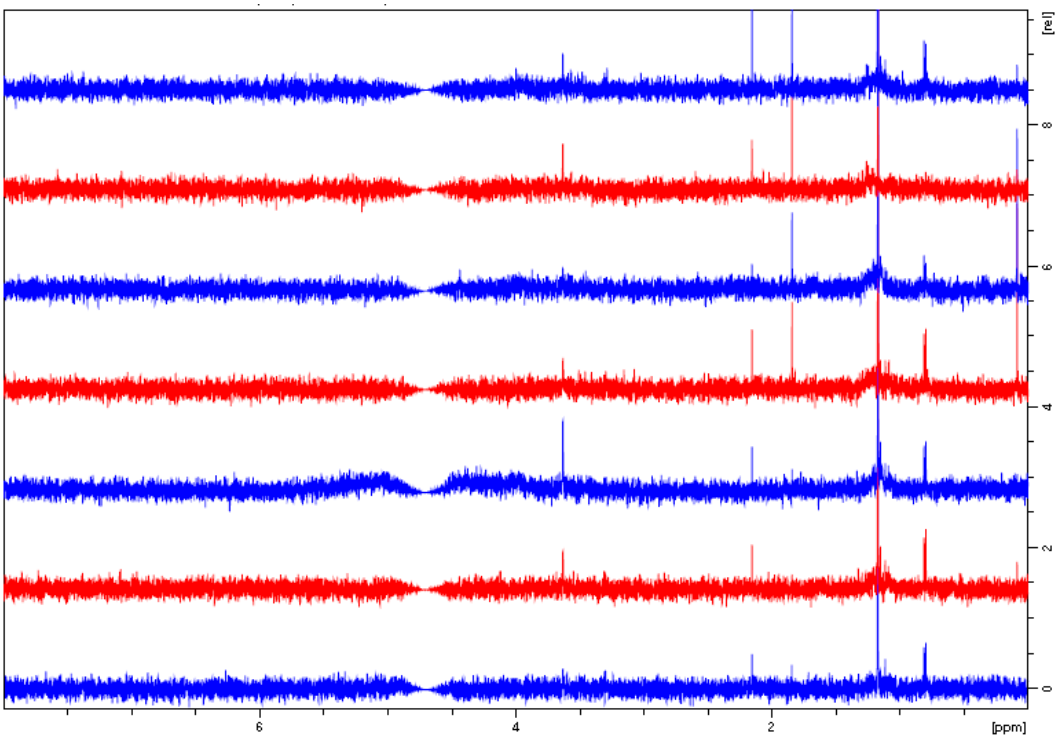

Figure 4.4.4 NMR Spectrum

[Note: Top – E3 Filtered, E3, E2 Filtered, E2, E1 Filtered, E1, Tap Water, Bottom]

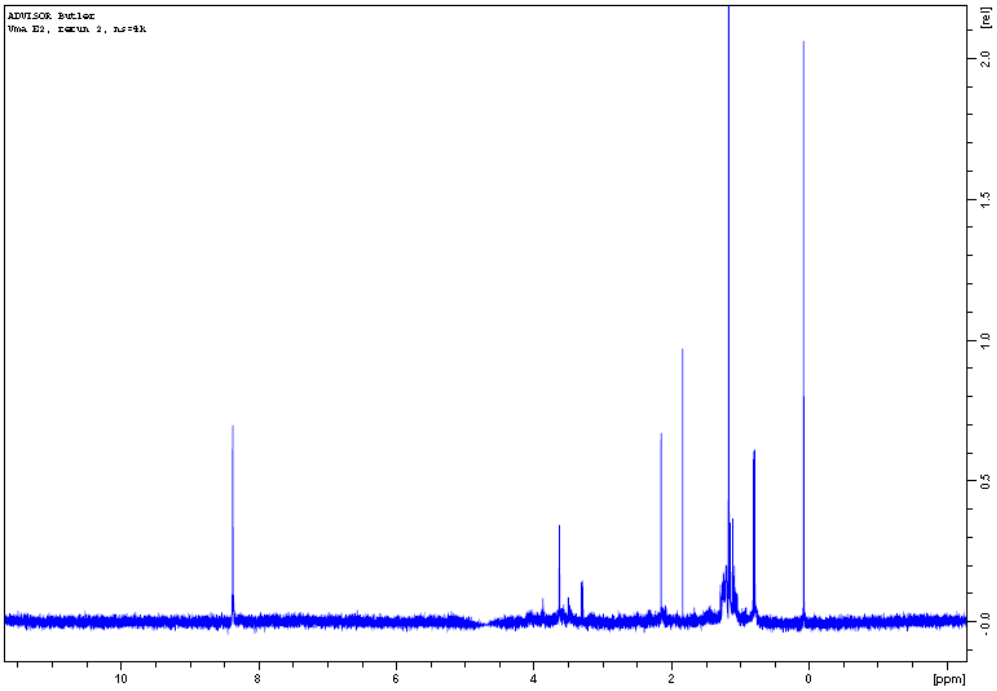

Figure 4.4.5 High S/N NMR Spectrum for sample E2

Gas chromatography–mass spectrometry (GC-MS)

Figure 4.6 shows the chromatograms of the two samples. The peaks in the spectrum confirms the presence of compounds in the effluent water samples. To identify these compounds, the mass spectrums were matched with the spectrums of compounds in National Institute of Standards and Technology (NIST) library (Linstrom and Mallard 2017). Table 4.4.6 shows the identified compounds for sample 1 and 2. Further work is required to improve the accuracy of compounds identification and to measure the corresponding weights using Mass Spectrometry.

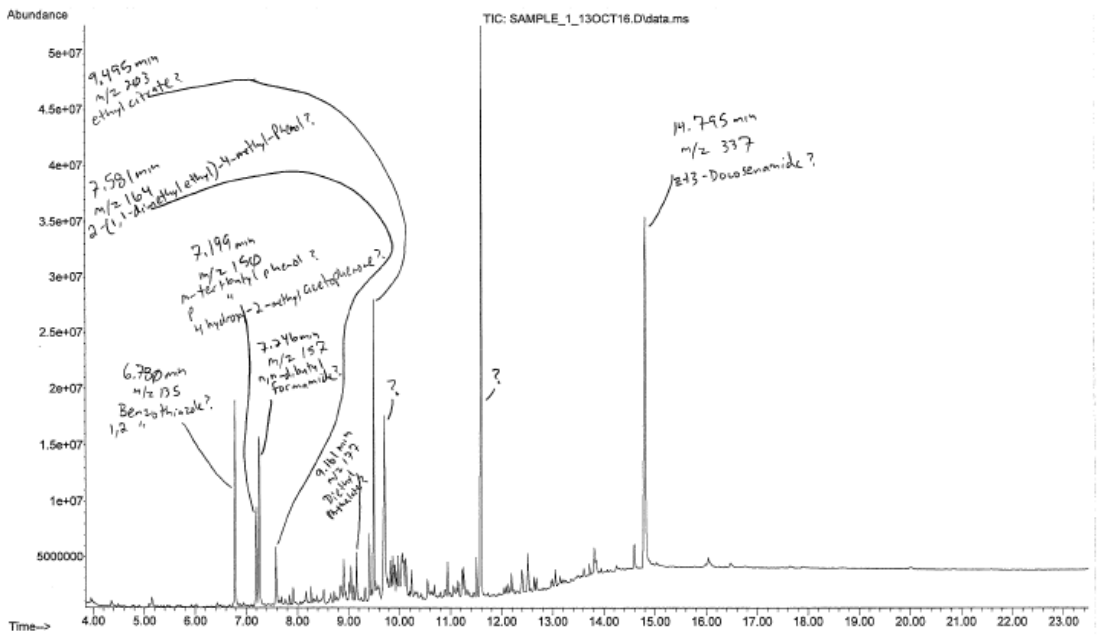

(a) Sample 1

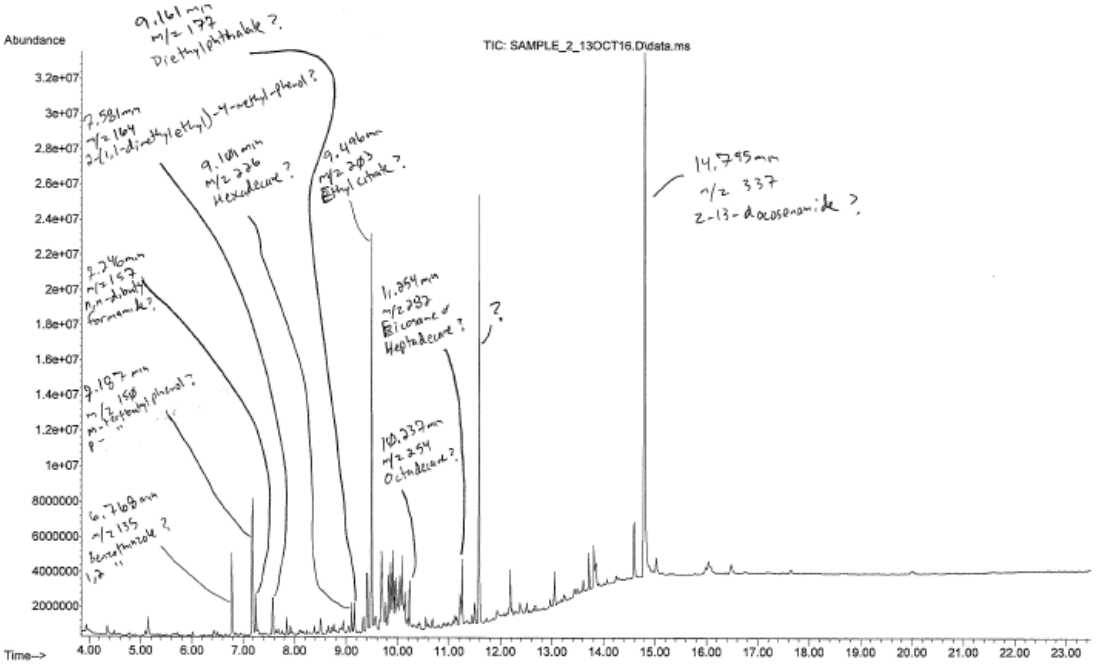

(b) Sample 2

Figure 4.4.6 GC/MS Chromatograms

Table 4.4.2 Results of GC/MS – Identified Compounds

Sample 1 - 10PI#1

S.NO.	Name of Compound	m/z	Ret. time
1	Benzothiazole	135	6.78
2	m-tert-Butylphenol/4-Hydroxy-2-methylacetophenone	150	7.199
3	n, n-d, butylformamide	157	7.246
4	2-(1,1-dimethyl ethyl)-4-methyl-phenol	164	7.581
5			
6	Diethyl phthalate	177	9.161
7	Ethyl citrate	203	9.495
9	z-13-Docosenamide	337	14.795

Sample 2 - 10PI#2

S. NO.	Name of Compound	m/z	Ret. time
1	Benzothiazole/ 1,2 Benzothiazole	135	6.77
2	m-tert-Butylphenol/p-tert-Butylphenol	150	7.19
3	n, n-d, butylformamide	157	7.25
4	2-(1,1-dimethyl ethyl)-4-methyl-phenol	164	7.58
5	Hexadecane	226	9.10
6	Diethyl phthalate	177	9.16
7	Ethyl citrate	203	9.50
8	Octadecane	254	10.24
9	Eicosane/Heptadecane	287	11.25
10	z-13-Docosenamide	337	14.80

4.4.4 Conclusions

1. The results of Dissolved organic carbon looks promising for use with effluent analysis.

2. The NMR was not able to detect the low intensities of asphalt compounds in the effluent water samples from the MIST.

3. The GC/MS was able to identify traces of asphalt binder compounds in the MIST effluent.

References

Linstrom, P. J., and Mallard, W. E. (2017). "NIST Chemistry WebBook, NIST Standard Reference Database Number 69." National Institute of Standards and Technology, Gaithersburg MD, 20899.

Chapter 5

Main Study

5.1 Objective

The objective of this phase was to develop and validate a method for identifying the mixtures with potential of moisture induced material loss and to understand the impact of mixture strength, stiffness and material loss on moisture susceptibility of Hot Mix Asphalt (HMA).

5.2 Materials

A moisture susceptible (PI) and a non-moisture susceptible (SM) were used for the study. The mix design details of these mixes were provided in Table 5.1.

Table 5.1. Mix design information for PI and SM mixes

PI mix

NMAS: 12.5 mm (Fine-Graded); N_{design}: 50 gyrations; Asphalt Binder: PG 64-28

Material	Proportions[a]	Sieve Size (mm)	Percent Passing
19 mm		19	100
12.5 mm	86.25%	12.5	90-100
9.5 mm	(Quarry)	9.5	78-90
Classifier Sand		4.75	64-78
Sand	13.75%	2.36	38-46
		1.18	23-31
Asphalt Content	5.9%	0.60	14-20
		0.30	8-12
		0.15	5-9
		0.075	3.9-6.0

SM mix

NMAS: 12.5 mm (Coarse-Graded); N_{design}: 75 gyrations; Asphalt Binder: PG 64-28

Material	Proportions[a]	Sieve Size (mm)	Percent Passing
19 mm	73.75% (Quarry)	19	100
12.5 mm		12.5	90-100
9.5 mm		9.5	74-88
Sand	26.25 %	4.75	43-57
		2.36	31-39
Asphalt Content	5.4%	1.18	20-28
		0.60	13-19
		0.30	8-12
		0.15	5-9
		0.075	3.5-7.0

[a]Batches made by stockpile sizes after washing, drying and separating into different sizes based on the source (Quarry/ Natural Sand).

5.3 Methods

The test plan for this study is shown in Figure 5.1.

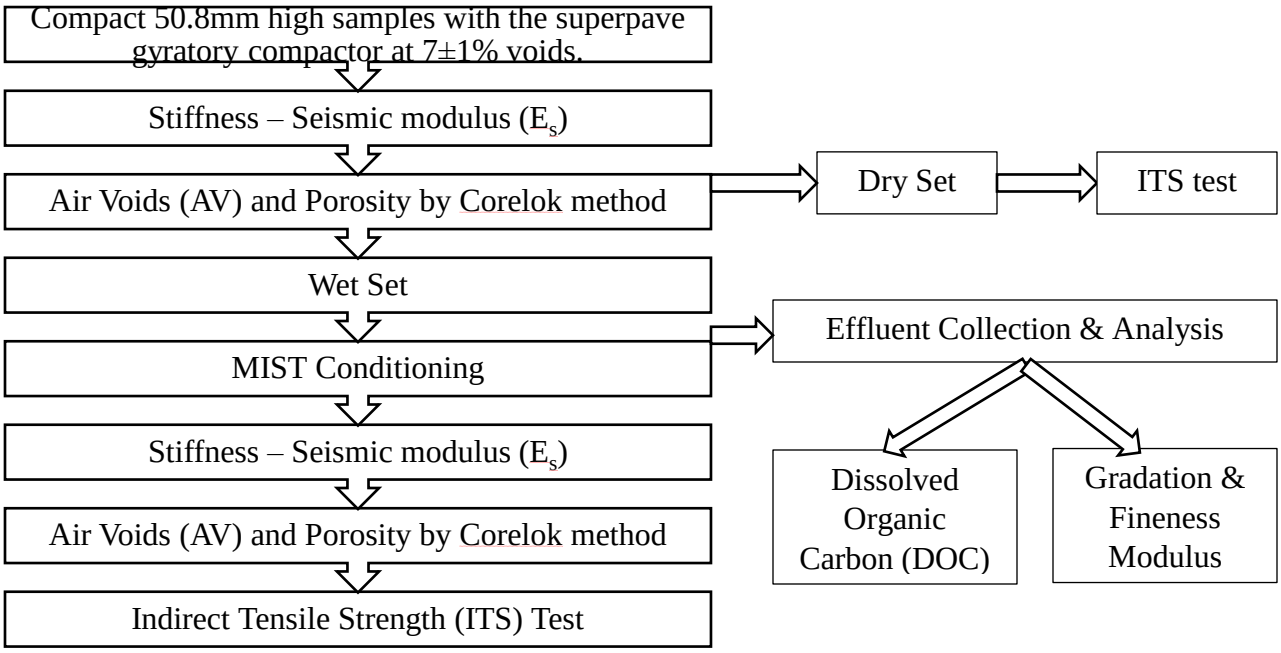

Figure 5.1 Test Plan – Main study

The methods are as described in previous chapters except the following.

5.3.1 Moisture Conditioning - MIST

A MIST protocol of 10,000 cycles at 60^0C and 207 kPa (30 psi) with a pre MIST dwell of 20 hours at 60^0C was used.

5.3.2 Seismic Modulus

The seismic modulus measurements were taken according to the method described in section 3.1.2.3 with following revisions to the test parameters:

i. Transducers: An erratic travel time measurement would be possible from an incomplete longitudinal compression wave (P-waves) within the specimen and also from the effects of specimen boundary. So, it is advisable to have at least two complete passes of P-waves within the specimen to get a representative travel time. Therefore, a higher frequency transducers, (150kHz) were considered for the study instead of the previously used 54 kHz

frequency transducers based on the following calculations (P.C with Soheil Nazarian and Ilker Boz, 2016).

Minimum theoretical thickness, mm = Maximum of 2 * (wave length) or 2 * top size aggregate

Where, Wave length, mm = compression velocity/frequency

= 2* (3800/150) or 2*25

= 51 or 50 mm [51 mm or 2 inch]

ii. Coupling agent: The high vacuum grease was replaced with lubricating gel for the following reasons:
    a. To avoid clogging of specimen voids due to the use of high vacuum grease
    b. To avoid contamination of post MIST water samples which are considered for effluent analysis

Also, to capture the effects of moisture damage, the locations of the travel time readings on the dry samples were marked (5 spots) on the specimen using a fabricated template, such that the testing on the wet samples could be done on the same exact spots.

5.3.3 Image Analysis

Amelian et al. (2014) investigated the digital image analysis approach to objectively evaluate boiling water test instead of regular subjective visual assessment, and also studied the relationship between the results of image analysis and AASHTO T 283 test. The authors concluded the image analysis approach was able to detect stripping from boiling water test and also a good correlation was found between stripping percentages of samples from boiling water test using image analysis and indirect tensile strength test results. The results of AASHTO T 283 with TSR showed a good correlation with the results of boiling water test. Hamzah et al. (2014) studied the fracture surfaces of failed specimens in direct tension mode after F-T conditioning using image analysis technique, to determine the nature of failure – adhesion or breakage of aggregates. The authors concluded that the image analysis technique was effective in visualizing the stripping failures due to moisture conditioning. The image analysis also revealed the fact that the PG 76 binder mixtures were prone

to breakage of aggregates due to the lower percentage of adhesive failures whereas the PG-64 binder mixtures showed an opposite trend.

A high-resolution 16.1 megapixel digital camera was used to take pictures of sample surface before and after MIST conditioning, under similar conditions. To quantify the changes in the pictures of sample surface due to MIST conditioning, number of black pixels for each picture was determined. A pixel with a RGB threshold value less than or equal to 50 was considered as black pixel. The number of black pixels associated with each image were counted by a Python based application software (P.C with Mohammed Salhi, 2017).

5.4 Results and Discussion

Table 5.2 shows the results of volumetric and mechanical tests, and effluent analysis of the PI and SM mixes at two different air void contents – 10±1 & 7±1%.

Table 5.2 Results of Volumetric, Mechanical and Effluent Analysis

MIX	Before MIST Conditioning				After MIST Conditioning				Effluent Analysis		
	Air Voids (%)	Porosity (%)	Seismic Modulus (Mpa)	ITS (kPa)	Air Voids (%)	Porosity (%)	Seismic Modulus (Mpa)	ITS (kPa)	**LOM (gm)**	**FM**	**DOC (ppm)**
PI	10.6	9.1	10656	420	9.8	6.7	10774	406	0.0367	1.21	1.599
PI	9.7	8.8	12061	476	9.1	7.1	12107	548	0.0494	1.78	0.914
PI	9.5	8.7	11964	489	9.2	7.1	11867	502	0.9398	1.11	2.141
PI	6.9	5.1	12803	717	7.5	4.2	12419	456	0.017	1.56	0.944
PI	6.5	4.3	13437	720	7.6	5.3	12545	528	0.021	0.97	1.090
PI	6.4	4.9	13551	681	6.8	4.4	12895	566	0.047	1.96	2.186
SM	12.0	10.6	11014	625	11.3	9.3	11632	363	0.1162	3.15	1.405
SM	10.0	8.4	12279	570	9.8	8.5	11375	533	0.0358	2.96	1.736
SM	10.1	8.8	12284	555	9.8	8.2	11932	520	0.0849	2.41	1.694
SM	7.6	5.9	13222	644	9.5	7.09	13126	478	0.0523	3.73	0.856
SM	7.2	5.5	14427	615	7.2	5.9	13392	597	0.0864	2.51	1.553
SM	6.7	5.3	14522	601	6.9	5.5	13909	616	0.0300	2.86	2.927

Table 5.3 Average Values of Volumetric, Mechanical properties and Effluent Analysis

MIX	Before MIST Conditioning				After MIST Conditioning				Effluent Analysis		
	Air Voids (%)	Porosity (%)	Seismic Modulus (Mpa)	ITS (kPa)	Air Voids (%)	Porosity (%)	Seismic Modulus (Mpa)	ITS (kPa)	**LOM (gm)**	**FM**	**DOC (ppm)**
PI	9.9	8.9	11560	462	9.3	7.0	11583	485	0.342	1.37	1.551
PI	6.6	4.8	13264	706	7.3	4.7	12619	517	0.028	1.50	1.407
SM	10.7	9.3	11859	583	10.3	8.7	11646	472	0.079	2.84	1.612
SM	7.2	5.6	14057	620	7.9	6.2	13476	564	0.056	3.03	1.779

5.4.1 Effect of Air voids

Figure 5.2 and 5.3 shows the percentage change in air voids and porosity due to MIST conditioning of PI and SM mixes. The samples at higher Pre MIST air void contents showed positive percentage change in air voids indicating compaction whereas those at lower construction voids showed negative percentage indicating dilatation.

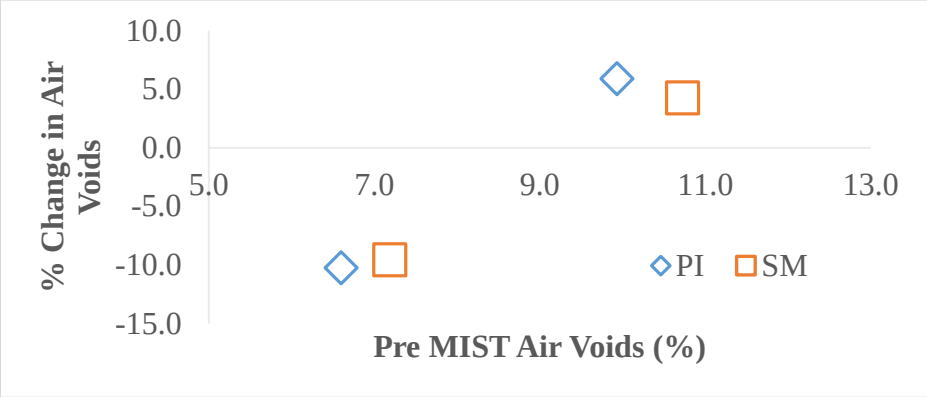

% change = ((Pre – Post)/Pre)*100

Figure 5.2 Average %Change in Air Voids due to MIST Conditioning

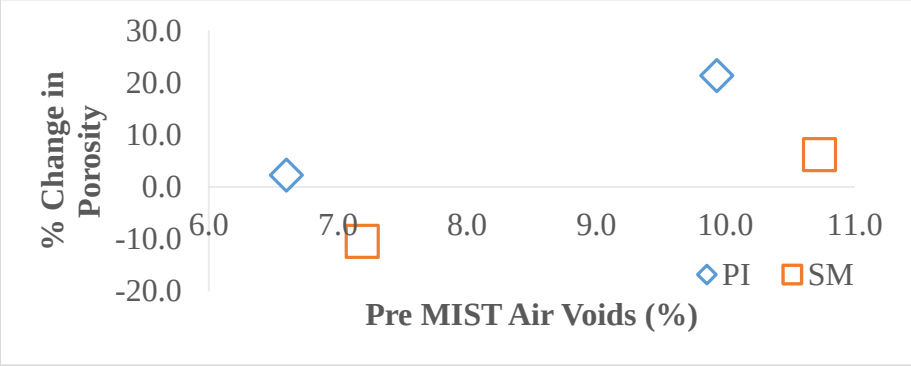

Figure 5.3 Average % Change in Porosity due to MIST Conditioning

Figure 5.4 and 5.5 shows the percentage change in modulus and strength due to MIST conditioning in PI and SM mixes. It is suspected that the part of loss in modulus especially at higher air voids could be masked by the effect of compaction. It is evident from lower percentage change in modulus and strength at higher air void contents which could be due to higher post MIST modulus values due to the masking effect. Therefore, the data associated with 10% air voids is not considered for further analysis in this study.

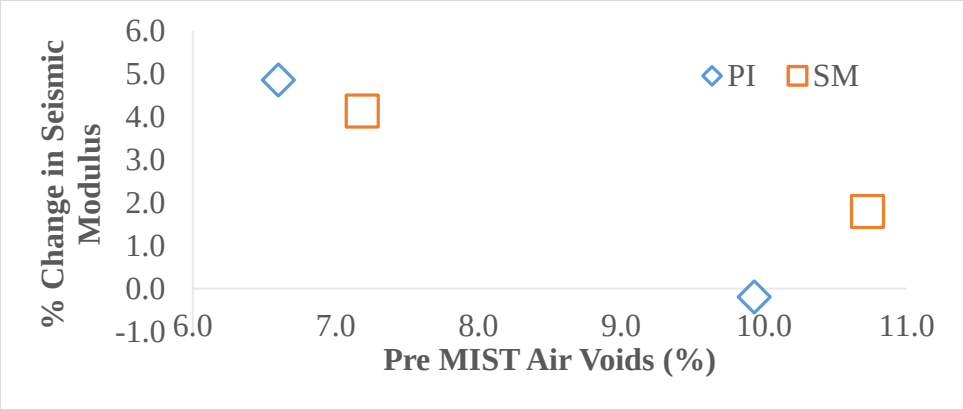

Figure 5.4 Average %Change in Seismic Modulus due to MIST Conditioning

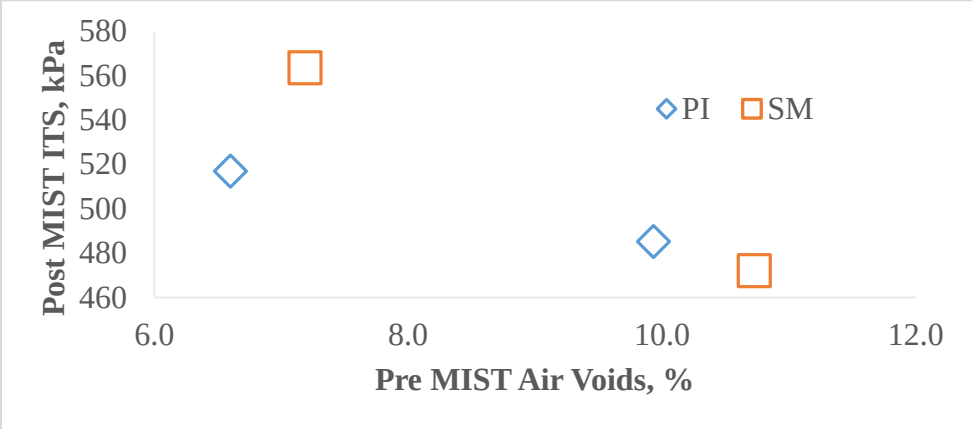

Figure 5.5 Average % Change in indirect tensile strength due to MIST Conditioning

5.4.2 Stiffness

Table 5.4 shows the results of seismic modulus tests for PI and SM mixes at 7±1% air voids. On an average, the loss in modulus was higher in the case of PI mix as compared to SM mix (Figure 5.6). A paired t test conducted upon these results showed that the change in seismic modulus in the case of PI mix was significantly different whereas it was insignificant in the case of SM mix (Table 5.5).

Table 5.4 Results of Seismic Modulus

MIX	Seismic Modulus (Mpa)	
	Before MIST	After MIST
PI	12803	12419
PI	13437	12545
PI	13551	12895
SM	13222	13126
SM	14427	13392
SM	14522	13909

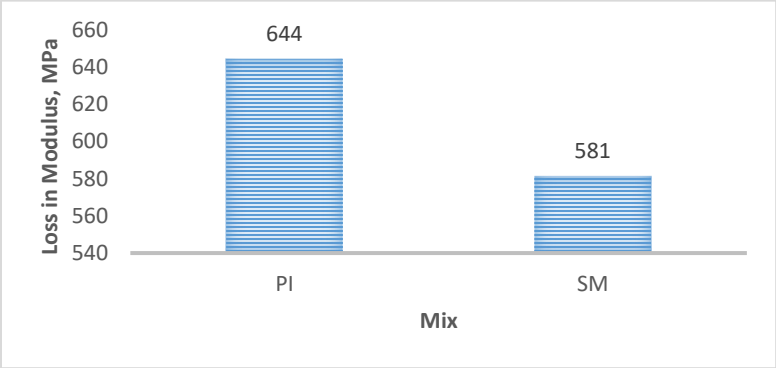

Figure 5.6 Average values of loss in Seismic Modulus

Table 5.5 Statistical Analysis – Seismic Modulus - PI and SM mixes @10,000 MIST cycles

Mix	Mean	Std. Deviation	Std. Error Mean	t	df	Sig. (2-tailed)
PI	644.0	254.21	146.77	4.388	2	.048
SM	581.3	470.30	271.53	2.141	2	.166

5.4.3 Strength

Table 5.6 shows the results of indirect tensile strength for PI and SM mixes at 7±1% air voids. On an average, the loss in strength and also the post-MIST ITS were lower in the case of PI mix when compared to SM mix (Figure 5.7). A paired t test conducted upon these results showed the change

in ITS in the case of PI mix was significantly different whereas it was insignificant in the case of SM mix (Table 5.7).

Table 5.6 Results of Indirect Tensile Strength (ITS)

Mix	ITS (kPa)	
	Before MIST	After MIST
PI	717	456
PI	720	528
PI	681	566
SM	644	478
SM	615	597
SM	601	616

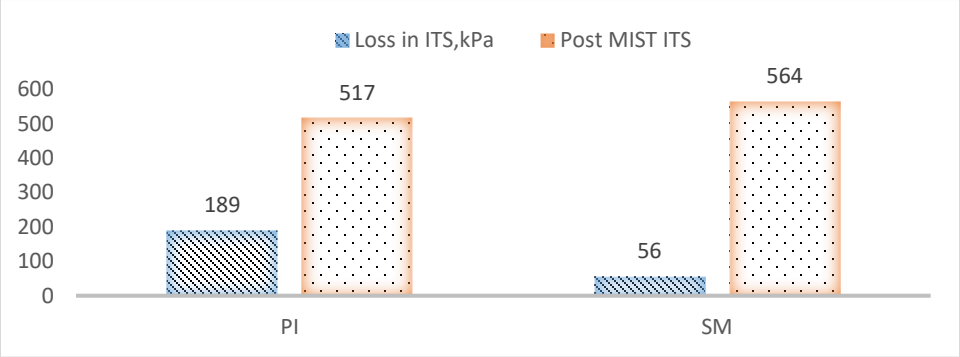

Figure 5.7 Average values of loss in ITS and post-MIST ITS

Table 5.7 Statistical Analysis – ITS - PI and SM mixes @10,000 MIST cycles

Mix		Sum of Squares	Df	Mean Square	F	Significance
PI	Between Variation	53804.6	1	53804.6	29.712	**0.006**
	Within Variation	7243.6	4	1810.9		
	Total Variation	61048.2	5			
SM	Between Variation	4735.0	1	4735.0	1.562	0.279
	Within Variation	12125.0	4	3031.3		
	Total Variation	16860.0	5			

5.4.4 Strength and Modulus

The rate of change in ITS, that was calculated by knowing the conditioning period of 10 hours, was seen to have a good correlation with the pre-MIST seismic modulus (Es) (Figure 5.8). This can be explained by the fact that mixes with higher stiffness experience lower strain under the applied stress in the MIST and are hence less susceptible to deterioration of the mix. The equation developed from the pooled data of SM and PI mixes is as follows:

Rate of Change in ITS, kPa, per hour = 219.21 - 0.0151*(pre-MIST Es) (5.1)

R^2 = 0.95; Where Es = pre-MIST Seismic Modulus

This equation can be utilized to estimate the loss of ITS throughout the design life of the pavement, if the number of hours the pavement is subjected to moisture is known. The data can then be utilized to estimate the minimum initial E_s that is required to ensure a minimum ITS of the mix throughout the design life.

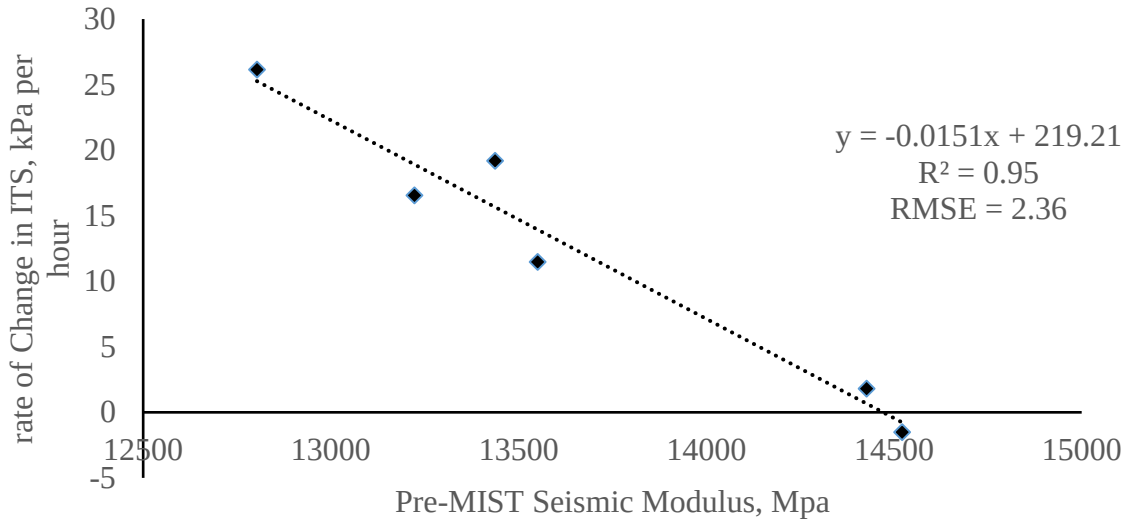

Figure 5.8 Plot of pre-MIST Seismic Modulus versus rate of change in ITS as a result of moisture conditioning

The relationship presented in Equation 5.1 can be explained as follows. The change in tensile strength in mixes during the conditioning process is due to the growth of cracks formed by the repeated/pulse stressing the mix in water. The dependence of the crack growth rate (at a specific temperature) on the material is exhibited by the relationship between the rate of change in the

indirect tensile strength and the pre-conditioning Seismic Modulus value. The equation can also be utilized to estimate the expected change in ITS due to an expected variation in the pre-MIST Seismic Modulus.

5.4.5 Monte Carlo Simulation – Pooled data

For the data used in this study, a mean and a standard deviation of 13,660 MPa and 681 MPa were observed for the pre-MIST Seismic Modulus. Utilizing these values, a Monte Carlo simulation of the change in ITS, was conducted and the results are shown in Figure 5.9. The 90% confidence interval for loss of ITS (per hour of moisture conditioning) is -4 to 30 kPa, with a mean of 13 kPa per hour.

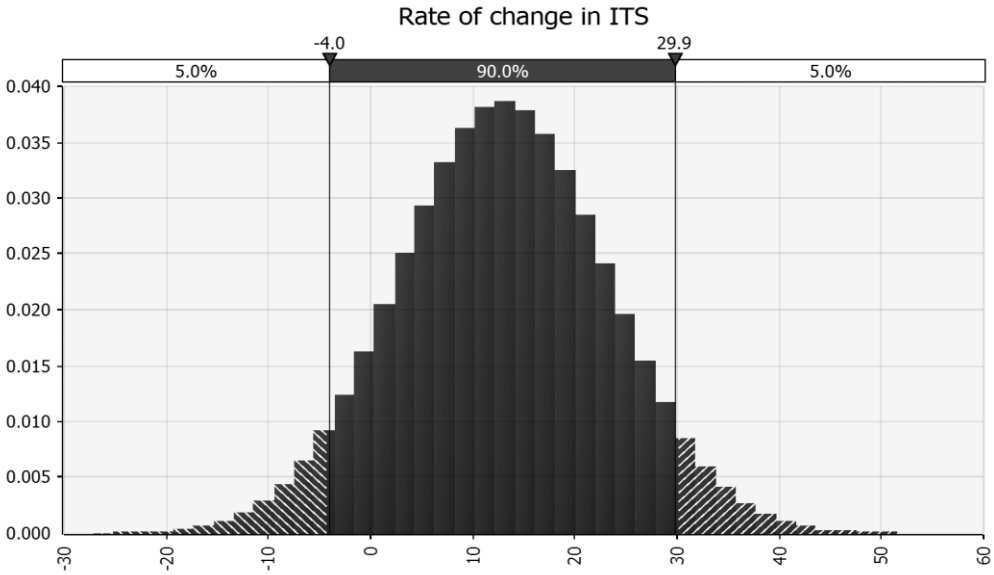

Figure 5.9 Results of Monte Carlo analyses for rate of change in Indirect Tensile Strength, considering pooled data

5.4.6 Estimation of Pre-MIST Threshold Values

Since the PI mix is identified as a moisture susceptible mix, and the SM is identified as a non-moisture susceptible mix, the mean and standard deviation values of the pre-MIST E_s were utilized separately to determine the expected range of change in ITS by conducting a Monte Carlo analysis. The results (Figure 5.10) show a 90% confidence interval of 9 to 27 kPa per hour for the PI mix and -11 to 25 kPa per hour for the SM mix. Note that the average predicted rate of change for the PI and the SM mixes are 19 and 7 kPa per hour respectively.

As mentioned in Chapter 4.1: Study upon 26 HMA mixes from MDOT, it showed that the two poor performing mixes have ITS values at or below 500 kPa whereas the good performing ones have >500 kPa post-MIST ITS values (Figure 5.11). Hence 500 kPa can be taken as a minimum desirable ITS after the expected number of hours of moisture damage for adequate performance of a mix in the field. Therefore, knowing the number of hours of expected moisture damage conditioning (or exposure to moisture in the field), and taking the minimum value of 500 kPa, it is possible to estimate a threshold value of pre-MIST Es for different values of Pre-MIST ITS, using Equation 5.1 (Figure 5.12).

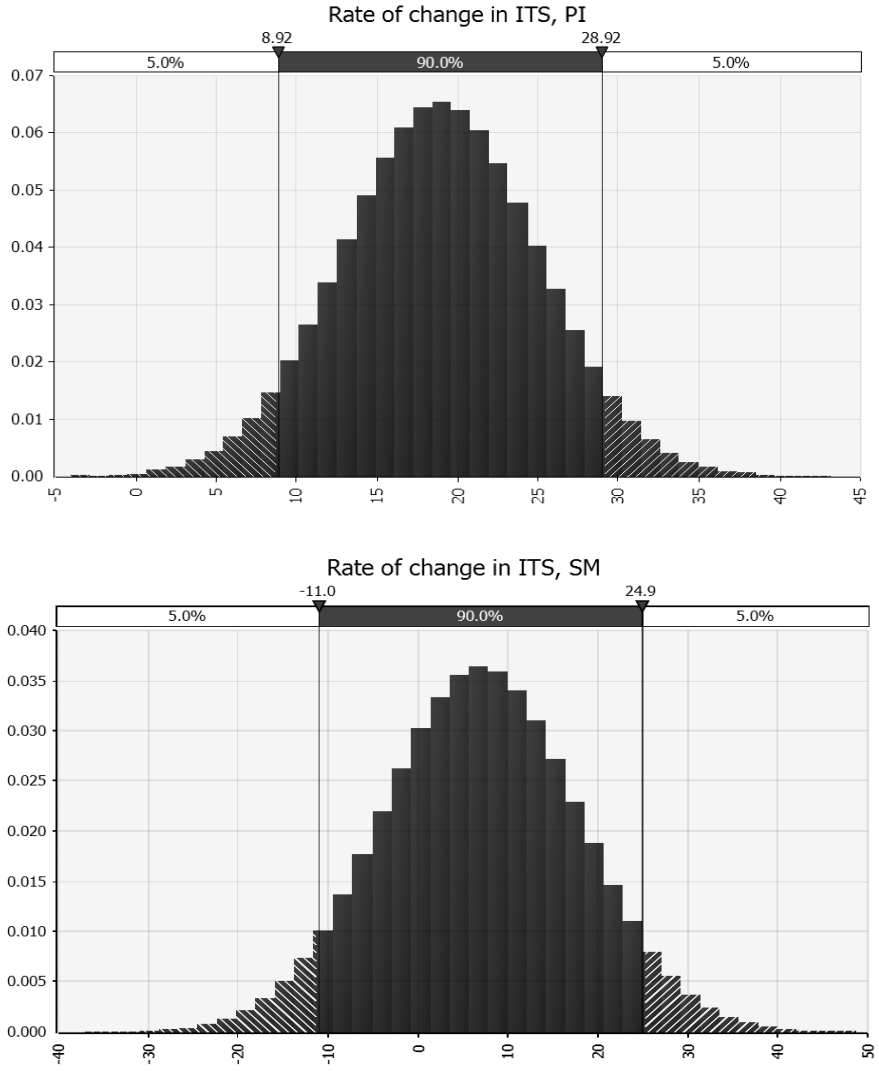

Figure 5.10. Results of Monte Carlo analyses for rate of change in Indirect Tensile Strength, considering PI and SM mixes

The utilities of the plots presented in Figure 5.12 are as follows:

- Both MIST conditioning and Indirect Tensile Strength tests are time consuming, and a desirable option will be to minimize the chance of finding out, after MIST conditioning, that the mix does not meet the minimum retained strength.
- Instead of using ITS and MIST first, the mix designer can assume a pre-MIST ITS on the basis of his/her experience with similar mixes, check the seismic modulus of the designed mix (which will take a very short period of time and is nondestructive) and then utilize the chart to determine whether the Seismic Modulus meets the minimum value for the specific time of conditioning.
- Then the same samples could be utilized for pre-MIST indirect tensile strength tests. If after testing, the strengths are higher than what were assumed, the mix can be assumed to be adequately resistant as the minimum required seismic modulus value decreases with an increase in the pre-MIST ITS, for a specific duration of moisture conditioning.
- If however, the strength is found to be lower than the assumed value, the designer can improve the mix design. This will help the agency to reduce the chance of ending up with mixes that fail to meet the minimum post-conditioning ITS requirement, and reduce the time of actual MIST conditioning.

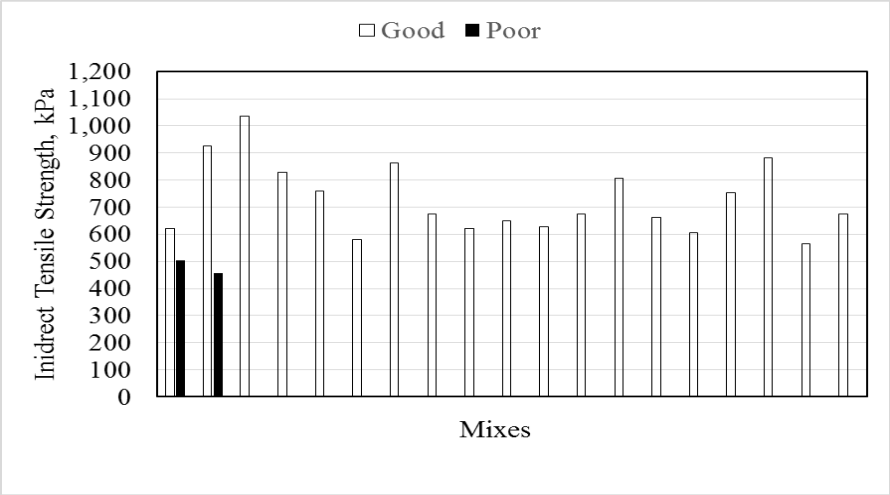

Figure 5.11. Plots of post-MIST ITS versus observed field performance

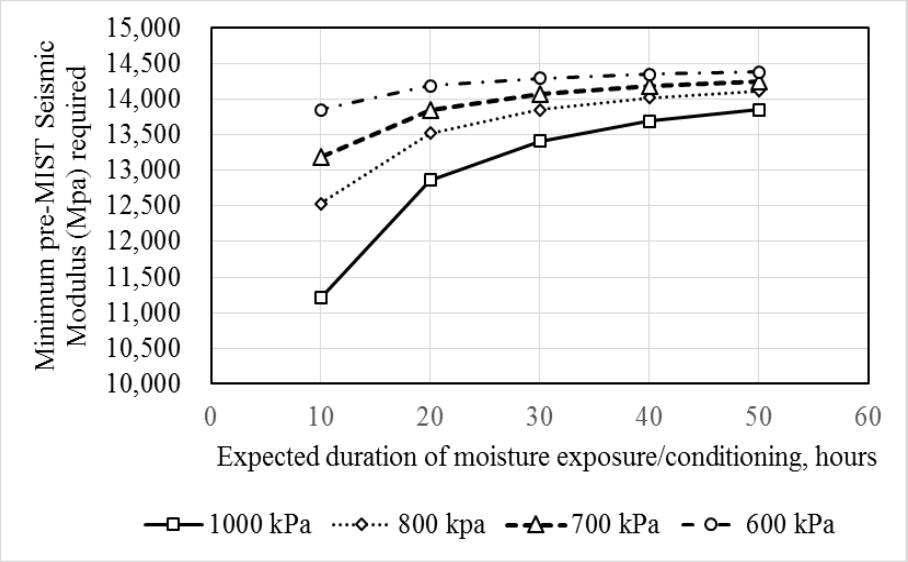

Figure 5.12. Plots of threshold values of pre-MIST Seismic Modulus versus duration of moisture conditioning for different pre-MIST ITS

5.4.7 Comparison of the loss in properties – Radar Chart

The present study evaluated a number of properties of the two mixes. Figure 5.13 combines the data for the loss in three different properties – modulus, strength and materials, due to the moisture conditioning process for the two mixes. A similar chart could be used to evaluate and compare mixes during regular mix design. A mix with a smaller footprint area in the chart is expected to be with a higher resistance against moisture damage. It also shows the relative impact of moisture on the three different properties. In this case, it can be seen that even though the SM mix loses a higher amount of material, the loss in stiffness and strength are comparatively lower, most likely because of the better quality of aggregates. On the other hand, because of the soft aggregates, the PI mix shows a much higher loss of stiffness and strength. A template chart with a footprint area of a good performing mix could be utilized to evaluate new mixes during the mix design process.

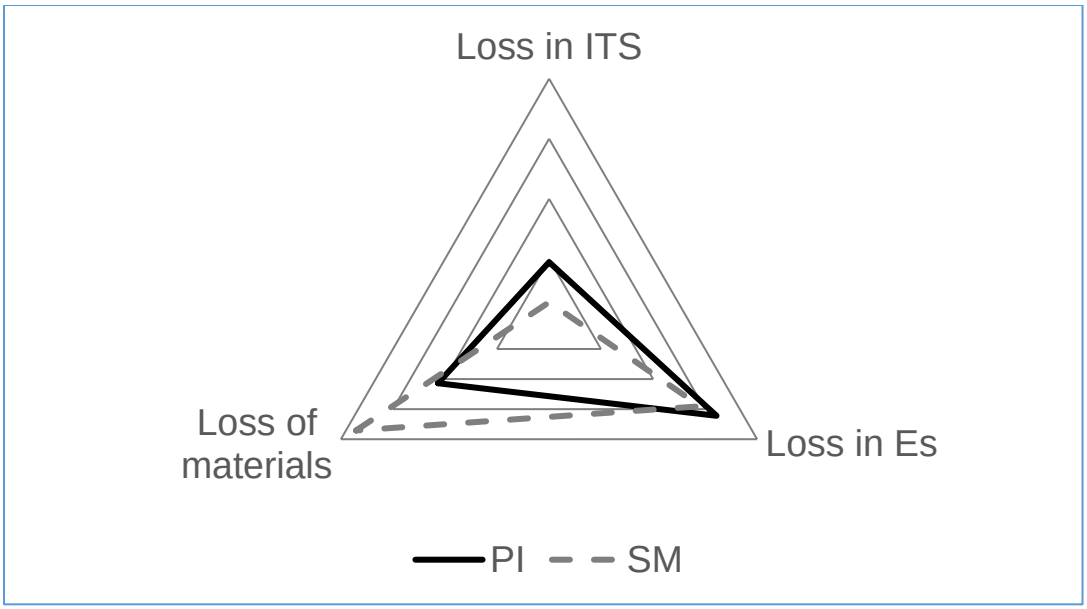

Figure 5.13. A comparison of the loss in properties of PI and SM mixes

5.4.8 Effluent Analysis

Table 5.8 and Figure 5.14 show the results of effluent analysis on PI and SM mix specimens at 7±1% air voids. Though the loss of material (LOM), Dissolved Organic Carbon (DOC) contents and Fineness Modulus (FM) between PI and SM mixes were not statistically significant (Table 5.9), SM mix showed higher values than PI mix (Figure 5.14). It is suspected that the lower value of FM, which indicates a finer gradation, of the PI mix is due to the damage (for example by fracturing) of the relatively soft aggregates whereas changes in the SM mix are due to partial loss of asphalt binder and aggregates/mastic (Figure 5.15). Even though the PI mix has been reported to be showing materials loss in the field, both the mixes showed some loss during the conditioning process (not significantly different). This means that the loss of materials, as detected from the effluent, is not a causal factor for the differences in performance of the mixes – rather, it is an indication of the type and amount of material that can be expected from the two mixes, as a result of the moisture damage.

Table 5.8 Results of Effluent Analysis

Mix	Effluent Analysis		
	LOM (gm)	FM	DOC (ppm)
PI	0.017	1.56	0.944
PI	0.021	0.97	1.090
PI	0.047	1.96	2.186
SM	0.052	3.73	0.856
SM	0.086	2.51	1.553
SM	0.030	2.86	2.927

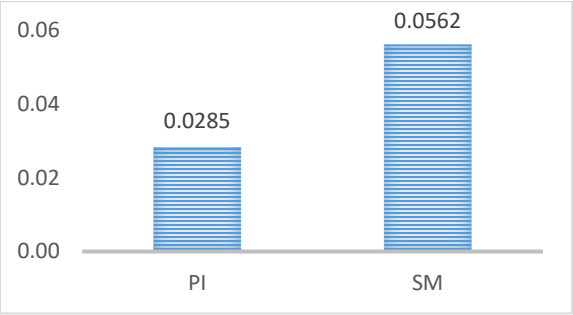

(a) Loss of Material

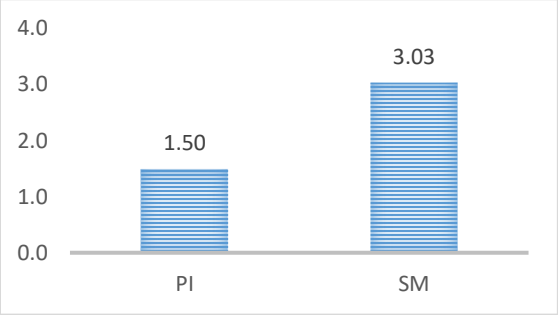

(b) Fineness Modulus

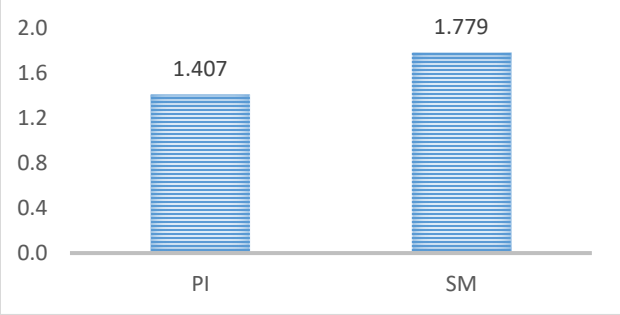

(c) Dissolved Organic Carbon (DOC)

Figure 5.14 Results of Effluent Analysis – LOM, FM & DOC

Table 5.9 Statistical Analysis – ANOVA of results of Effluent Analysis

Mix		Sum of Squares	Df	Mean Square	F	Significance
DOC	Between Variation	0.208	1	0.208	0.264	0.634
	Within Variation	3.143	4	0.786		
	Total Variation	3.350	5			
LOM	Between Variation	0.0012	1	0.0012	2.160	0.216
	Within Variation	0.0021	4	0.0005		
	Total Variation	0.0033	5			
FM	Between Variation	3.5420	1	3.5420	11.023	**0.029**
	Within Variation	1.2853	4	0.3213		
	Total Variation	4.8274	5			

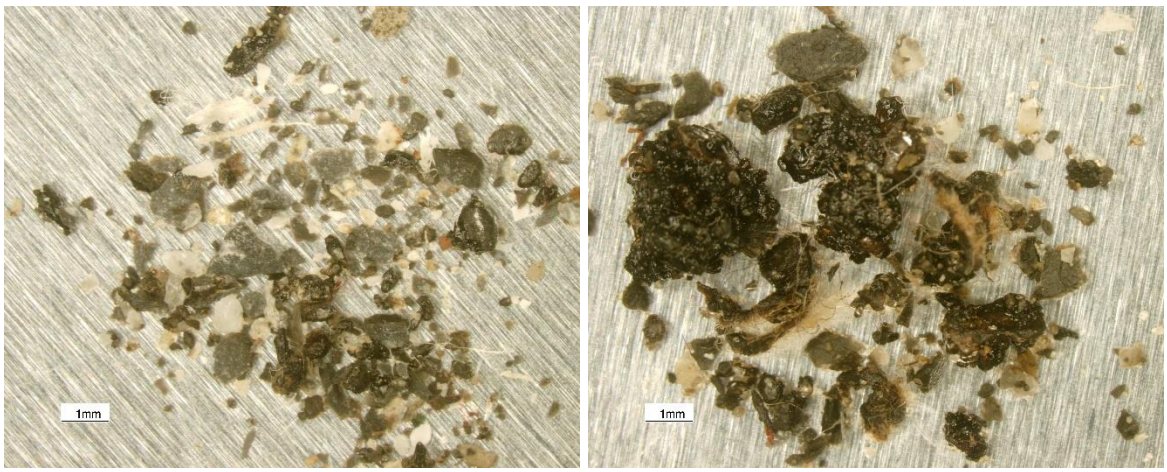

(a) PI mix **(b) SM mix**

Figure 5.15 Typical materials collected from the effluent after MIST conditioning – 1X Magnification

5.4.9 Relations between effluent and mechanical properties

The Dissolved Organic Carbon (DOC) content is observed to have a positive correlation with post-MIST ITS (Figure 5.16). The correlation in Figure 5.16 can be explained by the fact that a higher DOC indicates a higher loss of asphalt binder from the mix, and mixes with reduced

asphalt content are expected to be at higher tensile strength. This observation is important since in many cases designers rely on the retained strength or the post conditioning strengths only, to evaluate the mix's resistance against moisture damage. While this is a reasonable approach, it should be used with caution since, a loss of the binder, which is a precursor to more serious damage of loss of aggregates and gradual loosening of mix in the field, may falsely indicate a high resistance against moisture damage after the laboratory conditioning process.

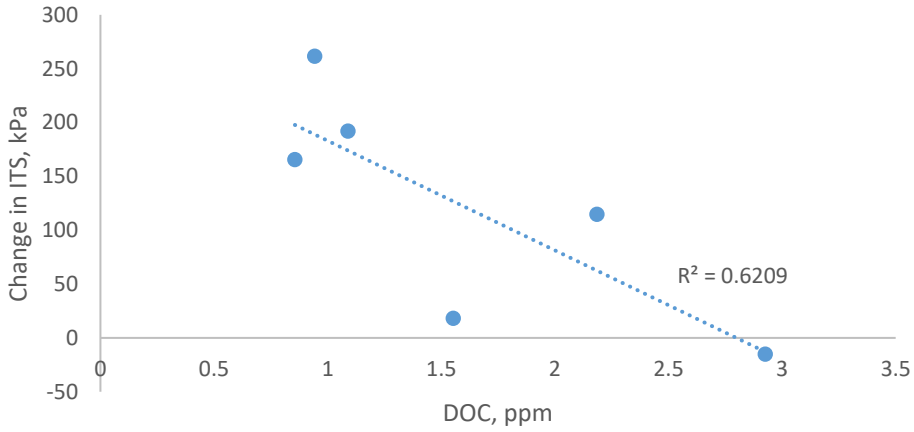

Figure 5.16 Change in ITS Vs. DOC

The fineness modulus (FM) of the aggregate material lost during the MIST conditioning shows a negative correlation with change in indirect tensile strength as a result of MIST conditioning (Figure 5.17). This is because, a lower FM indicates a finer gradation, and a finer gradation indicates more breakdown of larger aggregates, which would have a higher weakening effect on the strength of the mix. A higher FM most likely means that larger size aggregates are displaced by moisture, as whole particles, and there is relatively less aggregate breakdown in the mix. This is evident from a higher FM for the materials lost by the SM mix, as compared to that of the PI mix (Figure 5.14 (b)). Note that an outlier was removed from the dataset, which improved the correlation significantly.

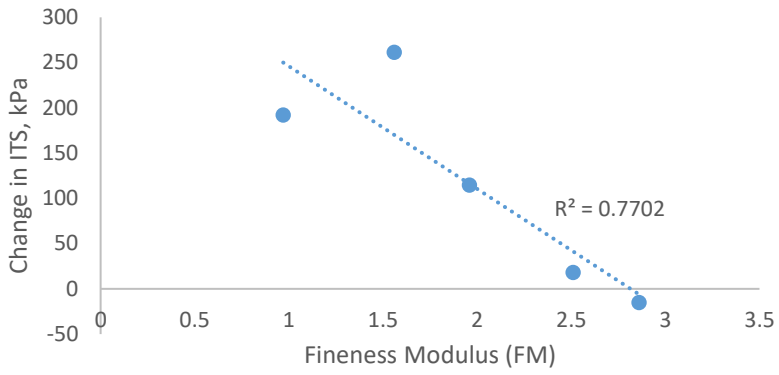

Figure 5.17 Change in ITS Vs. Fineness Modulus

5.5 Effect of Lime on moisture damage

Hydrated lime is the most commonly used anti stripping agent to improve the performance of hot mix asphalt against moisture induced damage (Gorkem and Sengoz 2009; Huang et al. 2005; Zou et al. 2016). The addition of hydrated lime to aggregates reduces the acidic nature of aggregates leading to improved adhesion between aggregates and asphalt binder (Nejad et al. 2013). Improved characteristics such as mastic stiffening, toughening, and advanced bonding characteristics at mastic-aggregate interfaces due to the use of hydrated lime were reported by Kim et al. (2008).

In this study, samples of PI and SM mix with lime were prepared by adding 3% (by wt. of aggregates) water followed by spreading 1.5% (by wt. of aggregates) lime to aggregate batches and mixing them together thoroughly. The marinated mixtures were cured for 48 hours at room temperature. A set of three numbers of 50.8 mm high gyratory specimens were prepared at 7±1% and 10±1% air voids, for PI and SM mixes. Table 5.10 and 5.11 shows the results of volumetric, mechanical test properties and effluent analysis of PI and SM mix specimens with lime after MIST conditioning.

Figure 5.18 shows the results of impact of lime on change in ITS values for PI and SM mix. Though, both mixes with lime showed a decrease in change in ITS, the PI mix with lime showed a higher change in ITS value.

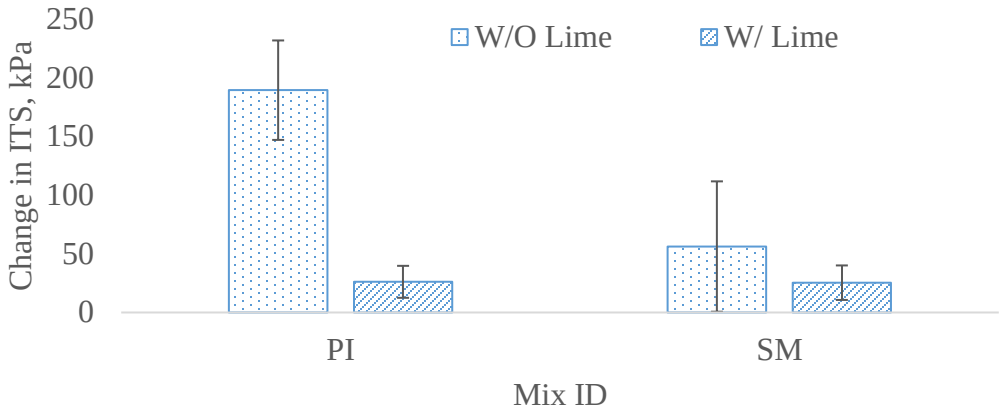

Figure 5.18 Change in ITS with addition of Lime

Figure 5.19 shows the results of change in DOC with addition of lime. Both mixes showed a decrease in DOC with addition of lime.

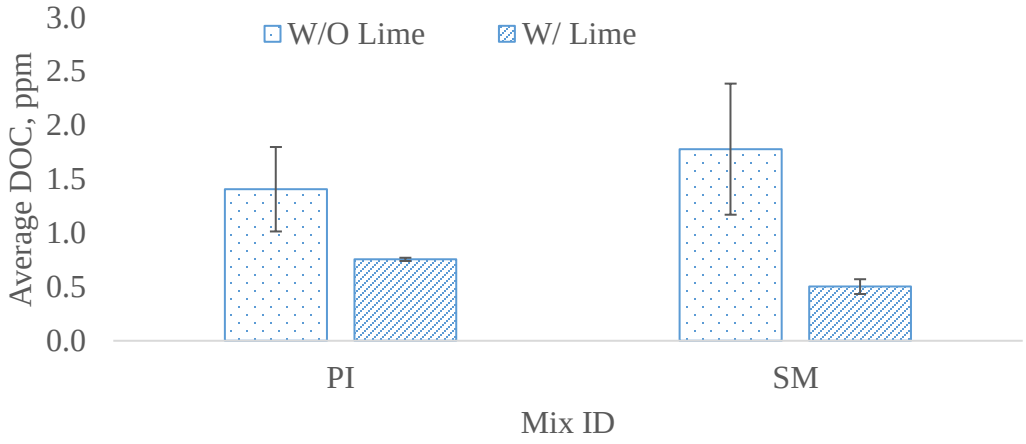

Figure 5.19 Change in DOC with addition of Lime

Table 5.10 Results of PI and SM mix specimens with addition of Lime

MIX	**Before MIST Conditioning**				**After MIST Conditioning**				**Effluent Analysis**		
	Air Voids (%)	Porosity (%)	Seismic Modulus (Mpa)	ITS (kPa)	Air Voids (%)	Porosity (%)	Seismic Modulus (Mpa)	ITS (kPa)	**LOM (gm)**	**FM**	**DOC (ppm)**
PI+L	8.0	6.6	13288	624	7.2	4.8	13570	580	0.0678	1.43	0.766
PI+L	6.0	4.5	14814	581	5.7	3.3	14725	582	0.0642	3.40	0.726
PI+L	8.0	6.5	12854	587	7.4	4.9	12496	551	0.2841	4.78	0.775
SM+L	6.0	4.1	15713	645	6.2	4.5	15411	591	0.0269	2.2	0.407
SM+L	6.1	4.0	16100	589	6.3	4.5	15312	575	0.0354	3.15	0.465
SM+L	6.1	4.2	15571	585	6.4	4.7	14663	577	0.0295	1.97	0.636

Table 5.11 Averaged results of PI and SM mix specimens with addition of Lime

MIX	**Before MIST Conditioning**				**After MIST Conditioning**				**Effluent Analysis**		
	Air Voids (%)	Porosity (%)	Seismic Modulus (Mpa)	ITS (kPa)	Air Voids (%)	Porosity (%)	Seismic Modulus (Mpa)	ITS (kPa)	**LOM (gm)**	**FM**	**DOC (ppm)**
PI+L	7.4	5.9	13652	597	6.8	4.4	13597	571	0.139	3.20	0.756
SM+L	6.1	4.1	15795	606	6.3	4.6	15128	581	0.027	2.20	0.503

5.5.1 Image Analysis – Lime Samples

Table 5.12 shows the results of image analysis of MIST conditioned samples. Though, both mixes showed significant change in black pixels due to MIST conditioning, slightly higher percentage change was found for the PI mix. Also, it is evident from Figure 5.20 that, higher the DOC or LOM higher is the percentage change in number of black pixels.

Table 5.12 Number of Black Pixels – Lime Samples

MIX	Before MIST	After MIST	% Change	Average	P-Value at 95%*
PI+L	2111524	1705867	19.2	21.3	0.0394
PI+L	2270454	1608881	29.1		
PI+L	2221170	1873482	15.7		
SM+L	2313986	1861917	19.5	20.5	0.002
SM+L	2402004	1876144	21.9		
SM+L	2519823	2011506	20.2		

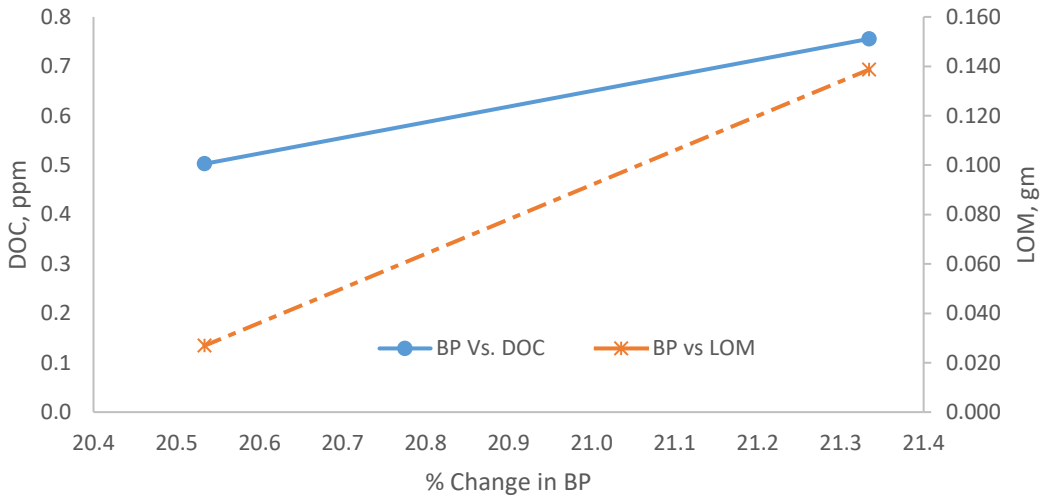

Figure 5.20 DOC and LOM versus % Change in Black Pixels (BP)

The results show that a reduction in black pixels (BP) can be expected for both types of mixes after moisture conditioning.

5.6 Reduction of MIST Conditioning Cycles from 10,000 to 5,000

Each 1,000 cycles in the MIST takes about 1 hour, and hence a reduction in the number of cycles is desirable to limit the total conditioning time. The E_s results from tests conducted with samples conditioned to 15,000 and 10,000 cycles were found to be similar. In both cases significant difference between Es values of pre & post-conditioned samples were found for the PI mixes but not the SM mixes. The effect of MIST conditioning cycles were assessed by reducing the number of cycles from 10,000 to 5,000 (tests were conducted with samples from the PI mix only). The pressure was increased from 138 kPa to 207 kPa and the temperature was increased from 25^0C to 60^0C. Tables 5.13 shows the results of volumetric and mechanical tests, and effluent analysis from samples that were conditioned for 5,000 cycles.

Table 5.13 Results of tests conducted on PI samples conditioned to 5,000 cycles in the MIST

	Before MIST Conditioning				After MIST Conditioning				LOM (gm)	FM	DOC (ppm)
	Air Voids (%)	Porosity (%)	Seismic Modulus (Mpa)	ITS (kPa)	Air Voids (%)	Porosity (%)	Seismic Modulus (Mpa)	ITS (kPa)			
PI	9.6	8.7	12605	420	8.6	6.0	11766	378	0.0168	1.08	1.030
PI	9.6	8.1	11282	476	9.0	6.8	11082	406	0.0207	0.85	0.382
PI	9.2	8.0	12107	489	8.2	6.4	11505	425	0.0366	1.21	0.306
PI	6.5	5.1	13881	717	6.8	4.5	13051	492	0.0564	2.31	1.113
PI	6.6	5.2	13796	720	6.8	4.4	13043	448	0.0378	1.98	0.874
PI	6.6	5.2	13120	681	7.1	4.7	12594	443	0.0449	2.13	0.552

Table 5.14 Average results of tests conducted on PI samples conditioned to 5,000 cycles in the MIST

	Before MIST Conditioning				After MIST Conditioning				LOM (gm)	FM	DOC (ppm)
	Air Voids (%)	Porosity (%)	Seismic Modulus (Mpa)	ITS (kPa)	Air Voids (%)	Porosity (%)	Seismic Modulus (Mpa)	ITS (kPa)			
PI	9.4	8.3	11998	462	8.6	6.4	11451	403	0.025	1.05	0.573
PI	6.6	5.2	13599	706	6.9	4.5	12896	461	0.046	2.14	0.846

Statistical analysis conducted on the results of seismic modulus and indirect tensile strength tests showed similar significance difference as obtained in the case of samples conditioned to 10,000 cycles (Table 5.15). Also no significant difference was found between the results of tests conducted on samples conditioned to 10,000 and 5,000 cycles (Table 5.16). Therefore, it can be inferred that the number of cycles in the MIST, can be reduced to 5,000 cycles for regular testing.

Table 5.15 Statistical Analysis – MIST 5,000 Results

Paired t test						
Property	Mean	Std. Deviation	Std. Error Mean	t	df	Sig. (2-tailed)
Es	703.0	158.05	91.25	7.704	2	.016
AV	-0.3	0.15	0.09	-3.780	2	.063
Poro	0.6	0.15	0.09	7.181	2	.019
ANOVA - ITS						
Property		Sum of Squares	Df	Mean Square	F	Significance
ITS	Between Variation	90285.8	1	90285.8	149.20	**0.0003**
	Within Variation	2420.5	4	605.1		
	Total Variation	92706.3	5			

Table 5.16 ANOVA of mix properties– MIST 10,000 cycles vs. 5000 cycles

Mix		Sum of Squares	Df	Mean Square	F	Significance
%Change in Es	Between Variation	0.1554	1	0.1554	0.0713	0.803
	Within Variation	8.7181	4	2.1795		
	Total Variation	8.8735	5			
Post Indirect Tensile Strength (ITS)	Between Variation	4694.69	1	4694.69	2.43	0.194
	Within Variation	7742.34	4	1935.58		
	Total Variation	12437	5			
%Change in AV	Between Variation	41.5178	1	41.5178	2.202	0.212
	Within Variation	75.4325	4	18.8581		
	Total Variation	117	5			
%Change in Poro	Between Variation	207.67	1	207.667	0.8224	0.416
	Within Variation	1010.06	4	252.515		
	Total Variation	1217.73	5			
Dissolved Organic Carbon (DOC)	Between Variation	0.4710	1	0.471	1.744	0.257
	Within Variation	1.0802	4	0.270		
	Total Variation	1.5512	5			
Loss of Material (LOM)	Between Variation	0.00048	1	0.00048	2.728	0.174
	Within Variation	0.00070	4	0.00018		
	Total Variation	0.00119	5			

5.6.1 Image Analysis - MIST 5,000 Cycles

Table 5.17 shows the results of image analysis from samples that were conditioned to 5,000 cycles. Though, the samples at both air void contents showed significant difference in change in black pixels due to MIST conditioning, a higher change in percentage of black pixels was found for samples with 7% air voids. Also, from the pooled data of both air void contents (Figure 5.22), it is evident that the higher the DOC or LOM higher is the percentage change in number of black pixels. Therefore, it seems that there is loss of materials during the MIST conditioning process and this loss causes a change in the color of the sample.

Table 5.17 Image Analysis - No. of Black Pixels - MIST 5000 Cycles

Mix	Before MIST	After MIST	% Change	Average	P-Value at 95%*
10PI#1	2125332	1934894	9.0	12.8	0.0315
10PI#2	2248670	1882735	16.3		
10PI#3	2519733	2185716	13.3		
7PI#1	2221454	1692525	23.8	22.5	0.0135
7PI#2	2232348	1837086	17.7		
7PI#3	2290760	1692510	26.1		

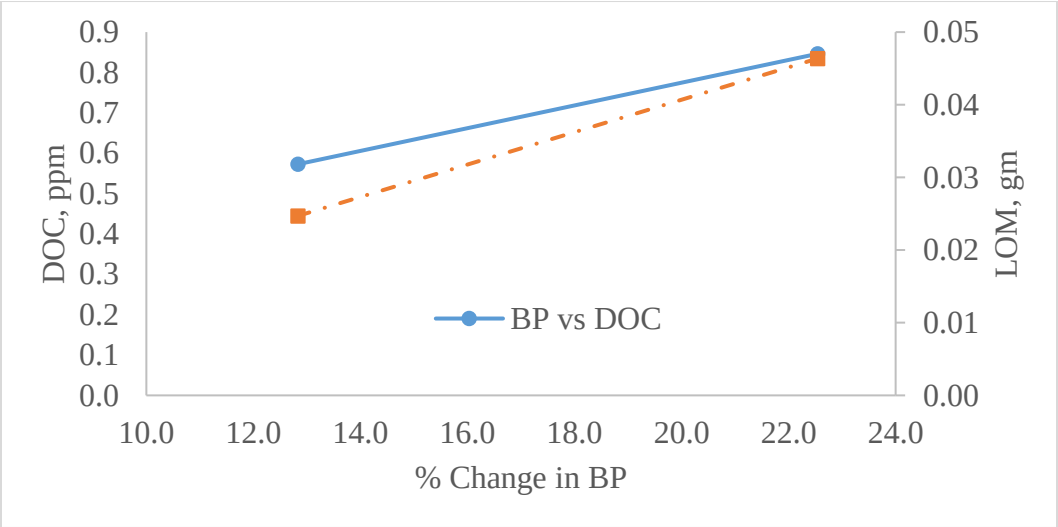

Figure 5.22 DOC and LOM vs. %Change in Black Pixels

5.7 Conclusions and Recommendations

1. The use of the Moisture Induced Stress Tester (MIST) can be considered as an appropriate laboratory conditioning process to simulate combined moisture-traffic induced damage in HMA
2. The dynamic modulus test in indirect tensile mode was found to be insensitive to changes in the mix due to moisture conditioning
3. The Ultrasonic Pulse Velocity (UPV) test was found to be sensitive to changes in mixes as a result of the moisture conditioning process
4. Mixes undergoing a higher loss of asphalt binder during moisture conditioning will exhibit higher tensile strengths.
5. Mixes with aggregate breakdown exhibit lower tensile strengths.
6. The rate of change in indirect tensile strength during moisture conditioning is strongly correlated to the pre-conditioning modulus of the mix, and the proposed equation can be utilized to estimate the loss of strength for a given mix during mix design.
7. Threshold values of seismic modulus of pre-conditioning mixes for different durations of moisture conditioning can be utilized during mix design to screen poor mixes in a fast and nondestructive manner.
8. A combination of the MIST and the UPV and the Indirect Tensile Strength (ITS) test can be used successfully to evaluate the resistance of HMA against moisture damage.
9. The protocol for MIST conditioning is suggested as a combination of a 20 hour dwell period and 5,000 cycles at 207 kPa and 60^0C.

References

Amelian, S., Abtahi, S. M., and Hejazi, S. M. (2014). "Moisture susceptibility evaluation of asphalt mixes based on image analysis." *Construction and Building Materials*, 63, 294-302.

Gorkem, C., and Sengoz, B. (2009). "Predicting stripping and moisture induced damage of asphalt concrete prepared with polymer modified bitumen and hydrated lime." *Construction and Building Materials*, 23(6), 2227-2236.

Hamzah, M. O., Kakar, M. R., Quadri, S. A., and Valentin, J. (2014). "Quantification of moisture sensitivity of warm mix asphalt using image analysis technique." *Journal of Cleaner Production*, 68, 200-208.

Huang, S.-C., Robertson, R. E., Branthaver, J. F., and Petersen, J. C. (2005). "Impact of Lime Modification of Asphalt and Freeze–Thaw Cycling on the Asphalt–Aggregate Interaction and Moisture Resistance to Moisture Damage." *Journal of Materials in Civil Engineering*, 17(6), 711-718.

Kim, Y.-R., Lutif, J. S., Bhasin, A., and Little, D. N. (2008). "Evaluation of Moisture Damage Mechanisms and Effects of Hydrated Lime in Asphalt Mixtures through Measurements of Mixture Component Properties and Performance Testing." *Journal of Materials in Civil Engineering*, 20(10), 659-667.

Nejad, F. M., Hamedi, G. H., and Azarhoosh, A. R. (2013). "Use of Surface Free Energy Method to Evaluate Effect of Hydrate Lime on Moisture Damage in Hot-Mix Asphalt." *Journal of Materials in Civil Engineering*, 25(8), 1119-1126.

Zou, J., Roque, R., Lopp, G., Isola, M., and Bekoe, M. (2016). "Impact of Hydrated Lime on Cracking Performance of Asphalt Mixtures with Oxidation and Cyclic Pore Pressure." *Transportation Research Record: Journal of the Transportation Research Board*, 2576, 51-59.

Chapter 6

Use of System dynamics to understand moisture induced material loss of Hot Mix Asphalt (HMA)

6.1 Objective

The objectives of this phase of the study were to understand the problem of moisture induced material loss of Hot Mix Asphalt (HMA) using systems approach and to develop a system dynamics model.

6.2 System dynamics

System dynamics (SD) is a system based approach (Forrester. 1971; Sterman. 2000) that can be used to map out the different components of a system that is relevant to a problem, and simulate the interactions between them over time. Stocks, flows, converters and connectors are the main components that represent various form of the system model. Generally, the rate of increase or decrease of any parameter is known as "flow" whereas the parameters themselves are indicated as "stocks". In addition there are converters that generate outputs by converting one variable to other variable during each step of the simulation. Finally, there are "connections" that complete the model by linking the different stocks, flows and controllable parameters. The concept is based in numerically integrating sets of equations in a time-step process (for example, through Euler or Runge-Kutta method). The model outputs numerical values at different intervals of time, and they can be utilized for visualizing trends in the changes of different parameters or flow rates. The main utility of SD is not so much as predicting actual numerical values, as it is for predicting trends of the data and evaluating simultaneous and feedback based impacts of multiple factors – something which cannot be achieved through analytical approach. The most powerful feature of this approach is the consideration of the concept of feedback in the model.

Mallick et al. (2013) have studied the benefits of using recycled asphalt pavement (RAP) to avoid the depletion of natural aggregates due to road construction, maintenance and rehabilitation activities, using system dynamics. The authors presented a model that shows all the parameters involved in the process. The several simulations were also conducted to understand the respective effects of aggregate depletion and use of RAP for road construction. The study suggests a high

rate of recycling in order to avoid the depletion of natural aggregates and also the increase in fuel costs involved in transporting natural aggregates. Mallick et al. (2014) have investigated the impact of climate change on the long-term performance of pavements using system dynamics. A model that links all the parameters – climatic, economical and pavement performance that are involved was presented along with various simulations of parameters with respect to time. Mallick et al. (2014) have examined the effects of road construction activities such as depletion of natural aggregates, increase in haul distances, alternative options of recycling and environmental impacts using system dynamics model. Mallick et al. (2015) developed a SD based methodology to assess the vulnerability of roadways to flood-induced damage. Mallick and Solaimanian (2015) have utilized system dynamics model to investigate the performance of Porous Friction Courses (PFC). Mallick and Radzicki (2017) have studied various sustainable policies in road construction using system dynamics modeling approach.

6.3 Moisture induced material loss of Hot Mix Asphalt (HMA)

In general, most of the moisture damage evaluation studies focus on determining the loss of mix properties or performance in the laboratory due to moisture conditioning. However, there is no study found in the literature, so far, that have seen the effects of material lost from the mix and their corresponding impacts upon the mix properties. From the current main study, it was found that the mixes do lose materials in the form of aggregates and/or asphalt binder compounds which could influence the mix properties. Based on the laboratory study and field experience, it has been hypothesized that the mix loses aggregates and asphalt binder with time in the presence of traffic and moisture. Mixes show compaction (air voids are found to decrease over time) along with the loss of material which decreases the mix stiffness and strength gradually. Also, the asphalt binder stiffness increases due to oxidative aging. Several factors, many of which are interrelated, change simultaneously over time, and hence SD was considered to be an appropriate methodology for exploration.

6.4 Model

The moisture induced material loss of material was modeled using an objected oriented program, Stella (ISEE systems inc. 2016). Figure 6.1 presents the system dynamics model for moisture induced material loss of HMA. Table 6.1 and 6.2 show the various parameters and their corresponding equations used in the model. Note that the relations between parameters were developed on the basis of observations from this research.

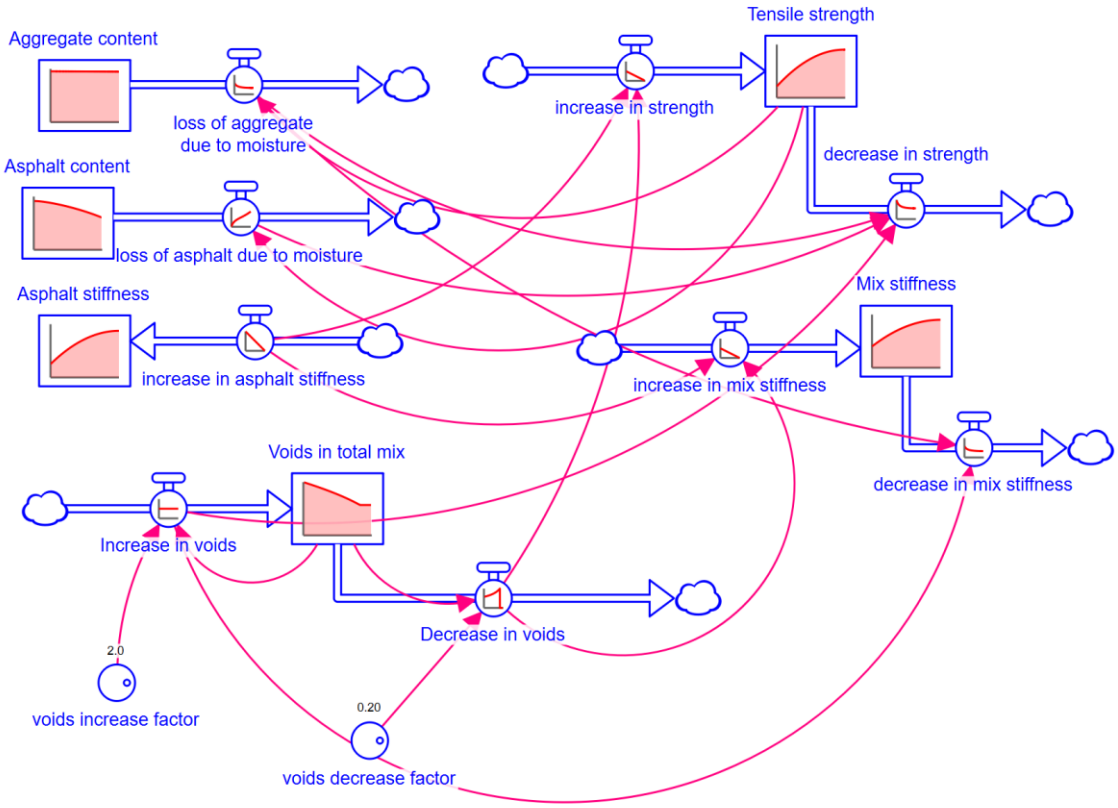

Figure 6.1. Exploratory System Dynamics Model of Moisture induced material loss of HMA

Table 6.1 Details of parameters used in the system dynamics model

Parameter (x)	Initial Value	Remarks
Aggregate content	95.5%	An initial aggregate content of 95.5% was considered and the loss of aggregate content with time was expressed as a function of tensile strength.
Asphalt content	4.5%	An initial asphalt content of 4.5% was considered and the loss of asphalt content with time was expressed as a function of tensile strength.
Asphalt stiffness (dynamic shear modulus, G*)	2,000 MPa	An initial asphalt stiffness of 2,000 MPa was considered and the increase in asphalt stiffness with time was expressed as a function of time.
Voids in total mix	7%	An initial voids of 7% were considered, and a factor of 2 and 0.2 were used to calculate increase and decrease in voids, respectively with time. Note that the increase in air voids was not generally observed with HMA sampels.
Mix stiffness (seismic modulus, Es)	4,000 MPa	An initial mix stiffness of 4000 MPa was considered. The increase in mix stiffness was expressed as a function of increase in asphalt stiffness and decrease in voids whereas decrease in mix stiffness was expressed as a function of loss of aggregates and increase in voids.
Tensile strength	800 kPa	An initial tensile strength of 800 kPa was considered .The increase in strength with time was expressed as a function of increase in asphalt stiffness and decrease in air voids whereas the decrease in strength was expressed as a function of loss of aggregates and asphalt and increase in voids.

Table 6.2. Equations used in the system dynamics model

Aggregate_content(t), % = Aggregate_content(t - dt) + (- loss_of_aggregate_due_to_moisture) * dt *Outflows:* loss_of_aggregate_due_to_moisture = 0.005+10 * 1/ Tensile_strength
Asphalt_content(t), % = Asphalt_content(t - dt) + (- loss_of_asphalt_due_to_moisture) * dt *Outflows:* loss_of_asphalt_due_to_moisture = 2 * TIME / Tensile_strength
Asphalt_stiffness(t), MPa = Asphalt_stiffness(t - dt) + (increase_in_asphalt_stiffness) * dt *Inflows:* increase_in_asphalt_stiffness = GRAPH(TIME) (0.0, 100.0), (10.0, 90.0), (20.0, 80.0), (30.0, 70.0), (40.0, 60.0), (50.0, 50.0), (60.0, 40.0), (70.0, 30.0), (80.0, 20.0), (90.0, 10.0), (100.0, 0.0)
Mix_stiffness(t), MPa = Mix_stiffness(t - dt) + (increase_in_mix_stiffness - decrease_in_mix_stiffness) * dt *Inflows:* increase_in_mix_stiffness = increase_in_asphalt_stiffness + Decrease_in_voids *Outflows:* decrease_in_mix_stiffness = loss_of_aggregate_due_to_moisture + Increase_in_voids
Tensile_strength(t), kPa = Tensile_strength(t - dt) + (increase_in_strength - decrease_in_strength) * dt *Inflows:* increase_in_strength = increase_in_asphalt_stiffness + Decrease_in_voids *Outflows:* decrease_in_strength = loss_of_aggregate_due_to_moisture * 250 + loss_of_asphalt_due_to_moisture + Increase_in_voids * 100
Voids_in_total_mix(t), % = Voids_in_total_mix(t - dt) + (Increase_in_voids - Decrease_in_voids) * dt *Inflows:* Increase_in_voids = IF(Voids_in_total_mix > 8) THEN(Voids_in_total_mix * voids_increase_factor) ELSE(0) *Outflows:* Decrease_in_voids = IF(Voids_in_total_mix > 4) THEN(voids_decrease_factor / Voids_in_total_mix) ELSE(0) voids_decrease_factor = 0.2 voids_increase_factor = 2

6.5 Simulations, Results and Discussion

6.5.1 Reference Mode

Figure 6.2 shows the plots of various parameters with typical values and the corresponding changes over time. The plots provide an understanding of different parameters involved in the system. It was noticed that the loss of aggregate and asphalt binder content along with the deterioration of asphalt properties affect the mix stiffness and tensile strength. The mix stiffness was found to be continuously increasing whereas tensile strength increases to a maximum value and then decreases. Similar trends were also found with laboratory tests and are generally mentioned in the literature.

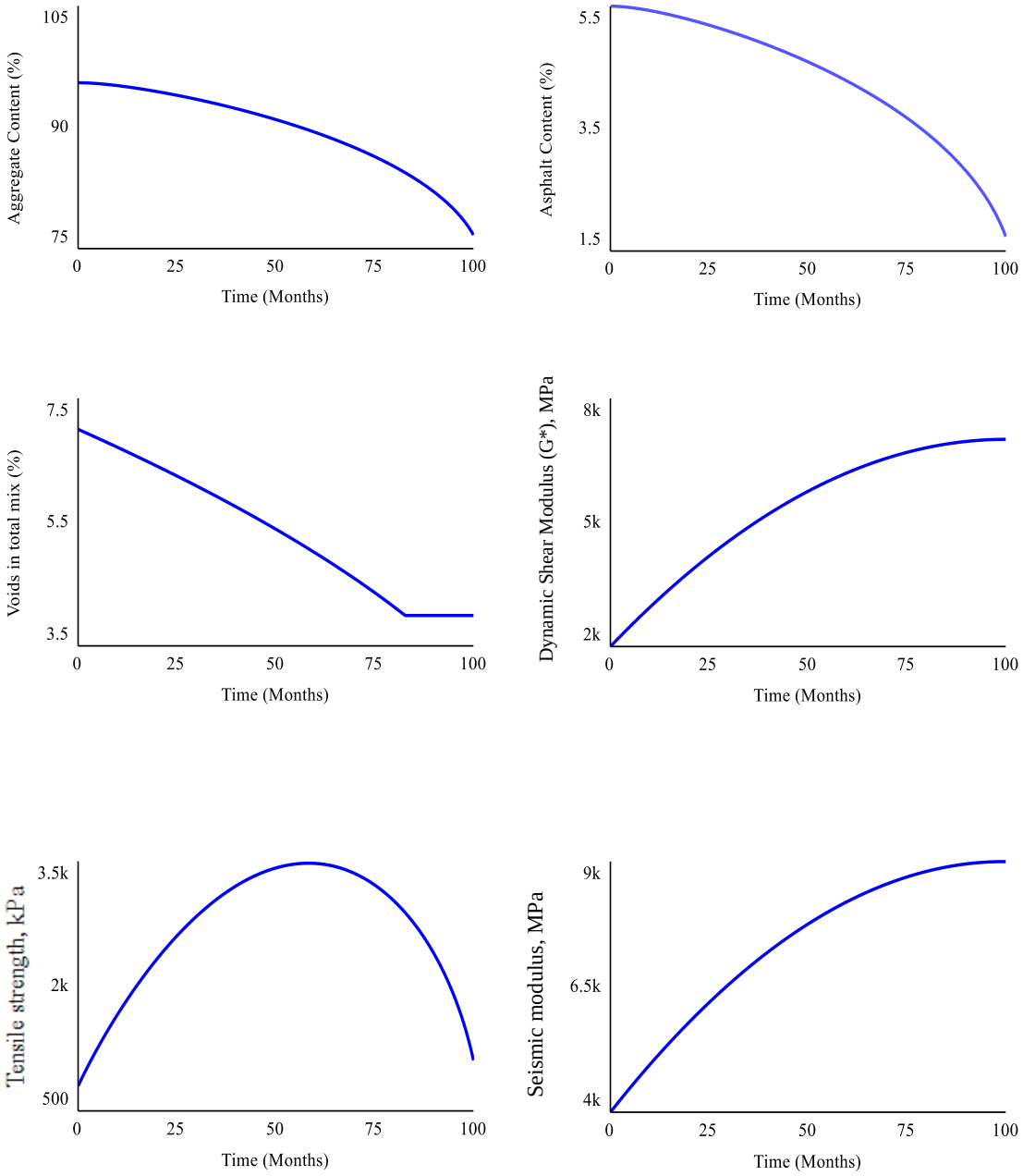

Figure 6.2. Plots of different parameters versus Time (Reference mode)

6.5.2 Tensile Strength

Figure 6.3 shows the results of simulation runs with different initial tensile strength values (600, 800, 1,000 and 1,200 kPa) and their corresponding changes due to moisture conditioning with time up to 10 years. The reuslts capture the siginificant impact of initial tensile strength on the performance of the pavement. A higher initial tensile strength of the mix produces a performance.

The mix with an initial tensile strength of ≤ 600kPa, reached a critical tensile strength of 500kPa (as discussed in Chapter 5.4.6) in less than 8 years whereas a mix with a higher initial strength of ≥ 1000 kPa remained at a higher than the critical tensile strength for the 10 year period. A general understanding from this study is that a mix with inadequate initial tensile strength suffers early damage and results in an increase in the maintenance cost whereas a mix with adequate initial tensile strength serves the entire period without early damages and increase in maintenance costs.

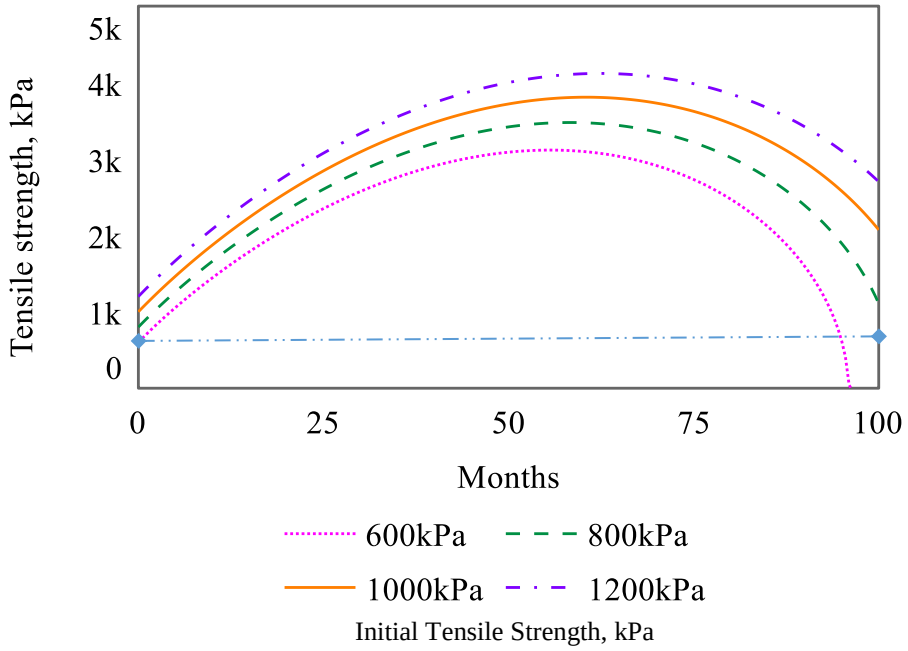

Figure 6.3. Effect of initial tensile strength on moisture damage of HMA

6.6 Conclusions

The system dynamics model was able to simulate the trends of the loss of material and changes in mix properties over time. The time-dependent simulations with various scenarios of initial values would be very helpful to understand the corresponding changes in the pavement performance. The model was successful to demonstrate the changes of each parameter visually through graphs and tables. The accuracy of the model's performance would increase with the use of validated equations and field correlations.

Recommendations

The use of system dynamics for modeling and understanding moisture damage of HMA should be explored. The proposed model can be improved with better equation and correlation that can be obtained from laboratoy and field studies.

References

ISEE systems inc. (2016). STELLA Pro 1.1.2 [software]. Lebanon (NH).

Mallick, R., Radzicki, M., Daniel, J., and Jacobs, J. (2014). "Use of system dynamics to understand long-term impact of climate change on pavement performance and maintenance cost." Transportation Research Record: Journal of the Transportation Research Board(2455), 1-9.

Mallick, R., Tao, M., Daniel, J., Jacobs, J., and Veeraragavan, A. (2015). "Development of a methodology and a tool for the assessment of vulnerability of roadways to flood-induced damage." Journal of Flood Risk Management.

Mallick, R. B., Radzicki, M., Nanagiri, Y. V., and Veeraragavan, A. (2013). "The impact of road construction on depletion of natural aggregates and consequence of delay in recycling pavement-key factors in sustainable road construction." Indian Highways, 41(12).

Mallick, R. B., and Radzicki, M. J. (2017). "Using System Dynamics to Identify, Evaluate, and Implement Sustainable Policies and Practices in the Road Construction Industry." Sustainability Issues in Civil Engineering, Springer, 105-121.

Mallick, R. B., Radzicki, M. J., Zaumanis, M., and Frank, R. (2014). "Use of system dynamics for proper conservation and recycling of aggregates for sustainable road construction." Resources, Conservation and Recycling, 86, 61-73.

Mallick, R. B., and Solaimanian, M. (2015). "Achieving Safer Roads Through the Use of System Dynamics and Porous Friction Courses." Transportation Research Record: Journal of the Transportation Research Board(2524), 71-82.

Forrester JW. (1971). World Dynamics.WrightAllen Press.Cambridge.

KarlssonRobert and IsacssonUlf. (2012). “Investigations on Bitumen Rejuvenator Diffusion and Structural Stability.” Journal of the Association of Asphalt Paving Technologists, (72), 463-501.

Sterman, J.D. (2000). Business Dynamics: Systems Thinking and Modeling for a Complex World, McGraw-Hill (Boston).

Chapter 7

Moisture susceptibility evaluation of asphalt mixes – A framework

Based on this study, it can be concluded that the Moisture Induced Stress Tester (MIST) conditioning along with any one of the mechanical tests - nondestructive ultrasonic pulse velocity (UPV) (recommended) or indirect tensile strength (ITS) can be used to simulate and identify field moisture damage for Hot Mix Asphalt (HMA) in the laboratory. The UPV test is recommended over ITS as the modulus value of the mix can be used in Mechanistic-Empirical (ME) design and life-cycle cost analysis. This information may also be helpful to the pavement agencies while strategizing repairs for the moisture damaged pavement. A framework to utilize the MIST, UPV or ITS is suggested in Table 7.1.

Table 7.1 Framework to evaluate moisture susceptible asphalt mixes with UPV

Step 1

Determine the theoretical maximum density (TMD) of the asphalt mix, separately

Step 2

Fabricate a minimum of three gyratory compacted HMA specimens with construction voids of 7±1% and a thickness of 50 mm

Step 3

Determine the bulk specific gravity (BSG) of HMA specimens using Corelok method

Step 4

Determine the air voids of the HMA specimens based on BSG and TMD

Step 5

UPV: Determine the seismic modulus (Es) of HMA specimens

(Or)

ITS: Determine the indirect tensile strength of three HMA specimens, separately (Dry ITS)

Step 6

UPV: Estimate the design modulus (Ed) using the empirical equation from Es

ITS: Use the other three specimens for moisture conditioning (Wet ITS)

Step 7

Moisture condition the mixes using MIST for 5,000 Cycles at 60^0C and 30 psi with a pre-MIST dwell of 20 hours at 60^0C

Step 8

After conditioning, keep the specimens in a water bath maintained at 25^0C for 2-3 hours and then fan dry the specimens for 3 days

Step 9

UPV: Repeat the steps from 3 to 6

ITS: Repeat the steps from 3 to 5

Step 10

UPV: Determine whether the difference in modulus (Ed) before and after MIST is significant or not, using statistical analysis such as paired t-test. A statistically significant difference in modulus (lower post-MIST modulus) indicates a moisture susceptible mix which can be discarded.

ITS: Determine whether the difference in strength before and after MIST is significant or not using statistical analysis such as one-way ANOVA. A statistically significant difference in strength indicates a moisture susceptible mix which can be discarded. Also, determine the retained tensile strength by dividing wet ITS to dry ITS.
